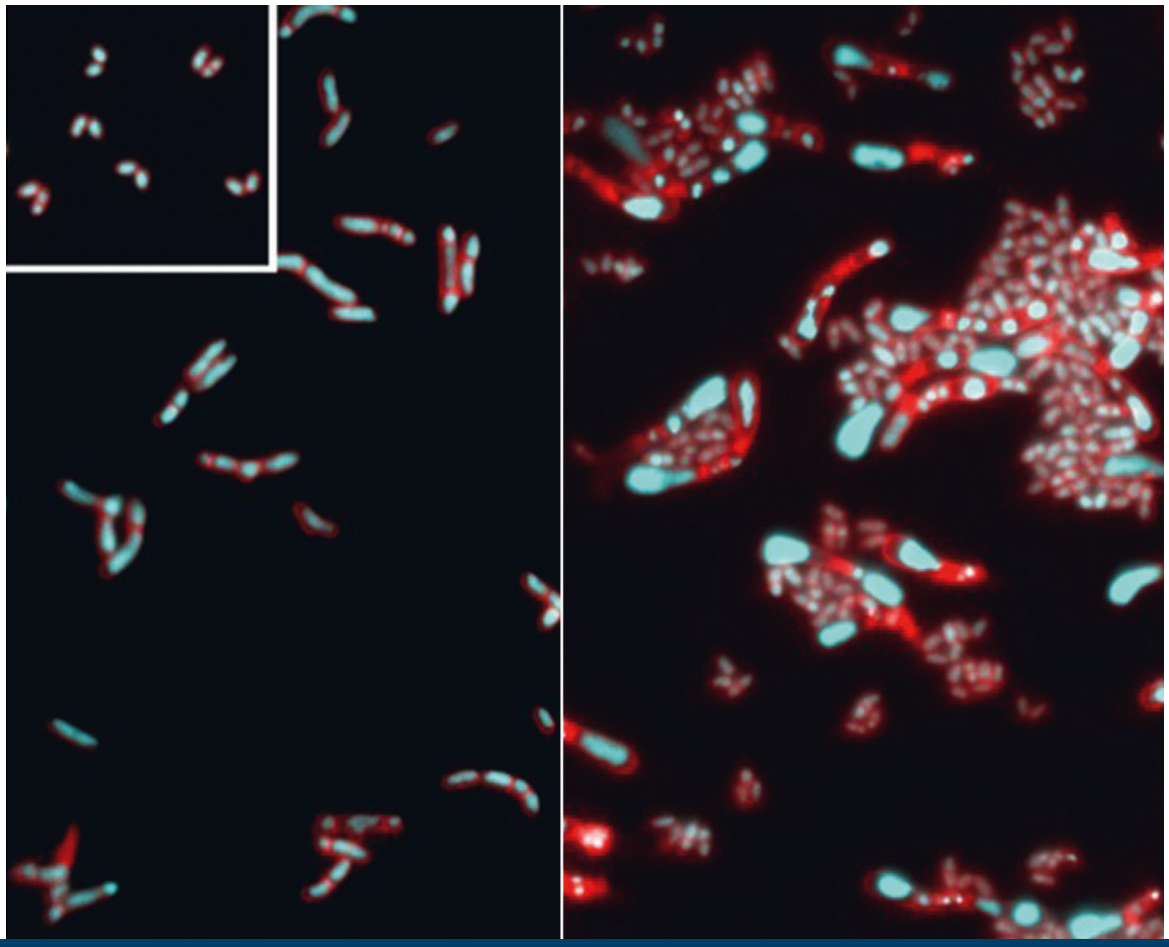

# Novel insights into the transcriptional regulation of cell division in *Corynebacterium glutamicum*

Kim Julia Kraxner

Schlüsseltechnologien / Key Technologies
Band / Volume 241
ISBN 978-3-95806-560-4

Mitglied der Helmholtz-Gemeinschaft

JÜLICH
Forschungszentrum

Schriften des Forschungszentrums Jülich
Reihe Schlüsseltechnologien / Key Technologies Band / Volume 241

Forschungszentrum Jülich GmbH
Institut für Bio-und Geowissenschaften
Biotechnologie (IBG-1)

# Novel insights into the transcriptional regulation of cell division in *Corynebacterium glutamicum*

Kim Julia Kraxner

Schriften des Forschungszentrums Jülich
Reihe Schlüsseltechnologien / Key Technologies Band / Volume 241

ISSN 1866-1807 ISBN 978-3-95806-560-4

Bibliografische Information der Deutschen Nationalbibliothek.
Die Deutsche Nationalbibliothek verzeichnet diese Publikation in der
Deutschen Nationalbibliografie; detaillierte Bibliografische Daten
sind im Internet über http://dnb.d-nb.de abrufbar.

| | |
|---|---|
| Herausgeber und Vertrieb: | Forschungszentrum Jülich GmbH<br>Zentralbibliothek, Verlag<br>52425 Jülich<br>Tel.: +49 2461 61-5368<br>Fax: +49 2461 61-6103<br>zb-publikation@fz-juelich.de<br>www.fz-juelich.de/zb |
| Umschlaggestaltung: | Grafische Medien, Forschungszentrum Jülich GmbH |
| Druck: | Grafische Medien, Forschungszentrum Jülich GmbH |
| Copyright: | Forschungszentrum Jülich 2021 |

Schriften des Forschungszentrums Jülich
Reihe Schlüsseltechnologien / Key Technologies, Band / Volume 241

D 61 (Diss. Düsseldorf, Univ., 2020)

ISSN 1866-1807
ISBN 978-3-95806-560-4

Vollständig frei verfügbar über das Publikationsportal des Forschungszentrums Jülich (JuSER)
unter www.fz-juelich.de/zb/openaccess.

In dieser Dissertation beschriebene Ergebnisse wurden in der folgenden Originalpublikation veröffentlicht:

Kim Julia Kraxner, Tino Polen, Meike Baumgart, Michael Bott (2019) The conserved actinobacterial transcriptional regulator FtsR controls expression of *ftsZ* and further target genes and influences growth and cell division in *Corynebacterium glutamicum*. BMC Microbiology 19:179

**Table of Contents**

## Abbreviations

| | |
|---|---|
| ® | registered trademark |
| °C | degree Celsius |
| µ | growth rate |
| µg | microgram |
| µL | microliter |
| A | nucleobase adenine |
| ag | attogram |
| ATCC | American Type Culture Collection |
| BHI(S) | Brain Heart Infusion (+ Sorbitol) |
| bp | base pairs |
| C- | carboxyl-terminal end |
| C | nucleobase cytosine |
| CA | California |
| CDC | Centers for Disease Control and Prevention |
| CGP3 | *Corynebacterium glutamicum* prophage 3 |
| CGXII | minimal medium for *Corynebacterium glutamicum* |
| ChAP-Seq | chromatin affinity purification with subsequent sequencing |
| ChIP | chromatin immunoprecipitation |
| $Cm^R$ | chloramphenicol resistance |
| $CO_2$ | carbon dioxide |
| CoA | coenzyme A |
| D | *dexter*, D-configuration (e.g. of an amino acid) |
| Da | Dalton |
| dcw | division cell wall |
| DNA | deoxyribonucleic acid |
| DNase | desoxyribonuclease |
| DSMZ | Deutsche Sammlung von Mikroorganismen und Zellkulturen |
| DTT | dithiothreitol |
| e.g. | *exempli gratia*, for example |
| EDTA | ethylenediaminetetraacetic acid |
| EMSA | electrophoretic mobility shift assay |
| *et al.* | *et alii* |
| etc. | *et cetera* |
| eYFP | enhanced yellow fluorescent protein |
| FHA | forkhead-associated |
| *g* | standard gravity, 9.80665 $m/s^2$ |

| | |
|---|---|
| G | nucleobase guanine |
| GDH | glutamate dehydrogenase |
| GmbH | Gesellschaft mit beschränkter Haftung |
| GOGAT | glutamate-2-oxoglutarate aminotransferase |
| GS | glutamate synthase |
| HPLC | high performance liquid chromatography |
| HTH | helix-turn-helix |
| IL | Illinois |
| Inc. | Incorporation |
| IPTG | isopropyl β-D-1-thiogalactopyranoside |
| k | kilo |
| $Kan^R$ | kanamycin resistance |
| L | *laevus*, L-configuration (e.g. of an amino acid) |
| L | liter |
| LB | lysogeny broth |
| Ltd. | private company limited by shares |
| MALDI | matrix-assisted laser desorption/ionization |
| MEME | Multiple Em for Motif Elicitation |
| mg | milligram |
| mL | milliliter |
| mM | millimolar |
| mRNA | messenger RNA |
| MS | mass spectrometry |
| MSG | monosodium glutamate |
| N- | amino-terminal end |
| $NAD^+$/NADH | nicotinamide adenine dinucleotide, oxidized/reduced |
| $NADP^+$/NADPH | nicotinamide adenine dinucleotide phosphate, oxidized/reduced |
| NCBI | National Ceter for Biotechnology Information |
| ng | nanogram |
| nm | nanometer |
| $OD_{600}$ | optical density at 600 nm |
| ODHC | 2-oxoglutarate dehydrogenase complex |
| *ori* | origin of replication |
| PAGE | polyacrylamide gel electrophoresis |
| PBS | phosphate-buffered saline |
| PCR | polymerase chain reaction |
| pg | picogram |

| | |
|---|---|
| pH | potential of hydrogen |
| PhD | *philosophiae doctor* |
| pI | isoelectric point |
| pmol | picomol |
| psi | pound-force per square inch |
| qPCR | quantitative PCR |
| RBS | ribosome binding site |
| RNA | ribonucleic acid |
| rpm | revolutions per minute |
| SDS | sodium dodecyl sulfate |
| SNP | single nucleotide polymorphism |
| T | nucleobase thymine |
| t | ton |
| TCA | trichloroacetic acid |
| TCA cycle | tricarboxylic acid cycle |
| TE | transposable element |
| TEV | tobacco etch virus |
| ™ | Trademark |
| ToF | time of flight |
| TSS | transcriptional start site |
| UK | United Kingdom |
| USA | United States of America |
| V | Volt |
| v/v | volume per volume |
| w/v | weight per volume |
| WHO | World Health Organization |
| WT | wild type |
| Δ | delta/deletion |
| ΔT | temperature difference |

Abbreviations not included in this section are according to international standards, as for example listed in the author guidelines of the American Society for Biochemistry and Molecular Biology.

# 1. Summary

## 1.1. English Summary

In the first part of this doctoral thesis the transcriptional regulation of the *odhI* gene (cg1630) of *Corynebacterium glutamicum* was analyzed. OdhI in its unphoshorylated state functions as inhibitor of the 2-oxoglutarate dehydrogenase complex (ODHC) by binding to the OdhA subunit. Phosphorylation of OdhI by serine/threonine protein kinases abolishes this effect. Inhibition of ODHC activity by OdhI was shown to be crucial for overproduction and secretion of L-glutamate, which is used as a flavour enhancer. Since downstream of *odhI* two genes presumably encoding transcriptional regulators (cg1631 and cg1633) are located, it was speculated that these could be involved in transcriptional regulation of *odhI*. However, transcriptome analysis of deletion mutants lacking cg1631 or cg1633 and DNA affinity chromatography with the *odhI* promoter did not support this hypothesis. Furthermore, no other potential transcriptional regulators of *odhI* could be identified. Thus, there is currently no evidence for transcriptional regulation of *odhI*.

The second part of this thesis addresses the regulation of cytokinesis in *C. glutamicum*. In contrast to e.g. *Escherichia coli* and *Bacillus subtilis*, knowledge about regulators of cytokinesis in Actinobacteria is very limited. In this study, the so far uncharacterized Cg1631 protein was discovered to be a transcriptional regulator of the *ftsZ* gene in *C. glutamicum* encoding the key player of bacterial cell division. Therefore, Cg1631 was named FtsR, standing for FtsZ regulator. Both deletion and overexpression of *ftsR* caused growth defects and an altered cell morphology, emphasizing an important function of FtsR in cell division or cell wall synthesis. The wild-type phenotype could be restored by plasmid-based complementation. Chromatin affinity purification with subsequent next generation sequencing (ChAP-Seq) identified a region in the *ftsZ* promoter as a major FtsR binding site, but revealed also additional potential target genes. With the ChAP-Seq results a putative DNA-binding motif could be identified for FtsR. Transcriptional activation of *ftsZ* expression by FtsR was underlined by DNA microarray experiments, electrophoretic mobility shift assays (EMSAs), and reporter gene studies. Analysis of strains expressing *ftsZ* under control of the gluconate-inducible *gntK* promoter revealed that the phenotype of the Δ*ftsR* mutant is not solely caused by reduced *ftsZ* expression but involves additional factors. In summary, FtsR was identified as the first transcriptional regulator of *ftsZ* in *C. glutamicum*. Furthermore, since FtsR and its DNA-binding site in the promoter region of *ftsZ* are highly conserved in Actinobacteria, it can be assumed that this regulatory mechanism is also relevant for the control of cell division in related *Actinobacteria*. This makes FtsR a promising target for the development of new antimicrobial drugs against pathogenic relatives of *C. glutamicum*.

## 1.2. Deutsche Zusammenfassung

Im ersten Teil dieser Doktorarbeit wurde die Transkriptionsregulation des *odhI*-Gens (cg1630) von *Corynebacterium glutamicum* analysiert. OdhI wirkt in seinem nichtphosphorylierten Zustand als Inhibitor des 2-Oxoglutarat-Dehydrogenase-Komplexes (ODHC) durch Bindung an die OdhA-Untereinheit. Die Phosphorylierung von OdhI durch Serin/Threonin-Proteinkinasen hebt diesen Effekt auf. Die Hemmung der ODHC-Aktivität durch OdhI ist entscheidend für die Überproduktion und Sekretion von L-Glutamat, das als Geschmacksverstärker verwendet wird. Da sich stromabwärts von *odhI* zwei Gene befinden, die vermutlich für Transkriptionsregulatoren (cg1631 und cg1633) kodieren, wurde spekuliert, dass diese an der Transkriptionsregulation von *odhI* beteiligt sein könnten. Die Transkriptomanalyse der Deletionsmutanten ∆cg1631 und ∆cg1633 sowie DNA-Affinitäts-chromatographie mit dem *odhI*-Promotor stützten diese Hypothese jedoch nicht. Darüber hinaus konnten keine anderen potenziellen Transkriptionsregulatoren von *odhI* identifiziert werden. Daher gibt es derzeit keine Hinweise auf eine Transkriptionsregulation von *odhI*.

Der zweite Teil dieser Arbeit befasst sich mit der Regulation der Zytokinese bei *C. glutamicum*. Im Gegensatz zu z.B. *Escherichia coli* und *Bacillus subtilis* ist das Wissen über Regulatoren der Zytokinese bei Actinobakterien sehr begrenzt. In dieser Arbeit wurde entdeckt, dass das bisher nicht charakterisierte Cg1631-Protein ein Transkriptionsregulator des *ftsZ*-Gens in *C. glutamicum* ist, das den Schlüsselakteur der bakteriellen Zellteilung codiert. Daher wurde Cg1631 als FtsR bezeichnet und steht für FtsZ-Regulator. Sowohl Deletion als auch Überexpression von *ftsR* verursachten Wachstumsdefekte und eine veränderte Zell-morphologie, was auf eine Funktion von FtsR bei Zellteilung oder Zellwandsynthese hindeutet. Der Wildtyp-Phänotyp konnte durch plasmidbasierte Komplementation der ∆*ftsR*-Mutante wiederhergestellt werden. Chromatin-Affinitätsreinigung mit anschließender Sequenzierung (ChAP-Seq) bestätigte die Bindung von FtsR an den *ftsZ*-Promotor und identifizierte weitere potenzielle FtsR-Zielgene. Mit den ChAP-Seq-Daten konnte ein mutmaßliches DNA-Bindungsmotiv für FtsR identifiziert werden. Die Aktivierung der *ftsZ*-Expression durch FtsR wurde durch DNA-Microarray-Experimente, elektrophoretische Retardationstests und Reportergenstudien bestätigt. Die Analyse von Stämmen, die *ftsZ* unter Kontrolle des Gluconat-induzierbaren *gntK*-Promotors exprimierten, ergab, dass der Phänotyp der ∆*ftsR*-Mutante nicht nur durch eine verringerte *ftsZ*-Expression verursacht wird, sondern zusätzliche Faktoren beinhaltet. Zusammenfassend wurde FtsR als erster Transkriptionsregulator von *ftsZ* in *C. glutamicum* identifiziert. Da FtsR und seine DNA-Bindungsstelle im *ftsZ*-Promotor in Actinobakterien hoch konserviert sind, wird angenommen, dass dieser Regulationsmechanismus auch für die Kontrolle der Zellteilung in verwandten Actinobakterien relevant ist. Dies macht FtsR zu einem vielversprechenden Ziel für die Entwicklung neuer antimikrobieller Wirkstoffe gegen pathogene Verwandte von *C. glutamicum*.

# 2. Introduction

## 2.1. *Corynebacterium glutamicum*

*Corynebacterium glutamicum* is a non-pathogenic, aerobic, Gram-positive soil bacterium which is used for the large-scale production of several L-amino acids and other industrially relevant compounds (Wendisch *et al.*, 2016, Eggeling & Bott, 2015, Eggeling & Bott, 2005). Moreover, it is a useful model organism for the *Corynebacteriales*, including pathogenic species such as *Corynebacterium diphtheriae* and *Mycobacterium tuberculosis,* which cause the fatal infectious diseases diphtheria and tuberculosis in humans, respectively (WHO, 2015, CDC, 2014, Lawn & Zumla, 2011, Hadfield *et al.*, 2000). Due to its industrial relevance and close relationship to pathogenic species, great efforts have been made in the last decades to unravel the regulatory network of *C. glutamicum*. About 140 transcriptional regulators were identified (Schröder & Tauch, 2010, Brinkrolf *et al.*, 2007) and approximately half of them have been characterized to date. This leads to a better understanding of the biomolecular circuits in this organism, which is of major importance in order to further improve biotechnological production strains or drug discovery processes.

In the past, *C. glutamicum*, which has been isolated in Japan by Kinoshita *et al.* (1957), became famous due to its native ability to produce the flavor enhancer monosodium glutamate (MSG). Originally, MSG was discovered in 1908 by Professor Kikunae Ikeda, as he isolated it from the seaweed *Laminaria japonica* because he wanted to unravel what constitutes the unique taste of Japanese seaweed broth (Lindemann *et al.*, 2002). Generally, Ikeda had the vision that the findings of his research could result in a commercial application, for example in a seasoning that would help improve human nutrition and therefore lead to a longer life expectancy of the Japanese population (Sano, 2009). And indeed, it has been shown that MSG and its umami taste have various positive effects in relation to improving nutrition and health (Mouritsen, 2012). Back then, MSG has been produced by hydrolysis of plant proteins using hydrochloric acid or later on by direct chemical synthesis. The discovery and characterization of *C. glutamicum* opened up the possibility of bacterial MSG synthesis, which had the advantages of enantiopure production of the natural L-form of glutamic acid and to satisfy the increasing demand while reducing production costs and relieving the environment (Sano, 2009). Today, *C. glutamicum* is an important industrial amino acid producer which is used to produce amongst others several million tons of the above-mentioned flavor enhancer L-glutamate and the feed additive L-lysine (Becker & Wittmann, 2020).

By now, there are several conditions known which trigger glutamate overproduction and secretion: Biotin limitation (Shiio *et al.*, 1962), addition of detergents like Tween-40 or Tween-60 (Duperray *et al.*, 1992, Takinami *et al.*, 1966), addition of β-lactam antibiotics like penicillin G (Nunheimer *et al.*, 1970), or inhibitors of cell wall synthesis like ethambutol

(Radmacher *et al.*, 2005), glycerol, or fatty acid auxotrophy (Kimura *et al.*, 1997, Nakao *et al.*, 1972, Kanzaki *et al.*, 1967, Okazaki *et al.*, 1967), and high temperature cultivation of temperature-sensitive strains (Delaunay *et al.*, 1999, Momose & Takagi, 1978), which are all thought to influence cell wall composition or membrane permeability, but the actual molecular mechanism is not entirely unraveled to date (Kimura, 2002, Eggeling *et al.*, 2001). Indeed, a transporter involved in glutamate secretion, named YggB (Cg1434), has been identified (Nakamura *et al.*, 2007) and metabolic flux analyses confirmed a strongly reduced activity of the 2-oxoglutarate dehydrogenase complex (ODHC) during cultivation of *C. glutamicum* under producing *versus* non-producing conditions, indicating that regulation of the ODHC plays an important role in glutamate production (Kataoka *et al.*, 2006, Shirai *et al.*, 2005, Shimizu *et al.*, 2003, Kawahara *et al.*, 1997).

## 2.2. 2-Oxoglutarate dehydrogenase and its regulation in *C. glutamicum*

ODHC is a multimeric enzyme composed of three subunits that catalyzes the conversion of 2-oxoglutarate, $NAD^+$, and coenzyme A to succinyl-CoA, NADH + $H^+$, and $CO_2$ in the tricarboxylic acid (TCA) cycle (Usuda *et al.*, 1996). The first subunit E1 is the OdhA protein encoded by the gene cg1280, harboring the actual 2-oxoglutarate dehydrogenase activity. The E2 and E3 subunits of the ODHC are called AceF (Cg2421) and LpdA (Cg0790) and encode a dihydrolipoamide acetyltransferase and a dihydrolipoamide dehydrogenase, respectively (Ikeda & Nakagawa, 2003, Kalinowski *et al.*, 2003, Schwinde *et al.*, 2001). The substrate 2-oxoglutarate marks an important branch point in the metabolism of *C. glutamicum*. Besides the conversion to succinyl-CoA by the ODHC in the TCA cycle it can also be reductively aminated to glutamate by the glutamate dehydrogenase Gdh (Cg2280), which is mainly active under nitrogen excess (Börmann *et al.*, 1992). Glutamate is converted to glutamine by the glutamine synthetase GlnA (Cg2429), which serves together with the glutamate-2-oxoglutarate aminotransferase GOGAT (encoded by *gltBD*, cg0229, and cg0230) for the assimilation of ammonium under nitrogen-limiting conditions (Jakoby *et al.*, 1997). The 2-oxoglutarate dehydrogenase reaction and the nitrogen metabolism in *C. glutamicum* are schematically illustrated in Figure 1.

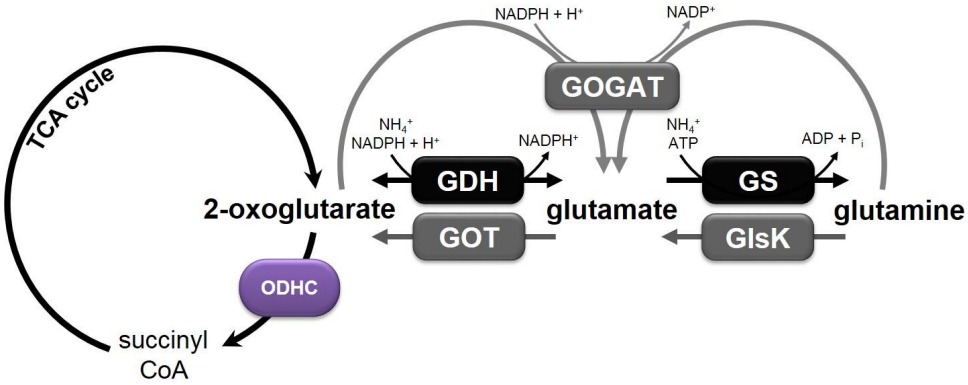


**Figure 1: Schematic illustration of the 2-oxoglutarate dehydrogenase reaction and of the nitrogen metabolism in *C. glutamicum*.** Ammonium assimilation is mediated by the reactions carried out by the glutamate dehydrogenase (GDH) and glutamine synthetase (GS)/glutamate-2-oxoglutarate aminotransferase (GOGAT), whereas glutamine catabolism involves the glutaminase K (GlsK) and the glutamate-oxaloacetate transaminase reaction.

Because the GDH shows a 30 to 70 times lower affinity to the substrate 2-oxoglutarate compared to the ODHC (Shiio & Ozaki, 1970), inhibition of ODHC activity is necessary for efficient glutamate production. How this occurs has been unraveled by the discovery of a novel kind of regulation of the ODHC, which results in an increased flux of 2-oxoglutarate to glutamate (Bott, 2007). It was found out that the 15 kDa small inhibitor protein OdhI (Cg1630) is involved in the regulation of the ODHC, which in turn is regulated by a complex signalling cascade. The findings obtained in previous studies so far led to the assumption of the following mechanism, which is schematically illustrated in Figure 2: in the presence of L-glutamine as sole carbon and nitrogen source, it is bound by the membrane-associated lipoprotein GlnH (Cg3045). The signal is then transmitted from GlnH *via* protein-protein interaction to the integral membrane protein GlnX (Cg3044), consisting of four transmembrane helices with the N- and C-terminus located in the cytoplasm. GlnX activates hereupon the soluble serine/threonine protein kinase PknG (Cg3046). Hence, PknG dissociates from the cytoplasmic membrane and phosphorylates the OdhA inhibitor protein OdhI at its threonine-14 residue. In its phosphorylated state, OdhI is inactive and not able to inhibit the ODHC, so that the complex is present in its active state. Under these conditions, a normal flux of glutamine through the TCA cycle towards succinyl-CoA occurs. The loss of interaction of phosphorylated OdhI with the ODHC is very likely caused by a conformational change which is triggered by the phosphorylation through PknG. OdhI consists of a non-folded N-terminal domain with two phosphorylation sites (Thr14 and Thr15) and a C-terminal forkhead-associated (FHA) domain. Phosphorylation through PknG at the threonine-14 residue causes a conformational change of the non-folded N-terminus which in turn can be bound by the FHA domain. This auto-inhibition leads to an inactive OdhI protein.

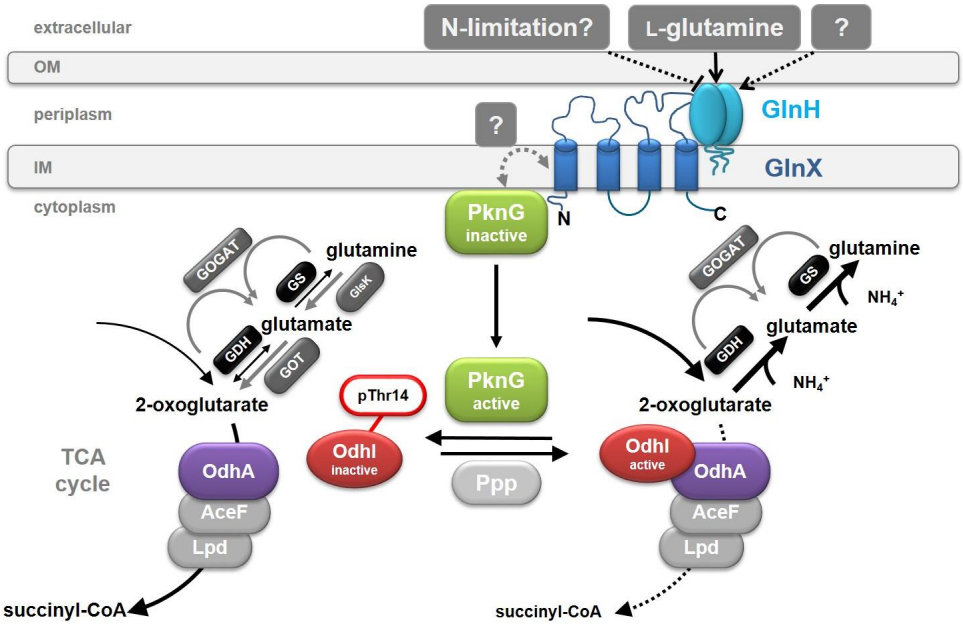


**Figure 2: Model of the GlnX-GlnH-PknG-OdhI signal transduction cascade in *C. glutamicum*.** Illustrated is the model of the GlnX-GlnH-PknG-OdhI signal transduction cascade in *C. glutamicum* as proposed based on the previous findings. A detailed description of the mechanism can be found in the text.

In the absence of the proteins of the cascade, the signal can neither be detected nor transmitted and consequently, OdhI can no longer be phosphorylated by the kinase PknG. In its unphosphorylated state, the inhibitor protein binds to the OdhA subunit of the ODHC, inhibiting its activity, which leads to a reduced conversion of 2-oxoglutarate to succinyl-CoA in the TCA cycle and an increased flux towards glutamate. Due to dephosphorylation of OdhI by the phospho-serine/threonine protein phosphatase Ppp (Cg0062), this process is reversible. The proposed model is based on the findings of Bosco (2011), Krawczyk *et al.* (2010), Schultz *et al.* (2009), Schultz *et al.* (2007), Gebel (2006), and Niebisch *et al.* (2006).

## 2.3. Cell division in *C. glutamicum*

Bacterial reproduction is usually characterized by cellular growth followed by binary fission of a mother cell into two daughter cells. During this process, the bacteria need to coordinate several distinct processes such as DNA replication, biogenesis of the new cell wall, and the division process itself. Although the overall process is similar, several different concepts have evolved in distinct bacterial groups. *Escherichia coli* and *Bacillus subtilis* represent two of the best studied species in this respect (Du & Lutkenhaus, 2017, Hajduk *et al.*, 2016).

Corynebacteria are rod-shaped with frequently engrossed cell poles during exponential growth, leading to the typical “club”-shaped morphology by which the name of this genus is

inspired (Cure & Keddie, 1973). Like for almost all other bacteria, the highly conserved FtsZ protein is also the key player of cell division in *C. glutamicum* (Donovan & Bramkamp, 2014, Adams & Errington, 2009). It is essential and the first protein that moves to the future division site, recruiting other proteins involved in this process (Margolin, 2005). Several FtsZ proteins together form the so-called Z-ring, which in rod-shaped bacteria is located in the middle of the cell, and constriction of this ring leads to a formation of two daughter cells (Adams & Errington, 2009, Margolin, 2005) (see Figure 3).

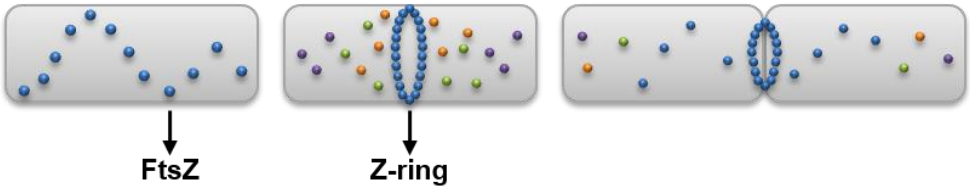


**Figure 3: Assembly and disassembly of FtsZ and the Z-ring.** On the left, a newborn cell with FtsZ proteins (blue) arranged in a spiral pattern is depicted, as known for *E. coli*. The cell in the middle already shows a formed Z-ring and the recruitment of other proteins of the divisome (violet, green, and orange). On the right site, a dividing cell with a contracting Z-ring is illustrated. Picture inspired by Margolin (2005).

Interestingly, *C. glutamicum* – as well as other Actinobacteria – is lacking homologs for several important cell division-related genes described for *E. coli* or *B. subtilis* (Table 1). Cell division in *C. glutamicum* is for example independent of the actin homolog MreB, which is essential for elongation of the lateral cell wall in *E. coli*, *Caulobacter crescentus*, and *B. subtilis* (Kruse *et al.*, 2005, Figge *et al.*, 2004, Jones *et al.*, 2001). In contrast to these species, *C. glutamicum* inserts new cell wall material at the poles, representing an apical elongation mechanism (Daniel & Errington, 2003). Besides *mreB*, also other typically essential cell division genes are missing, such as *ftsL* and *ftsN* (Letek *et al.*, 2008). Most of the genes required for cell division and peptidoglycan synthesis are located in the so-called division cell wall (*dcw*) cluster, which is highly conserved throughout the bacterial kingdom (Mingorance *et al.*, 2004). Several studies of this cluster in Actinobacteria revealed that its arrangement in *Corynebacteria* and *Mycobacteria* clearly differs from many other bacteria (Tamames *et al.*, 2001). However, the most striking difference might be the complete absence of homologs of other known spatial and temporal, positive and negative regulators of cell division, as for example *ftsA, ezrA*, *slmA, sulA, zipA*, *zapA*, *min*, and *noc* are missing (Donovan & Bramkamp, 2014, Letek *et al.*, 2007). FtsA is a positive regulator of FtsZ assembly and supports membrane association of the Z-ring (Pichoff & Lutkenhaus, 2005, Beall & Lutkenhaus, 1992). The integral membrane protein EzrA negatively influences Z-ring assembly and is involved in mid-cell localisation of the Z-ring (Haeusser *et al.*, 2004, Levin *et al.*, 1999). SlmA and NocA are nucleoid occlusion effector proteins, known to inhibit assembly of the Z-ring over the nucleoid (Bernhardt & de Boer, 2003, Wu & Errington, 2004). SulA also inhibits Z-ring formation and is induced upon DNA damage

(Bi & Lutkenhaus, 1993, Huisman *et al.*, 1984). ZipA and ZapA are positive regulators of Z-ring assembly (Slayden *et al.*, 2006, Gueiros-Filho & Losick, 2002, Hale & de Boer, 1997), and the Min system consists of several proteins preventing division occurring at the cell poles (Bramkamp *et al.*, 2008, Raskin & de Boer, 1999, Levin *et al.*, 1992, de Boer *et al.*, 1989). Taking all these differences into account, it is obvious that in Actinobacteria cell division and its regulation must differ profoundly from the processes described for other well-studied rod-shaped bacteria like *E. coli,* and *B. subtilis* (Letek *et al.*, 2007, Flardh, 2003, Ramos *et al.*, 2003).

**Table 1: Putative cell division genes of *E. coli*, *B. subtilis*, *C. glutamicum,* and *M. tuberculosis*.** Known positive regulators (green), negative regulators (red), and essential cell division genes (blue) which are missing in *C. glutamicum* are written in bold letters. The table is based on Letek *et al.* (2008) and Donovan and Bramkamp (2014). For an overview of the predicted protein functions, see Donovan and Bramkamp (2014).

| gene name | *E. coli* | *B. subtilis* | *C. glutamicum* | *M. tuberculosis* |
|---|---|---|---|---|
| *amiC* | b2817 | BSU09420 (*lytE*)<br>BSU09370 (*lytF*) | cg3424 | rv3915 |
| *clpX* | b0438 | BSU28220 | cg2620 | rv2457c |
| *crgA* | ? | ? | cg0055 | rv0011c |
| *cwsA* | ? | ? | ? | rv008c |
| *divIVA* | ? | BSU15420 | cg2361 | rv2154c (*wag31*) |
| *divS* | b0958 (*sulA*) | BSU17860 (*yneA*) | cg2133 | rv2719 (*chiZ*) |
| ***ezrA*** | ? | BSU29610 | ? | ? |
| ***ftsA*** | b0094 | BSU15280 | ? | ? |
| *ftsB (divIC)* | b2748 | ? | cg1112 | rv1024 |
| *ftsE* | b3463 | BSU35260 | cg0914 | rv3102c |
| *ftsI* | b0084 | BSU15170 | cg2375 | rv2163c |
| *ftsK* | b0890 | BSU29800 (*ytpT*)<br>BSU16800 (*spoIIIE*) | cg2158 | rv2748c |
| ***ftsL*** | b0083 | BSU15150 | ? | ? |
| ***ftsN*** | b3933 | ? | ? | ? |
| *ftsQ (divB)* | b0093 | BSU15240 | cg2367 | rv2151c |
| *ftsW* | b0089 | BSU14850<br>BSU15210 (*spoVE*) | cg2370 | rv2154c |
| *ftsX* | b3462 | BSU35250 | cg0915 | rv3101c |
| *ftsZ* | b0095 | BSU15290 | cg2366 | rv2150c |

*(Continued)*

**Table 1.** *Continued.*

| gene name | *E. coli* | *B. subtilis* | *C. glutamicum* | *M. tuberculosis* |
|---|---|---|---|---|
| *ftsX* | b3462 | BSU35250 | cg0915 | rv3101c |
| *ftsZ* | b0095 | BSU15290 | cg2366 | rv2150c |
| ***minC*** | b1176 | BSU28000 | ? | ? |
| ***minD*** | b1175 | BSU27990 | ? | ? |
| *minJ* | ? | BSU35220 | ? | ? |
| *minE* | b1174 | ? | ? | ? |
| ***mreB*** | b3251 | BSU14470 (*mreBH*)<br>BSU28030 (*mreB*)<br>BSU36410 (*mbl*) | ? | ? |
| *mreC* | b3250 | BSU28020 | ? | ? |
| *mreD* | b3249 | BSU28010 | ? | ? |
| ***noc*** | ? | BSU40990 | ? | ? |
| *pldP* | ? | ? | cg1610 | rv1708 |
| *rodA* | b0634 | BSU38120 | cg0061 | rv0017c |
| *sepF* | ? | BSU15390 | cg2363 | rv2147c |
| ***slmA*** | b3641 | ? | ? | ? |
| ***sulA*** | b0958 | ? | ? | ? |
| *ugtP* | ? | BSU21920 | ? | ? |
| ***zapA*** | b2910 | ? | ? | ? |
| *zapB* | b3928 | ? | ? | ? |
| *zapC* | b0946 | ? | ? | ? |
| ***zapD*** | b0102 | ? | ? | ? |
| ***zipA*** | b2412 | ? | ? | ? |

To date, *C. glutamicum* is an established model organism for industrial biotechnology and for pathogenic relatives, but we have a relatively narrow understanding about the exact regulation of its cytokinesis (Donovan & Bramkamp, 2014). However, it is known that accurate expression of FtsZ is critical for normal growth of *C. glutamicum* and *M. tuberculosis* and small variations lead to severe morphological changes and affect cell viability, suggesting that the intracellular levels of FtsZ are critical for proper cell division in these organisms (Letek *et al.*, 2007, Ramos *et al.*, 2005, Dziadek *et al.*, 2003). Thus, FtsZ levels must be subject to a tight regulation, which is supported by different studies of the *ftsZ* promoter region, showing a very complex

transcription of *ftsZ* in various bacteria (Letek *et al.*, 2007, Roy & Ajitkumar, 2005, Flardh *et al.*, 2000, Flardh *et al.*, 1997, Gonzy-Treboul *et al.*, 1992). A complex of the DNA-binding proteins WhiA (Cg1792) and WhcD (Cg0850) was reported to bind to the *ftsZ* promoter region (Lee *et al.*, 2018), however, the effect of this interaction on *ftsZ* expression remains to be elucidated. Previously, it was shown that the FtsZ protein can be phosphorylated *in vitro* by the serine/threonine protein kinases PknA, PknB, and PknL and is an *in vivo* substrate of the phospho-serine/threonine protein phosphatase Ppp (Schultz *et al.*, 2009), suggesting that the properties and activities of FtsZ can also be influenced by posttranslational regulation (Donovan & Bramkamp, 2014). However, a regulatory protein involved in direct control of *ftsZ* transcription has only been described for *Caulobacter crescentus* (Kelly *et al*., 1998). For the *Corynebacteriales* order, the regulation of cell division processes remains largely undiscovered.

## 2.4. Aim of this work

Originally, the focus of this thesis lay on studying the role of GlnX, GlnH, PknG, and OdhI in *C. glutamicum* in order to attain a deeper understanding of the signal transduction cascade which consists of these proteins. More specifically, one major objective was to investigate whether the inhibitory protein of the ODHC is potentially regulated on the transcriptional level. This seemed sensible because *odhI* (cg1630) is located upstream of the two genes (cg1631 and cg1633), which are annotated to encode transcriptional regulators. However, the experiments performed in this direction (DNA affinity chromatography with the *odhI* promoter, DNA microarrays) did not provide any evidence to support transcriptional regulation of *odhI*. Nevertheless, since studying the GlnH-GlnX-PknG-OdhI-ODHC signal transduction cascade was the initial objective of this work, a part of this introduction and the first chapters of the results section are related to this topic. In these initial studies, deletion mutants of the genes cg1631, cg1632, and cg1633 were constructed and analyzed. Thereby it was observed that deletion of cg1631 led to a severe growth defect and drastic morphological changes. Because there is hitherto no transcriptional regulator of cell division known for *C. glutamicum*, this phenotype was highly interesting and let us redefine the aims of this thesis towards the functional analysis of the previously uncharacterized protein Cg1631. In this context, we searched for the target genes of Cg1631 by a variety of complementary approaches and identified *ftsZ* to be activated by Cg1631. Therefore, Cg1631 was renamed FtsR, standing for *ftsZ* regulator. We show that FtsR is critical for normal growth and cell morphology of *C. glutamicum*, suggesting an important role of this protein in the regulation of cell division.

# 3. Materials and Methods

## 3.1. Bacterial strains, plasmids, and growth conditions

Bacterial strains and plasmids used in this study are listed in Table 2. The *C. glutamicum* type strain ATCC13032 or its prophage-free variant *C. glutamicum* MB001 were used as wild type or reference strain, as indicated. The parental strain ATCC13032 (DSM No. 20300) was obtained from the Deutsche Sammlung von Mikroorganismen und Zellkulturen GmbH (DSMZ, Braunschweig, Germany). The prophage-free strain MB001 was derived from an in-house stock but can also be obtained from the DSMZ (DSM No. 102070). First experiments were performed with ATCC13032, but to be able to discriminate between effects primarily caused by *ftsR* deletion or secondarily emerged due to phage-related effects, we later switched to the *C. glutamicum* MB001 strain. Deletion of the prophages did not lead to any negative effects on the physiology of *C. glutamicum* MB001 and due to its reduced complexity it is a useful platform organism for basic research (Baumgart *et al.*, 2013b).

For growth experiments, *C. glutamicum* was pre-cultivated for six to eight hours at 30 °C and 170 rpm in 5 mL BHI medium (BD Bacto™ Brain Heart Infusion, Becton Dickinson and Company, Heidelberg, Germany). The cells were harvested by centrifugation, washed with phosphate-buffered saline (PBS, 137 mM NaCl, 2.7 mM KCl, 4.3 mM $Na_2HPO_4$, 1.4 mM $KH_2PO_4$, pH 7.3) and used as inoculum for a second pre-culture in 20 mL CGXII minimal medium (Keilhauer *et al.*, 1993) supplemented with 3,4-dihydroxybenzoate (30 mg/L) as iron chelator and, if not stated otherwise, 2% (w/v) glucose as carbon source. This second pre-culture was incubated overnight at 30 °C and 120 rpm. After harvesting by centrifugation and washing with PBS, the cells were used for inoculation of the main culture, using CGXII medium with 3,4-dihydroxybenzoate (30 mg/L) and 2% (w/v) glucose as carbon source, if not stated otherwise.

Growth experiments were either performed in 100 mL shake flasks with 20 mL medium (initial optical density at 600 nm ($OD_{600}$) of 1.0) that were shaken at 30 °C and 120 rpm or in 48-well FlowerPlates® (m2p-labs GmbH, Baesweiler, Germany) containing a final culture volume of 800 µL (initial $OD_{600}$ of 0.5) that were shaken in a BioLector® system (m2p-labs GmbH, Baesweiler, Germany) at 30 °C and 1200 rpm. Growth was monitored as cell density by determining either $OD_{600}$ (shake flasks experiments, $OD_{600}$ measured with an Ultrospec 500 Pro UV/Vis spectrophotometer, Amersham Biosciences, Little Chalfont, United Kingdom) or as scattered light at 620 nm in the BioLector® (Kensy *et al.*, 2009), which is termed “backscatter” throughout this study.

For growth experiments with promoter exchange strains in which expression of the *ftsZ* gene was under control of the *gntK* promoter, the first pre-culture was supplemented with 0.1% (w/v) and the second pre-culture with 0.01% (w/v) gluconate and 1.99% (w/v) glucose as carbon source. The gluconate concentration of the main culture is indicated for each experiment.

For cloning purposes, *Escherichia coli* DH5α was used and routinely cultivated at 37 °C in lysogeny broth (LB, (Sambrook & Russell, 2001)). When required, the media were supplemented with 25 µg/mL kanamycin or 10 µg/mL chloramphenicol for *C. glutamicum* or with 50 µg/mL kanamycin or 34 µg/mL chloramphenicol for *E. coli*.

**Table 2: Bacterial strains and plasmids used in this study.**

| Strain or plasmid | Characteristics | Source or Reference |
|---|---|---|
| **Bacterial strains** | | |
| ***E. coli*** | | |
| DH5α | F$^-$ Φ80*dlac*Δ(*lacZ*)M15 Δ(*lacZYA-argF*) U169 *endA1 recA1 hsdR17* ($r_K^-$, $m_K^+$) *deoR thi-1 phoA supE44* λ$^-$ *gyrA96 relA1*; strain used for cloning procedures | Hanahan (1983) |
| ***C. glutamicum*** | | |
| ATCC13032 | biotin-auxotrophic wild type. | Kinoshita *et al.* (1957) |
| ATCC13032Δ*ftsR* | ATCC13032 with in-frame deletion of *ftsR* (cg1631) | this work |
| ATCC13032Δcg1632 | ATCC13032 with in-frame deletion of cg1632 | this work |
| ATCC13032Δcg1633 | ATCC13032 with in-frame deletion of cg1633 | this work |
| ATCC13032Δ*ramB* | ATCC13032 with in-frame deletion of *ramB* (cg0444) | Gerstmeir *et al.* (2004) |
| ATCC13032::*ftsZ-venus* | ATCC13032 with a chromosomal insertion of pK18*mob-ftsZ-venus* at the *ftsZ* locus; this strain has two chromosomal copies of *ftsZ* under control of its native promoter, one with and one without the fusion to *venus* | this work |
| ATCC13032Δ*ftsR*::*ftsZ-venus* | ATCC13032Δ*ftsR* with a chromosomal insertion of pK18*mob-ftsZ-venus* at the *ftsZ* locus; this strain has two chromosomal copies of *ftsZ* under control of its native promoter, one with and one without the fusion to *venus* | this work |
| MB001 | ATCC13032 with in-frame deletions of the prophages CGP1 (cg1507-cg1524), CGP2 (cg1746-cg1752), and CGP3 (cg1890-cg2071) | Baumgart *et al.* (2013b) |
| MB001Δ*ftsR* | MB001 with in-frame deletion of *ftsR* (cg1631) | this work |
| MB001::$P_{gntK}$-*ftsZ* | MB001 with a chromosomal promoter exchange of the native *ftsZ* promoter against the gluconate-inducible promoter of *gntK* (cg2732) | this work |
| MB001Δ*ftsR*::$P_{gntK}$-*ftsZ* | MB001::$P_{gntK}$-*ftsZ* with in-frame deletion of *ftsR* | this work |
| ***C. diphtheriae* ATCC27010** | genomic DNA of this strain was used as PCR template for amplification of the *ftsR* homolog CDC7B_1201 | DSM 44123 |
| ***M. tuberculosis* H37Rv** | genomic DNA of this strain was used as PCR template for amplification of the *ftsR* homolog rv1828 | ATCC 25618 |

*(Continued)*

**Table 2.** *Continued.*

| Strain or plasmid | Characteristics | Source or reference |
|---|---|---|
| **Plasmids** | | |
| pK18*mob* | Kan$^R$; plasmid for insertion of a DNA fragment into the chromosome of *C. glutamicum* (pK18 *ori*V$_{E.c.}$, *lacZα*) | Schäfer *et al.* (1994) |
| pK18*mob-ftsZ-venus* | Kan$^R$; pK18*mob* derivative for chromosomal insertion of the coding sequence for a fusion protein of FtsZ and the fluorescent protein Venus under control of the native *ftsZ* promoter | this work |
| pK19*mobsacB* | Kan$^R$; plasmid for allelic exchange in *C. glutamicum* (pK18 *ori*V$_{E.c.}$, *sacB*, *lacZ*α). | Schäfer *et al.* (1994) |
| pK19*mobsacB*-Δ*ftsR* | Kan$^R$; pK19*mobsacB* derivative for in-frame deletion of *ftsR*; contains PCR product covering the fused up- and downstream regions of *ftsR* | this work |
| pK19*mobsacB*-P$_{gntK}$-*ftsZ* | Kan$^R$; pK19*mobsacB* derivative for construction of MB001::P$_{gntK}$-*ftsZ;* contains a PCR fragment encompassing 691 bp of the upstream region of cg2366 (*ftsZ*) covering its promoter, followed by a terminator sequence, the *gntK* (cg2732) promoter and 523 bp of the *ftsZ* (cg2366) coding region | this work |
| pK19-P2732-*lcpA* | Kan$^R$; pK19*mobsacB* derivative used as template for the promoter exchange plasmid pK19*mobsacB*-P$_{gntK}$-*ftsZ* | Baumgart *et al.* (2016) |
| pAN6 | Kan$^R$; *C. glutamicum*/*E. coli* shuttle vector for regulated gene expression using P$_{tac}$ (P$_{tac}$ *lacI*$^q$ pBL1 *ori*V$_{Cg}$ pUC18 *ori*V$_{Ec}$) | Frunzke *et al.* (2008) |
| pAN6-*ftsR* | Kan$^R$; pAN6 derivative for expression of *ftsR* (252 amino acids) under control of P$_{tac}$ | this work |
| pAN6-*ftsR*-short | Kan$^R$; pAN6 derivative encoding an N-terminally shortened FtsR protein (224 amino acids) under control of P$_{tac}$ | this work |
| pAN6-*ftsR*-Strep | Kan$^R$; pAN6 derivative for expression of *ftsR* under control of P$_{tac}$ with a C-terminal Strep-tag® | this work |
| pAN6-CDC7B_1201 | Kan$^R$; pAN6 derivative for expression of *C. diphtheriae* CDC7B_1201 (*ftsR* homolog) under control of P$_{tac}$. | this work |
| pAN6-rv1828 | Kan$^R$; pAN6 derivative for expression of *M. tuberculosis* rv1828 (*ftsR* homolog) under control of P$_{tac}$. | this work |
| pEC-XC99E | Cm$^R$; *C. glutamicum*/*E. coli* shuttle vector for regulated gene expression using P$_{trc}$, (P$_{trc}$, *cat$_I$*, *lacI*$^q$, *rrnB*, *ori*V$_{E.c}$, *per* and *repA* (pGA1)$_{C.g.}$). | Kirchner and Tauch (2003) |
| pEC- *ftsR* | Cm$^R$; pEC-XC99E derivative for expression of *ftsR* under control of P$_{trc}$. | this work |
| pJC1-*venus*-term | Kan$^R$; pJC1 derivative carrying the Venus coding sequence and additional terminators (pCG1 *ori*$_{Cg}$, pACYC177 *ori*$_{Ec}$). | Baumgart *et al.* (2013a) |
| pJC1-P$_{ftsZ}$-*venus* | Kan$^R$, pJC1-*venus*-term derivative carrying the *ftsZ* promoter controlling expression of *venus* for promoter activity studies. | this work |

### 3.2. Recombinant DNA work and construction of insertion and deletion mutants

Routine methods such as PCR, DNA restriction and ligation, Gibson assembly, and transformation were performed using standard protocols (Sambrook & Russell, 2001, Hanahan, 1983, van der Rest *et al.*, 1999, Gibson, 2011). Phusion Green High Fidelity DNA Polymerase (Thermo Fisher Scientific Inc., Rockford, IL, USA) was used for cloning purposes. For all other PCRs, either the KAPA2G Fast ReadyMix PCR Kit (Kapa Biosystems, Wilmington, USA) or DreamTaq DNA Polymerase (Thermo Fisher Scientific Inc., Rockford, IL, USA) were used. The oligonucleotides used in this study (see Table 3) were purchased from Eurofins Genomics GmbH (Ebersberg, Germany) and DNA sequencing was also performed by this company. The Δ*ftsR* mutant of *C. glutamicum* and the promoter exchange strains carrying a DNA fragment with a transcription terminator sequence and the *gntK* promoter inserted into the chromosome between the native *ftsZ* promoter and the *ftsZ* coding region were constructed *via* a two-step homologous recombination protocol as described previously (Baumgart *et al.*, 2016, Niebisch & Bott, 2001), using plasmids pK19*mobsacB*-Δ*ftsR* and pK19*mobsacB*-$P_{gntK}$-*ftsZ*. The strains ATCC13032::*ftsZ*-venus and ATCC13032Δ*ftsR*::*ftsZ*-venus were constructed by chromosomal insertion of pK18*mob-ftsZ-venus* by single homologous recombination. In all tested clones of both strains, the plasmid did not insert into the intergenic region between cg1121 and cg1122, but into the *ftsZ* region. As the insertion plasmid was constructed in such a way that these mutants also carry one native copy of *ftsZ* and one fused to *venus*, these strains were used for microscopy, anyway.

**Table 3: Oligonucleotides used in this study for cloning, EMSAs, and DNA affinity purification.** Restriction sites are underlined. Bold letters represent the overlapping sequences needed for Gibson Assembly. If not stated otherwise, *C. glutamicum* genomic DNA was used as template.

| Oligonucleotide | Sequence (5' → 3') and properties | Commentary |
|---|---|---|
| **DNA affinity purification with $P_{odhI}$ and $P_{ftsZ}$** | | |
| AP_PodhI_fw | TGATCAGTCCGTGAGGGAAC | |
| AP_PodhI_rv_bio | *GAGGAGTCGTCGATGTGGAGACC*CAGC GCGGAATACTGAGGTG | overlap (in italics) homologous to the biotin-oligo used as reverse primer in a second PCR to create a biotinylated fragment |
| AP_PftsZ_fw | CATTAGCTCACCCTCAATGG | |
| AP_PftsZ_rv_bio | *GAGGAGTCGTCGATGTGGAGACC*GAGG CCTTCTTCAATCATGC | overlap (in italics) homologous to the biotin-oligo used as reverse primer in a second PCR to create a biotinylated fragment |
| biotin_oligo | 5'BIO- GAGGAGTCGTCGATGTGGAGACC | biotin-labelled sequence homologous to the overlap of the rv_bio primers for attachment of a biotin-tag to the resulting fragments; biotinylated molecules bind with high affinity to the Streptavidin-coated magnetic beads used for DNA affinity purification. |

*(Continued)*

**Table 3.** *Continued.*

| Oligonucleotide | Sequence (5' → 3') and properties | Commentary |
|---|---|---|
| **Construction of pK18*mob*- and pK19*mobsacB* derivatives** | | |
| M13-fw | CGCCAGGGTTTTCCCAGTCAC | for sequencing of pK18*mob-ftsZ-venus* and pK19*mobsacb*-Δ*ftsR* |
| M13-rv | AGCGGATAACAATTTCACACAGGA | |
| **Plasmid pK18*mob-ftsZ-venus* for chromosomal insertion of *ftsZ-venus*** | | |
| pK18_IRG-fw-V2 | **CCTGCAGGTCGACTCTAGAG**GTTTACG CAGCACAAGACCCC | for amplification of a fragment covering about 450 bp of the intergenic region between cg1121 and cg1122 |
| IGR-rv | TCCTCCATAATTAGAGAGCGTAAGGCC C | |
| PftsZ-fw | **CGCTCTCTAATTATGGAGGA**TGATGGT GACCATGTCATTGACACCG | for amplification of the promoter and the coding region of *ftsZ* |
| FtsZ-rv | **TCCTCGCCCTTGCTCACCAT**CTGGAGG AAGCTGGGTACATCCAG | |
| venus-fw | ATGGTGAGCAAGGGCGAGGAG | for amplification of the *venus* gene encoding the fluorescent protein Venus |
| pK18_venus-rv-V2 | **CAGCTATGACCATGATTACG**TTACTTG TACAGCTCGTCCATGCC | |
| FtsZ-Seq1 | **CATTAGCTCACCCTCAATGGTG** | for sequencing of pK18*mob-ftsZ-venus* |
| FtsZ-Seq2 | **GAACCTGTCCATCATGGAAGC** | |
| int-reg-fw | AGCACCTTCGGCAAGAAGTA | test of integration strains for integration into the intergenic region of cg1121-cg1122 |
| int-reg-rv | CATCGAAGGTGTCGCAAAC | |
| ftsQ-rv | AGCAATAACCGCAGGAAGCAC | |
| M13-fw | CGCCAGGGTTTTCCCAGTCAC | |
| ftsQ-fw | ACAAGGCAGGACTAGCGTGAAC | test of integration strains for integration into the chromosomal *ftsZ*-region |
| ftsZ-downstream-rv | TCGTGAAGACCTTGCGGAC | |
| pK18-IGR-fw | CTTGGTTCGAATATGCAGTTCGG | |
| eYFP-int_rv | CGACCAGGATGGGCACCAC | |
| **Deletion plasmid pK19*mobsacb*-Δ*ftsR*** | | |
| D_ftsR_1_fw | GATCGGATCCTCCGCACTCAACATCTA GAC | PCR product contains BamHI site for cloning in BamHI-cut pK19*mobsacb* |
| D_ftsR_2_rv | TGTTTAAGTTTAGTGGATGGGGATGTT GCTGCTACCTGCTGTGAATTAAA | |
| D_ftsR_3_fw | CCCATCCACTAAACTTAAACATAGAAA AAATGAGTTTTGTTGAACTT | PCR product contains HindIII site for cloning in HindIII-cut pK19*mobsacb* |
| D_ftsR_4_rv | GATCAAGCTTCGTCGCCTGAAGCAGAT TCC | |
| map_DftsR_fw | TCCGCACTCAACATCTAGAC | for verification of chromosomal *ftsR* deletion |
| map_DftsR_rv | CAGGTAAAGCCATCTGGTTC | |
| **Deletion plasmid pK19*mobsacb*-Δcg1632** | | |
| D_cg1632_1_fw | GATCGGATCCTCAGCCCGGAGAAGTTT CAG | PCR product contains BamHI site for cloning in BamHI-cut pK19*mobsacb* |
| D_ cg1632_2_rv | TGTTTAAGTTTAGTGGATGGGTTTTTC TATCAGTATCCAAGCTGCTCGCGAGTT GC | |
| D_ cg1632_3_fw | CCCATCCACTAAACTTAAACAAATGTG ACTAATCACACCCTCAGATTTCAAC | PCR product contains HindIII site for cloning in HindIII-cut pK19*mobsacb* |
| D_ cg1632_4_rv | GATCAAGCTTAGGTCGTTGGTGCCCAT GTC | |

*(Continued)*

**Table 3.** *Continued.*

| Oligonucleotide | Sequence (5' → 3') and properties | Commentary |
|---|---|---|
| **Deletion plasmid pK19*mobsacb*-Δcg1633** | | |
| D_cg1633_1_fw | GATCGGATCCTACATGGCTACCATCAC TAC | PCR product contains BamHI site for cloning in BamHI-cut pK19*mobsacb* |
| D_ cg1633_2_rv | TGTTTAAGTTTAGTGGATGGGTAGTTT CTCCGATTATTCAGCACCCATGTTTTA TTC | |
| D_ cg1633_3_fw | CCCATCCACTAAACTTAAACAAAACTC AGCGCAGTAAATCTTCAAGCC | PCR product contains HindIII site for cloning in HindIII-cut pK19*mobsacb* |
| D_ cg1633_4_rv | GATCAAGCTTCAAGCCCTCGACCGACT TGG | |
| **Promoter exchange plasmid pK19*mobsacb*-$P_{gntK}$-*ftsZ*** | | |
| ftsZ_upstream_fw | **CAGGTCGACTCTAGAGGATC**GAAGTGC TTCCTGCGGTTAT | for amplification of a fragment upstream of the *ftsZ* coding region with homologies to the pK19*mobsacb*-backbone and to the terminator sequence |
| ftsZ_upstream_rv | **CACTACCATCGGCGCTAC**TGTCGATGT CTCGCCTTTCG | |
| term_fw | GTAGCGCCGATGGTAGTG | for amplification of a fragment harboring the terminator and the $P_{gntK}$ coding sequence; template: pK19-P2732-cg0847 (Baumgart *et al.*, 2016) |
| Pcg2732-rv | GTCTTATCCTTTCTTTGGTGGCG | |
| PgntK_ftsZ_fw | **CACCAAAGAAAGGATAAGAC**ATGACCT CACCGAACAACTA | for amplification of a fragment of the first 523 bp of the *ftsZ* (cg2366) coding region (including start codon) with homologies to the $P_{gntK}$ sequence and the pK19*mobsacb*-backbone |
| ftsZ_start_rv | **AAAACGACGGCCAGTGAATT**GTCGTTT GGAATAACGATGA | |
| map_term-PgntK_insertion_fw | TGAGTGCGGAACCAGCTTCG | for verification of insertion of the terminator-$P_{gntK}$-fragment between $P_{ftsZ}$ and the *ftsZ* coding region on the chromosome |
| map_term-PgntK_insertion_rv | ACCATCACCGTGGAGCTGAC | |
| **Construction of pAN6 derivatives** | | |
| pAN6_check_fw | CATCGGAAGCTGTGGTATGG | for sequencing of pAN6 derivatives |
| pAN6_check_rv | CCTGGCAGTTCCCTACTCTC | |
| **pAN6-*ftsR*, *pAN6-ftsR*-short & pAN6-*ftsR*-Strep** | | |
| pAN6_ftsR_fw | **CTGCAGAAGGAGATATACATATGA**GTG CACTCCGTAAAAC | PCR product with overlaps for cloning of *ftsR* in the NdeI/EcoRI-cut pAN6 plasmid; with fw-primer, the *ftsR* start codon GTG is changed to ATG |
| pAN6_ftsR_short_fw | **CTGCAGAAGGAGATATACATATG**TCAA TTGGTGTGGTACT | |
| pAN6_ftsR_rv | **AAAACGACGGCCAGTGAATT**TCAGTAT CCAAGCTGCTCGC | |
| pAN6_ftsR_Strep_rv | **CTGTGGGTGGGACCAGCTAGT**GTATCC AAGCTGCTCGCGA | with pAN6_ftsR_fw amplification of a PCR product without stop codon with overlaps for in-frame cloning of *ftsR* upstream of a Strep-tag® coding region for expression of FtsR-Strep in the NdeI/NheI-cut pAN6 vector |
| **pAN6-CDC7B_1201** | | |
| CDC7B_1201_pAN6_fw | **GCCTGCAGAAGGAGATATACAT**ATGAG TGCACTTCCGCAACG | PCR product with overlaps for cloning of the CDC7B_1201 gene (*ftsR* homolog) in the NdeI/EcoRI-cut pAN6 vector; template: *C. diphtheriae* ATCC27010 genomic DNA |
| CDC7B_1201_pAN6_rv | **AAAACGACGGCCAGTGAATT**TTAACGG TTCAGCTCATCGCGC | |

*(Continued)*

**Table 3.** *Continued*.

| Oligonucleotide | Sequence (5' → 3') and properties | Commentary |
|---|---|---|
| **pAN6-rv1828** | | |
| rv1828_pAN6_fw | **GCCTGCAGAAGGAGATATACAT**GTGAGCGCACCCGATAGCC | PCR product with overlaps for cloning of the rv1828 gene (*ftsR* homolog) in the NdeI/EcoRI-cut pAN6 vector; template: *M. tuberculosis* H37rv genomic DNA |
| rv1828_pAN6_rv | **AAAACGACGGCCAGTGAATT**TCAGCGGTGAAGAACGTCGCGAAC | |
| **Construction of pEC-*ftsR*** | | |
| ftsR_BamHI_fw | GATCGGATCCGCCTGCAGAAGGAGATATAC | PCR product contains BamHI and XbaI sites for cloning in pEC-XC99E vector cut with these enzymes; template: pAN6-*ftsR*, amplified fragment harbors RBS from pAN6 |
| ftsR_XbaI_rv | GATCTCTAGATCAGTATCCAAGCTGCTCGC | |
| pEC-check_fw | TAATCATCGGCTCGTATAATGTGTG | for sequencing of pEC derivatives |
| pEC-check_rv | GCTTCTGCGTTCTGATTTAATCTG | |
| **Construction of pJC1-P*ftsZ*-*venus*** | | |
| pJC1_PftsZ_fw | **AGCGACGCCGCAGGGGGAT**CTTCCTGCGGTTATTGCTGTA | amplification of the *ftsZ*-promoter region equipped with overlaps homologous to the pJC1-*venus*-term vector backbone cut with SpeI and to the *venus* coding region |
| PftsZ_venus_rv | **CTCCTCGCCCTTGCTCAC**CATTGTCGATGTCTCGCCTTTCG | |
| venus_fw | ATGGTGAGCAAGGGCGAGGAG | PCR product with overlap for cloning into BamHI-cut pJC1-*venus*-term; template: pJC1-*venus*-term |
| venus_pJC1_rv | **AAAACGACGGCCAGTACTAG**TTACTTGTACAGCTCGTCCATGC | |
| pJC1_check_fw | TGAAGACCGTCAACCAAAGG | for sequencing of pJC1-*venus*-term derivatives |
| pJC1_check_rv | TACGGCGTTTCACTTCTGAG | |
| **30-bp oligonucleotides for Electrophoretic Mobility Shift Assays** | | |
| ftsZ_oligo | CGCTACCCTCAACCTTTACTTTAGGGTTGT | |
| ftsZ_oligo_compl | ACAACCCTAAAGTAAAGGTTGAGGGTAGCG | |
| cg1081_oligo | GAAGCCACATGACATATGTCATGAAAATTA | |
| cg1081_oligo_compl | TAATTTTCATGACATATGTCATGTGGCTTC | |
| **Competition-EMSA** | | |
| Cy3-ftsZ_prom_rv | Cy3*TCTTGGCGAGGTAGTTGTTC | 5'-Cy3-label |
| ftsZ_prom_rv | TCTTGGCGAGGTAGTTGTTC | |
| ftsZ_prom250_fw | AGTTCCGGTTCACCCGTTTC | |
| ftsZ_prom500_fw | AGTGCTTCCTGCGGTTATTG | |
| ftsZ_prom250up_rv | CTACCCAGCCACTTTAGCGG | |
| **qPCR for determination of the copy number of cg0834 and cg0840** | | |
| qPCR_cg0834_fw | TTCGAATTTGCCTGCGGTTG | |
| qPCR_cg0834_rv | AAACCAACCTCGCATTCACC | |
| qPCR_cg0840_fw | TCTGACCAACCAGTTGCAAG | |
| qPCR_cg0840_rv | CCACAGTGCGTTTTTATGGC | |
| qPCR_recF_fw | GGCTATCTTGCGCATTTGTC | |
| qPCR_recF_rv | TCTCGGCCTTGATTAACAGC | |

### 3.3. Fluorescence microscopy

The *C. glutamicum* cells were centrifuged and suspended in PBS containing 100 ng/mL Hoechst 33342 dye to stain DNA and and 300 ng/mL Nile red (Sigma-Aldrich Chemie GmbH, Taufkirchen, Germany) to stain membranes. After 10 minutes of incubation in the dark at room temperature, samples were spotted onto a glass slide covered with a thin agarose layer (1% (w/v) in TAE buffer (40 mM Tris, 1 mM $Na_2EDTA$, 20 mM glacial acetic acid, pH 8) and analyzed using a Zeiss Axio Imager M2 microscope equipped with a Zeiss AxioCam MRm camera and a Plan-Apochromat 100x/1.40-numerical aperture phase-contrast oil immersion objective and AxioVision 4.8 software (Carl Zeiss Microscopy GmbH, Jena, Germany). Hoechst 33342 fluorescence was visualized with filter set 49 and Nile red with filter set 63 HE (both Carl Zeiss AG). *C. glutamicum* strains producing the FtsZ-Venus fusion protein were directly used for microscopy without further staining.

### 3.4. Purification of FtsR

FtsR was purified using *C. glutamicum* ATCC13032Δ*ftsR* carrying the plasmid pAN6-FtsR-Strep. The preculture was prepared using a single colony from a fresh BHI agar plate to inoculate 20 mL BHI with 2% (w/v) glucose and 25 µg/mL kanamycin and incubated at 30 °C and 120 rpm for 6-8 hours. The main culture (500 mL of the same medium in a 2 L baffled flask) was inoculated with 1 mL of the preculture. Due to the growth defect of the strain, the culture was incubated overnight at 30 °C and 90 rpm. On the following morning, expression of *ftsR* was induced by addition of 50 µM isopropyl β-D-1-thiogalactopyranoside (IPTG) and cultivation was continued for four hours at 30 °C and 120 rpm. Subsequently, the cells were harvested by centrifugation (4 °C, 30 min, 3399 *g*) and resuspended in buffer A (100 mM Tris-HCl, 100 mM NaCl, pH 7.5) supplemented with cOmplete Mini EDTA-free protease inhibitor cocktail tablets (Roche Diagnostics GmbH, Mannheim, Germany). Cell disruption was performed by five passages through a French® pressure cell using an HTU-Digi-F-Press (G. Heinemann Ultraschall- und Labortechnik, Schwaebisch Gmuend, Germany) at a pressure of 103.4 MPa (15,000 psi). Cell debris was removed by centrifugation for 20 minutes at 5300 *g* and 4 °C, followed by ultracentrifugation for one hour at 84,000 *g* and 4 °C. The supernatant was directly used for affinity chromatography using a Strep-Tactin®-Sepharose® column (IBA, Göttingen, Germany) with 1 mL bed volume, equilibrated with buffer W (50 mM Tris-HCl, 250 mM NaCl, pH 7.5). After the protein extract had passed, the column was washed three times with 15 mL buffer W and FtsR-Strep was eluted ten times with 1 mL buffer E (buffer W with 15 mM D-desthiobiotin (Sigma-Aldrich Chemie GmbH, Steinheim, Germany)). Aliquots of the elution fractions were analysed by SDS-PAGE (Laemmli, 1970) and Coomassie staining and the fractions containing FtsR-Strep were pooled and concentrated using Amicon® Ultra-4

Centrifugal Filter Devices with a 10 kDa cut-off (Merck Millipore Ltd., Carrigtwohill, Cork, Ireland). FtsR-Strep was further purified by gel filtration using a Superdex™ 200 Increase 10/300 GL column attached to an ÄKTA™ pure 25 system (GE Healthcare Bio-Sciences AB, Uppsala, Sweden). The column was equilibrated with buffer W and elution was performed with a flow rate of 0.6 mL/minute.

### 3.5. Electrophoretic mobility shift assays (EMSAs)

Two complementary single-stranded 30-bp oligonucleotides (see Table 3) covering the putative FtsR-binding motif in the *ftsZ* promoter region were annealed by heating the samples containing 10 µM Tris-HCl pH 8.0, 50 mM NaCl, 1 mM EDTA and 10 µM of each oligonucleotide to 95 °C for five minutes, followed by a slow cooling to room temperature. This double-stranded oligonucleotide (final concentration 1 µM) was incubated at room temperature for 30 minutes with increasing concentrations (0 to 8.5 µM) of freshly purified dimeric FtsR protein (see Figure 25) in binding buffer (10 mM Tris-HCl pH 7.5, 30 mM NaCl, 1.5 mM $Na_2EDTA$). For this purpose, FtsR protein was used directly after elution from the Strep-Tactin®-Sepharose® column, because its binding capability seemed to decrease during the purification process. A 30-bp fragment located in the cg1081 promoter region was used as negative control (see Table 3). After incubation, a suitable volume of 6-fold concentrated sample buffer (0.1% (w/v) xylene cyanol, 0.1% (w/v) bromophenol blue, 20% (v/v) glycerol in 1x TBE (89 mM Tris base, 89 mM boric acid, 2 mM $Na_2EDTA$)) was added and the samples were separated by native PAGE. using 15% (w/v) polyacrylamide gels in 1x TBE buffer. Electrophoresis was performed on ice at 180 V for one hour. Subsequently, the gel was stained with SYBR® Green I Nucleic Acid Gel Stain (Invitrogen, Ltd., Paisley, UK) and photographed.

The competition-EMSA was performed as described previously (Garcia-Nafria *et al.*, 2013). In brief, a 271-bp DNA fragment covering the *ftsZ* promoter region including the binding site was amplified using the oligonucleotides ftsZ_prom250_fw and Cy3-ftsZ_prom_rv to generate Cy3-labelled DNA or the oligonucleotides ftsZ_prom250_fw/ftsZ_prom_rv to generate unlabeled specific competitor DNA. A 260-bp DNA fragment further upstream in the *ftsZ* promoter was amplified using the oligonucleotide pair ftsZ_prom500_fw/ftsZ_prom250up_rv and used as unspecific competitor DNA. Purified FtsR protein was incubated with the DNA fragment(s) in a total volume of 10 µL binding buffer. After addition of loading buffer and separation by native PAGE on a 10% polyacrylamide gel, the gel was scanned using a Typhoon Trio™ scanner (GE Healthcare Bio-Sciences AB, Uppsala, Sweden).

### 3.6. Promoter studies with $P_{ftsZ}$ fused to *mVenus*

In order to analyze transcriptional regulation of *ftsZ* by FtsR *in vivo*, a DNA fragment covering the *ftsZ* promoter region and the native ribosomal binding site extending from position -494 to +3 with respect to the *ftsZ* translational start site was fused to a DNA sequence coding for the fluorescent protein mVenus and cloned into the pJC1 vector backbone (for details see Tables 2 and 3). Strains carrying their chromosomal *ftsZ* gene either unter control of its native promoter or under control of the *gntK* promoter were transformed with the resulting plasmid pJC1-$P_{ftsZ}$-*venus*. For complementation studies, the strains were additionally transformed with pEC-*ftsR* or the empty plasmid pEC-XC99E as control. Growth experiments were performed in the BioLector® system as described above, with additional monitoring of the *ftsZ* promoter activity by online measurement of mVenus fluorescence at an excitation wavelength of 508 nm and an emission wavelength of 532 nm.

### 3.7. Chromatin affinity purification with subsequent Sequencing (ChAP-Seq)

For ChAP-Seq experiments, *C. glutamicum* ATCC13032Δ*ftsR* pAN6-FtsR-Strep and the negative control *C. glutamicum* ATCC13032Δ*ftsR* pAN6 were cultivated as described above for FtsR purification with 10 µM instead of 50 µM IPTG. FtsR-Strep was purified as described above with the following alterations: after harvesting (15 minutes, 6371 *g*, 4 °C), washing with 40 mL PBS, and a second centrifugation step (15 minutes, 5525 *g*, 4 °C), the supernatant was discarded and the cells were suspended in 20 mL PBS containing 1% (w/v) formaldehyde and incubated at room temperature for 20 minutes, followed by addition of glycine to a final concentration of 125 mM and incubation for another 5 minutes at room temperature. The cells were washed twice with 40 mL buffer A and suspended in 20 mL buffer A with a suitable amount of cOmplete Mini EDTA-free protease inhibitor cocktail tablets and 5 mg of RNase A (both Roche Diagnostics GmbH, Mannheim, Germany). After cell disruption using a French® press as described above, the crude extract was transferred to a sonication vessel, placed in an ice bath and sonified three times for 30 seconds using a Branson Sonifier 250 (G. Heinemann Ultraschall- und Labortechnik, Schwaebisch Gmuend, Germany) with a pulse length of 40% and an intensity of one to shear the genomic DNA. The sonified crude extract was used for Strep-Tactin® affinity chromatography as described above. The FtsR-containing elution fractions were pooled, 1% (w/v) SDS was added, and the sample was incubated overnight at 65 °C, followed by Proteinase K treatment (final concentration 400 µg/mL) for 3 hours at 55 °C. The DNA in the sample was purified by phenol-chloroform-isoamyl alcohol extraction (Chomczynski & Sacchi, 2006), precipitated with ethanol and sodium acetate, washed with 70% (v/v) ethanol, dried, and dissolved in 50 µL deionized water. Sequencing of the DNA fragments and data evaluation were performed as described previously (Pfeifer *et al.*,

2016). Genomic binding sites of FtsR were defined to have a sequence coverage that is at least 50-fold above the average genome coverage determined for the negative control strain *C. glutamicum* ATCC13032 pAN6.

### 3.8. DNA microarrays

DNA microarray analysis was performed to compare the mRNA levels of the ATCC13032Δ*ftsR* mutant with the wild type. Therefore, cells were cultivated in 50 mL CGXII medium with 2% (w/v) glucose and harvested on ice in the exponential growth phase. RNA sample preparation, labelling, hybridization, and comparative transcriptome analysis were performed as described previously (Vogt *et al.*, 2014). The full data set of this experiment has been deposited in the NCBI Gene Expression Omnibus and can be found under the GEO accession number GSE107921.

### 3.9. DNA affinity purification and MALDI-ToF-MS analysis

To identify putative regulatory proteins binding to the *odhI* or the *ftsZ* promoter region, DNA affinity purification was performed. The promoter region of *odhI* or *ftsZ* was amplified by PCR (*odhI*: primers AP_PodhI_fw and AP_PodhI_rv_bio, product size 590 bp, DNA fragment extending from -201 to +62 with respect to the translational start site of *odhI; ftsZ*: primers AP_PftsZ_fw and AP_PftsZ_rv_bio, product size 404 bp, DNA fragment extending from -285 to +96 with respect to the translational start site of *ftsZ*). The resulting fragments were tagged with biotin by a second PCR using the biotinylated oligonucleotide biotin_oligo and the respective forward primer, AP_PodhI_fw or AP_PftsZ_fw. The PCR products were purified by size exclusion chromatography using a column with 8 mL Sephacryl™ S-400 High Resolution Chromatography Media (GE Healthcare Bio-Sciences AB, Uppsala, Sweden) as bed material and TE buffer (10 mM Tris-HCl, 1 mM $Na_2EDTA$, pH 7.6). Fractions containing the desired DNA fragment were pooled, concentrated to about 500 µL using an Eppendorf concentrator plus (Eppendorf AG, Hamburg, Germany), and precipitated with ethanol. The precipitate was dissolved in 50 µL TE buffer and the DNA concentration was measured with a Colibri Microvolume Spectrophotometer (Berthold Detection Systems GmbH, Pforzheim, Germany) to assure a minimal amount of 220 pmol biotinylated DNA, which was required for the following steps. The DNA affinity chromatography was performed using Dynabeads® M-280 Streptavidin (Life Technologies AS, Oslo, Norway) as described in Pfeifer *et al.* (2016). In brief, the biotinylated DNA was coupled to the beads and incubated with crude cell extract of *C. glutamicum* ATCC13032 cells that had been cultivated in glucose minimal medium and harvested in the exponential growth pase. After several washing steps, the proteins were eluted using buffer containing 2 M NaCl. The elution fractions were subjected to protein

precipitation with trichloroacetic acid (TCA, 10% (w/v) final concentration) and washed once with acetone. The precipitated protein was dissolved in 20 µL Tris-HCl buffer pH 7.5 and analysed by SDS-PAGE (Laemmli, 1970) using a 12% Mini-PROTEAN® TGX™ gel (Bio-Rad Laboratories, Inc., Hercules, CA, USA). The gel was stained with GelCode® Blue Stain Reagent (Thermo Fisher Scientific Inc., Rockford, IL, USA). Proteins enriched with the promoter region of *odhI* or *ftsZ* were identified by peptide mass fingerprinting after tryptic in-gel digestion of the excised bands of the polyacrylamide gel, followed by MALDI-ToF-MS using an Ultraflex III TOF/TOF mass spectrometer (Bruker Daltonics, Bremen, Germany) as described previously (Schaffer *et al.*, 2001, Koch-Koerfges *et al.*, 2012).

### 3.10. Genome re-sequencing

For genome re-sequencing, *C. glutamicum* ATCC13032 and three independent clones of *C. glutamicum* ATCC13032Δ*ftsR* were cultivated overnight in 20 mL BHI medium and the DNA was prepared as described previously (Pfeifer *et al.*, 2017). Genomic DNA was purified using the NucleoSpin® Microbial DNA Kit (MACHEREY-NAGEL GmbH & Co. KG, Düren, Germany). 4 µg were used for library preparation and indexing with the TruSeq® DNA PCR-Free Sample Preparation Kit (illumina Inc., San Diego, CA, USA). Quantifications of the resulting libraries were conducted using KAPA Library Quantification Kits (PEQLAB Biotechnologie GmbH, Erlangen, Germany) and were normalized for pooling. A MiSeq™ sequencing device (illumina Inc., San Diego, CA, USA) was used for paired-end sequencing with a read-length of two times 150 bases. Data analysis and base calling were accomplished with the illumina® instrument software and stored as fastq output files. The sequencing data obtained were imported into CLC Genomics Workbench (Qiagen Aarhus A/S, Aarhus, Denmark) for trimming and base quality filtering. The output was mapped to accession BX927147 as the *C. glutamicum* ATCC13032 reference genome. The resulting mappings were used for the quality-based single nucleotide polymorphisms (SNPs) variant detection with CLC Genomics Workbench. The detected SNPs were manually inspected for relevance.

### 3.11. Quantitative PCR

To elucidate how many copies of the genes cg0834 and cg0840 were present in the genome of different *C. glutamicum* strains, quantitative PCR (qPCR) was performed. For this purpose, genomic DNA was isolated as follows: selected strains were incubated overnight in 5 mL BHI medium and harvested by centrifugation. The cells were washed in TE buffer (10 mM Tris-HCl, 1 mM $Na_2EDTA$, pH 7.6), centrifuged again and suspended in 1 mL TE buffer with 15 mg lysozyme. After three hours incubation at 37 °C, 3 mL lysis buffer (10 mM Tris-HCl, 400 mM NaCl, 2 mM $Na_2EDTA$, pH 8.2), 220 µL 10% (w/v) SDS and 150 µL proteinase K

(20 µg/mL) were added to the suspension and mixed carefully, followed by an additional incubation for two hours at 60 °C. Two milliliter of saturated saline solution (about 6 M NaCl) was added and the samples were shaken vigorously until a white precipitate appeared, which was spun down by centrifugation at room temperature for for 30 minutes at 16000 *g*. The cleared supernatant was transferred into a fresh reaction tube and the DNA was precipitated by careful mixing with 2.5 volumes of ice-cold absolute ethanol. The DNA was removed from the tube with a Pasteur pipette whose tip was bent before using a Bunsen burner, dipped into 70% ethanol in a fresh Eppendorf tube for washing, and air-dried for a few seconds. Subsequently, the DNA was solubilized in 200 µL TE buffer by incubation at 4 °C overnight. For quality control, the isolated genomic DNA was analyzed by agarose gel electrophoresis. The DNA concentration was determined using a Colibri Microvolume Spectrophotometer (Berthold Detection Systems GmbH, Pforzheim, Germany) and adjusted to 50 ng/µL. For the qPCR experiment, PCR fragments for the generation of standard curves were amplified with the KAPA2G Fast ReadyMix PCR Kit (Kapa Biosystems, Boston, Massachusetts, United States) using chromosomal *C. glutamicum* DNA as template and the oligonucleotides given in Table 3. The gene *recF* was used as reference gene, as it has proven to be well suitable in previous projects. The primers were designed with the Primer3plus online tool (Untergasser *et al.*, 2012), using the standard settings for qPCR and an annealing temperature of 60 °C. The amplified fragments were checked for purity by agarose gel electrophoresis. The standards were used in concentrations of 10 pg/µL to 100 ag/µL in a gradient cycle protocol to determine the optimal annealing temperature for the qPCR experiment. The setup of the cycling protocol was as following (see Table 4): three minutes pre-incubation at 95 °C (step 1), five seconds denaturation at 95 °C (step 2), and 25 seconds elongation at a temperature-gradient from 55.1 °C to 66.9 °C (step 3), 40 times repetition of steps two and three, followed by a melting curve analysis (step 4) from 60 °C to 95 °C, with $\Delta T$ = 1 °C for every 6 seconds.

**Table 4: Determination of the copy number of cg0834 and cg0840**. The qPCR program used for the determination of the copy number of cg0834 and cg0840 is shown.

| step # | °C | min:sec | go to step | loops |
|---|---|---|---|---|
| 1 | 95 | 3:00 | | |
| 2 | 95 | 0:05 | | |
| 3 | 55.1 to 66.9 | 0:30 | 2 | 39 |
| 4 | --- | melting curve analysis, 60 °C to 95 °C, 6 s with $\Delta T$ = 1 °C | | |

Again, agarose gel electrophoresis of the PCR products was performed. Based on this experiment, an annealing temperature of 59 °C was chosen for the qPCR experiment. The

qPCR reaction was performed using the innuMIX qPCR MasterMix SyGreen (Analytik Jena, Jena, Germany) and the qTOWER 2.2 (Analytik Jena, Jena, Germany), and the procotol stated in Table 4, but with a constant temperature of 59 °C in step three. The reaction mix contained 10 µL master mix (2x), 1 µL primer 1 (10 µM), 1 µL primer 2 (10 µM), 2 µL template (50 ng/µL) and 6 µL $H_2O$. The data were analyzed using the program qPCRsoft 3.1 (Analytik Jena, Jena, Germany) and the ΔΔCt method (Livak & Schmittgen, 2001).

### 3.12. Coulter counter measurements

Bacterial size distribution was determined *via* the Coulter principle using a MultiSizer 3 (Beckman Coulter, Krefeld, Germany) particle counter equipped with a 30 µm capillary. Briefly, for each measurement the bacterial cells at an $OD_{600}$ of about 0.1 were 20-fold diluted in CASYton assay buffer (Schärfe System GmbH, Reutlingen, Germany). Each sample (100 µL) was analyzed twice in the volumetric measurement mode. The data were visualized and extracted using the Beckman Coulter Multisizer 3 software package.

# 4. Results

## 4.1. Phylogenetic conservation of *odhI* (cg1630) and adjacent genes

The *odhI* (cg1630) gene and its immediate genomic vicinity including the three downstream genes *ftsR* (cg1631), cg1632, and cg1633 were found to be highly conserved within Actinobacteria (Figure 4).

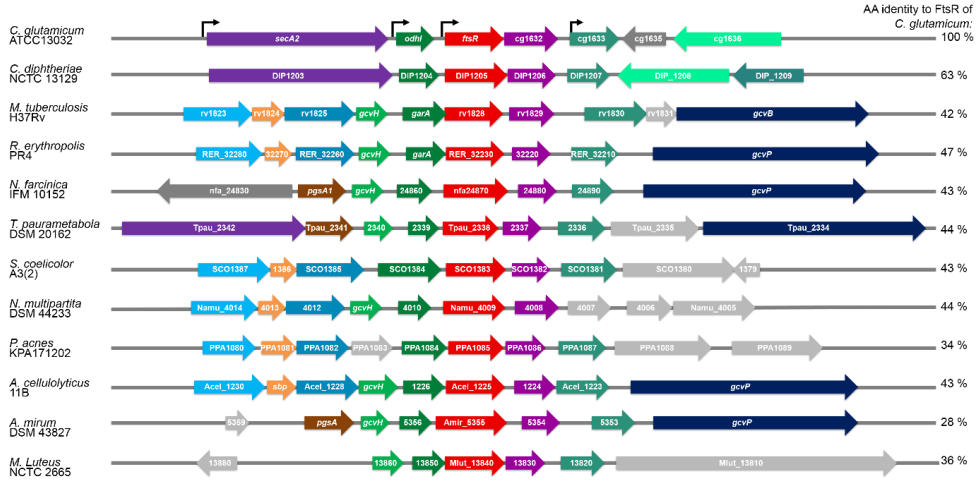


**Figure 4. Phylogenetic conservation of *odhI* (cg1630) and adjacent genes.** The *ftsR* (cg1631) gene and its homologs in different actinobacterial species of various genera are shown in red. Neighboring homologous genes are colored alike, whereas grey arrows indicate genes that are not conserved in the gene cluster. The black arrows indicate transcriptional start sites determined with RNA-Seq for *C. glutamicum* by Pfeifer-Sancar *et al.* (2013). Note that the cluster comprising *ftsR*, its upstream gene *odhI/garA*, and the two downstream genes encoding a bifunctional nuclease and a MerR-type transcriptional regulator is strongly conserved. The figure was prepared based on data of MicrobesOnline (Alm *et al.*, 2005) and ERGO (Overbeek *et al.*, 2003). The amino acid sequence identity of the FtsR homologs to *C. glutamicum* FtsR is given on the right side and was derived from NCBI BLAST (Altschul *et al.*, 1990). For lack of space, some locus tag prefixes were omitted in short genes. Gene lengths are approximately to scale. The full species names are as following: *Corynebacterium glutamicum, Corynebacterium diphtheriae, Mycobacterium tuberculosis, Rhodococcus erythropolis, Nocardia farcinica, Tsukamurella paurometabola, Streptomyces coelicolor, Nakamurella multipartita, Propionibacterium acnes, Acidothermus cellulolyticus, Actinosynnema mirum, Micrococcus luteus*.

The *odhI* gene encodes the 2-oxoglutarate dehydrogenase inhibitor protein OdhI, which acts as a phosphorylation-dependent switch, controlling the activity of the 2-oxoglutarate dehydrogenase complex (Niebisch *et al.*, 2006, Krawczyk *et al.*, 2010, Raasch *et al.*, 2014). The homologous protein of mycobacteria is GarA (Ventura *et al.*, 2013). The gene *ftsR* (cg1631) of *C. glutamicum* ATCC13032 encodes a protein of 252 amino acids (calculated mass 27.23 kDa), which was annotated as a transcriptional regulator of the MerR family due to the sequence similarity of the N-terminal region of FtsR to other members of the MerR family. The gene cg1632 encodes a putative bifunctional nuclease having both DNase and RNase

activity (PFAM PF02577). In *M. tuberculosis*, the homologous protein Rv1829 has been described as a carbon monoxide resistance gene (Zacharia *et al.*, 2013). cg1633 encodes another yet uncharacterized transcriptional regulator of the MerR family. Previous RNA-Seq analysis indicated that these neighboring genes are co-transcribed in various combinations: cg1629-cg1633 was annotated as primary operon and cg1630-cg1633 and cg1631-cg1633 as sub-operons (Pfeifer-Sancar *et al.*, 2013) (Figure 4). The genomic region upstream of *odhI* (cg1630) and downstream of cg1633 varies in different Actinobacteria.

An amino acid sequence alignment of FtsR homologs of different actinobacterial species revealed that especially the N-terminal part is highly conserved (Figure 5). Two features of the alignment are conspicuous, which are the variable length of the N-termini upstream of the highly conserved region starting with the sequence MSIG and the variable length of the region linking the N-terminal DNA-binding domain and the C-terminal regulatory domain. Notably, most of the other sequences are considerably shorter than *C. glutamicum* FtsR and indeed, a putative alternative start codon was found 28 amino acids downstream of the annotated start codon. However, complementation experiments with the two variants showed that the shorter protein version features a lower degree of complementation suggesting that the longer version is the protein natively synthesized *in vivo* (Figure 7).

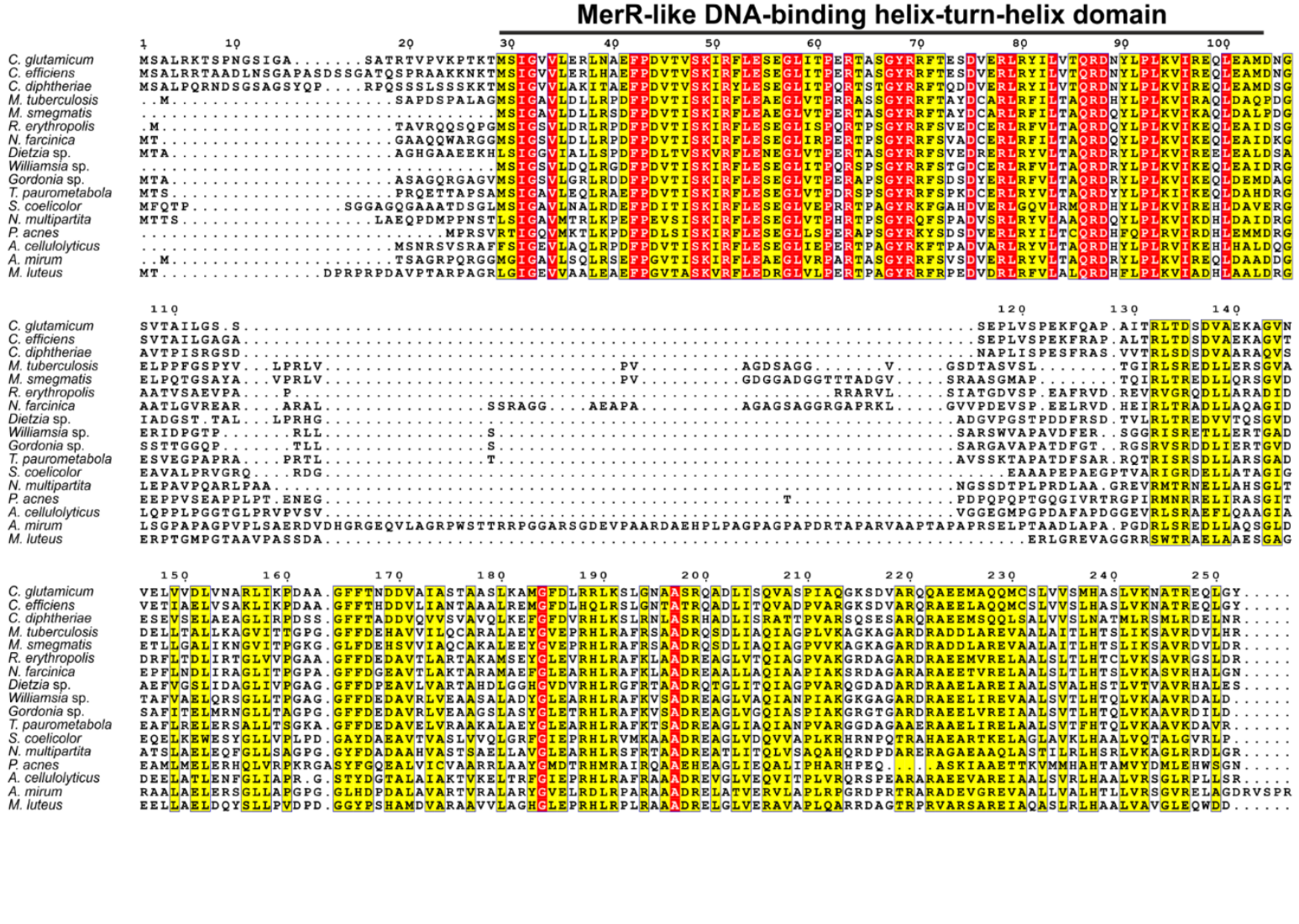
MerR-like DNA-binding helix-turn-helix domain
C. glutamicum
C. efficiens
C. diphtheriae
M. tuberculosis
M. smegmatis
R. erythropolis
N. farcinica
Dietzia sp.
Williamsia sp.
Gordonia sp.
T. paurometabola
S. coelicolor
N. multipartita
P. acnes
A. cellulolyticus
A. mirum
M. luteus

**Figure 5. Alignment of *C. glutamicum* FtsR and homologous proteins of other *Actinobacteria*.** The alignment was prepared using Clustal Omega (Sievers *et al.*, 2011) and edited using ESPript 3.0 (Robert & Gouet, 2014). Residues shown in yellow are at least 70% identical and residues indicated in red are fully conserved. The following proteins were aligned: *Corynebacterium glutamicum* FtsR (Cg1631); *Corynebacterium efficiens* CE1574; *Corynebacterium diphtheriae* DIP_1205; *Mycobacterium tuberculosis* Rv1828; *Mycobacterium smegmatis* MSMEG_3646; *Rhodococcus ruber* CS378_RS03820; *Nocardia farcinica* NFA_24870; *Dietzia* sp. H483_RS33310; *Williamsia* sp. ASG12_08425; *Gordonia effuse* GOEFS_105_00530; *Tsukamurella paurometabola* Tpau_2338; *Streptomyces coelicolor* SCO1383; *Nakamurella multipartite* NAMU_RS19840; *Propionibacterium acnes* PPA_RS05480; *Acidothermus cellulolyticus* ACEL_RS06295; *Actinosynnema mirum* AMIR_RS26540; *Micrococcus luteus* CRM77_RS01150.

### 4.2. Deletion of *ftsR* affects growth behavior

The possibility that *odhI* might be regulated on the transcriptional level seemed logical since it is located upstream of the two genes *ftsR* and cg1633 (Figure 4), which encode two transcriptional regulators. To elucidate if any of the three genes located downstream of *odhI* are involved in its regulation and to investigate their physiological role, in-frame deletion mutants of the genes *ftsR*, cg1632, and cg1633 were constructed and analyzed with respect to their growth behavior. Remarkably, the *ftsR* deletion strain grew significantly slower and to a lower final cell density (backscatter) compared to the wild type in CGXII minimal medium with glucose as carbon source, whereas the results for strains ∆cg1632 and ∆cg1633 were comparable with the wild type (Figure 6a).

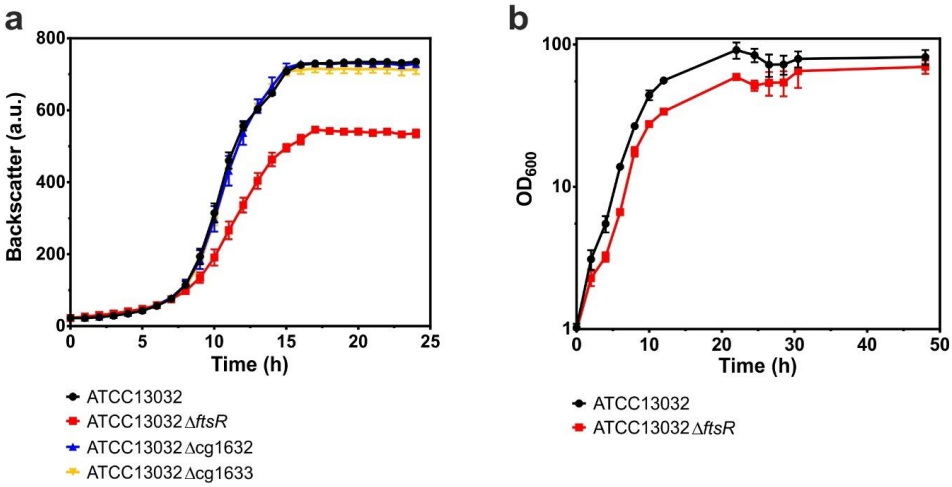


**Figure 6. Growth behavior of *C. glutamicum* ATCC13023 and *C. glutamicum* ATCC13023 with deleted *ftsR*, cg1632, or cg1633 in a BioLector microcultivaton system (a) and of strain Δ*ftsR* in shaking flasks (b).** The cells were first cultivated in BHI medium followed by two consecutive cultivations in CGXII minimal medium with 4% (w/v) glucose as carbon source. Means and standard deviations of three biological replicates of the second CGXII culture are presented.

For further investigation of the growth defect of the Δ*ftsR* mutant, an additional growth experiment for the determination of the growth rate in comparison to the wild type was performed in shaking flasks (Figure 6b). The mutant showed a growth rate of 0.32 ± 0.01 $h^{-1}$, which equals an 20% slower growth in comparison to the wild type (μ = 0.40 ± 0.00 $h^{-1}$).

### 4.3. Complementation experiments with *C. glutamicum* ATCC13032Δ*ftsR*

The consequences of *ftsR* overexpression in the wild type strain ATCC13032 were tested using the plasmid pAN6-*ftsR*, in which *ftsR* expression is controlled by the *tac* promoter. The promoter is known to be leaky in *C. glutamicum* and allows basal expression of the target gene

also in the absence of the inducer IPTG (Baumgart *et al.*, 2016). To confirm that the growth defect of the Δ*ftsR* mutant is caused by the *ftsR* deletion rather than by secondary mutations that might have occurred during construction of the mutants or polar effects on downstream genes, complementation experiments were performed with the plasmid pAN6-*ftsR* and two variants thereof. Without IPTG and with IPTG concentrations up to 10 µM, growth of ATCC13032 pAN6-*ftsR* was comparable to the reference strain ATCC13032 pAN6. However, when 100 µM IPTG was added, growth of ATCC13032 pAN6-*ftsR* was strongly inhibited (Figure 7). Thus, both the absence and the overexpression of *ftsR* had a negative effect on the growth performance. Plasmid pAN6-*ftsR*-Strep encodes an FtsR variant with a carboxyterminal linker sequence (AS) followed by a Strep-tag-II (WSHPQFEK). Plasmid pAN6-*ftsR*-short encodes an FtsR variant shortened by 28 amino acids at the N-terminus, which now consist of the amino acids MSIGV. An alternative start codon was found here, based on the alignment reported above (Figure 5). As shown in Figure 7, the growth defect of ATCC13032Δ*ftsR* pAN6 could partially be reversed by pAN6-*ftsR* and pAN6-*ftsR*-Strep, but not by pAN6-*ftsR*-short. This suggests that the longer FtsR variant composed of 256 amino acid residues represents the active protein and that its function is not disturbed by a C-terminal Strep-tag-II.

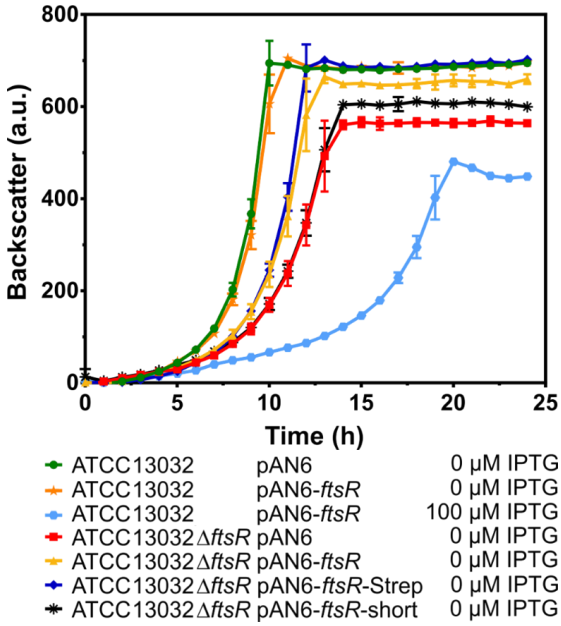


**Figure 7. Growth of an *ftsR* overexpressing strain and complementation of the Δ*ftsR* mutant with FtsR variants including an N-terminally shortened protein and a protein with a C-terminal Strep-tag-II.** The strains were pre-cultivated first in BHI medium and then in CGXII medium with 2% (w/v) glucose, followed by main cultivation in the same medium. All media were supplemented with kanamycin (25 µg/mL) and IPTG as indicated. Means and standard deviations of two biological replicates of the second CGXII culture are presented.

### 4.4. The morphological phenotype of *C. glutamicum* caused by *ftsR* deletion and overexpression

Phase-contrast and fluorescence microscopy with staining of DNA and membranes revealed strong morphological differences to wild type cells for both the Δ*ftsR* mutant and for the *ftsR* overexpressing strain (Figure 8, Figure 9).

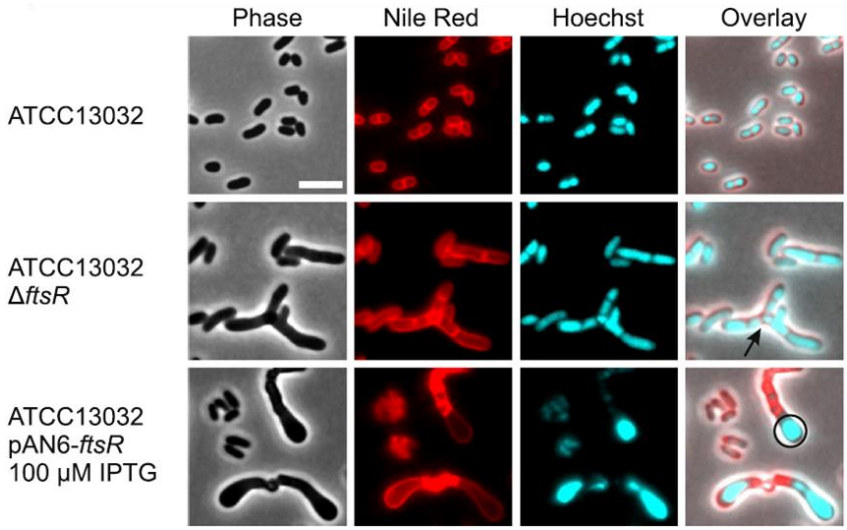


**Figure 8. Microscopic pictures of cells in the stationary phase**. To visualize membranes and DNA, cells were stained with Nile red and Hoechst 33342, respectively. The arrow points towards a branched cell and the circle indicates a high DNA concentration at the cell pole. The scale bar represents 5 µm.

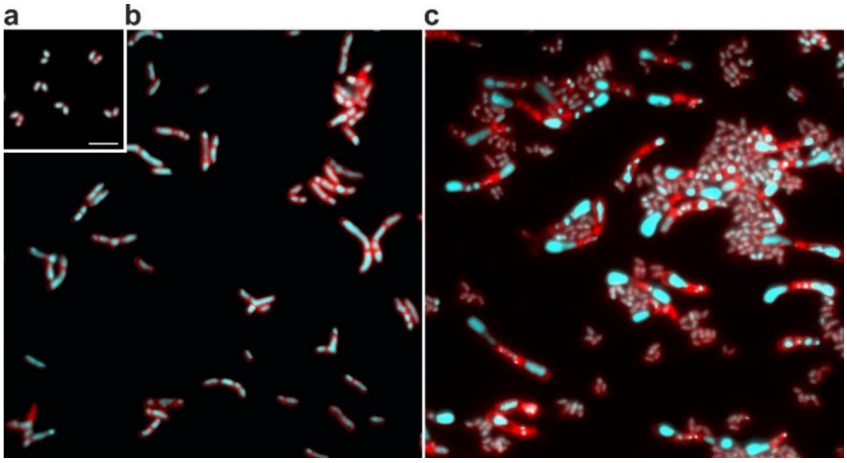


**Figure 9. Morphology of *C. glutamicum* ATCC13032 (a), ATCC13032Δ*ftsR* (b), and ATCC13032 pAN6-*ftsR* (c).** The cells were first cultivated in BHI medium followed by two consecutive cultivations in CGXII minimal medium with 2% (w/v) glucose as carbon source. For the plasmid-based overexpression (c), kanamycin (25 µg/mL) and IPTG (100 µM) were added. Fluorescence microscopy of stationary cells was performed. DNA was stained with Hoechst 33342 (cyan) and membranes with Nile red (red) as described in the Methods section. The scale bar is 5 µm.

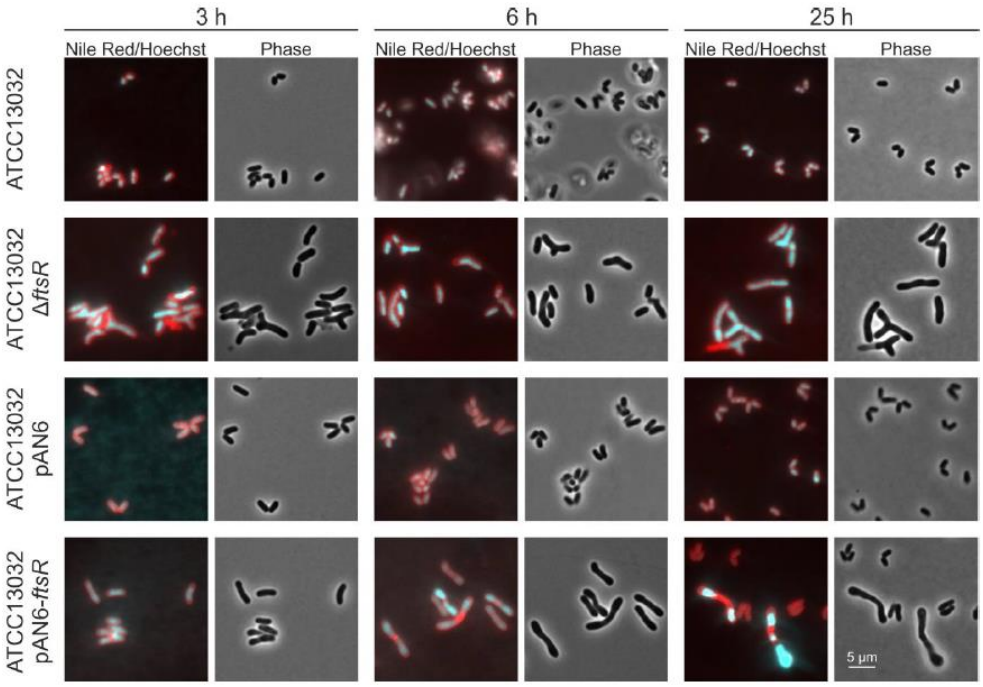


**Figure 10. Morphology of *C. glutamicum* ATCC13032, ATCC13032Δ*ftsR*, ATCC13032 pAN6, and ATCC13032 pAN6-*ftsR* in different growth phases.** See description of Figure 9.

Different cell morphologies were apparent both in the exponential and stationary growth phase; while the phenotype of the Δ*ftsR* mutant did not change much along the cultivation, the phenotype of the overexpression strain became more severe over time (Figure 10). This could be due to an accumulation of FtsR in the cells resulting from the overexpression. The Δ*ftsR* cells were elongated and some of them were branched (Figure 8, black arrow). Several cells had multiple septa at different positions in the cell. Overexpression of *ftsR* led to enlarged cells with DNA accumulated at the poles (Figure 8, black circle). These cells also contained additional septa, which were mostly located in the middle of the cells. However, only a fraction of the cells was enlarged, whereas the others remained small and inconspicuous. It should be noted that the small cells appear to be DNA-free in some pictures because the brightness was adjusted to the cells with the high DNA concentration. All small cells of the *ftsR* overexpression strain seem to contain similar DNA amounts comparable to the wild type. The reason for this population heterogeneity is yet unknown. It could result from different FtsR levels in the cells due to heterogeneous induction of pAN6-based *ftsR* expression, as previously reported for *eyfp* expression by the pAN6 parent plasmid pEKEx2 (Kortmann *et al.*, 2015). The observed morphological changes caused by *ftsR* deletion and overexpression, in particular the presence of multiple septa within a single cell that did not lead to a separation of the cells, hint toward a function of FtsR in cell division and to a potential role in the regulation of *ftsZ* expression.

To further evaluate the changes in cell size or rather cell volume, we analyzed the strains using a Coulter counter in the volumetric measurement mode. Figure 11 shows the size distribution at three different time points during cultivation (3 h, 6 h, 24 h). For the Δ*ftsR* strain in comparison to the wild type, the whole population was shifted to larger cell sizes at all time points and formed a single broad peak. The population of the *ftsR* overexpressing strain formed two peaks of different sizes at 24 h, differing weakly or strongly in size from wild type carrying pAN6. As mentioned above, this could be due to heterogeneous expression from plasmid pAN6-*ftsR*. Overall, these measurements confirmed that the *ftsR* deletion strain comprises a homogeneous population of cells with increased size in different growth phases. In contrast, the strain overexpressing *ftsR* showed a homogeneous population of enlarged cells in the exponential growth phase, and two populations with cells of different sizes in the stationary phase. These results coincide with the cell size distribution observed by microscopy.

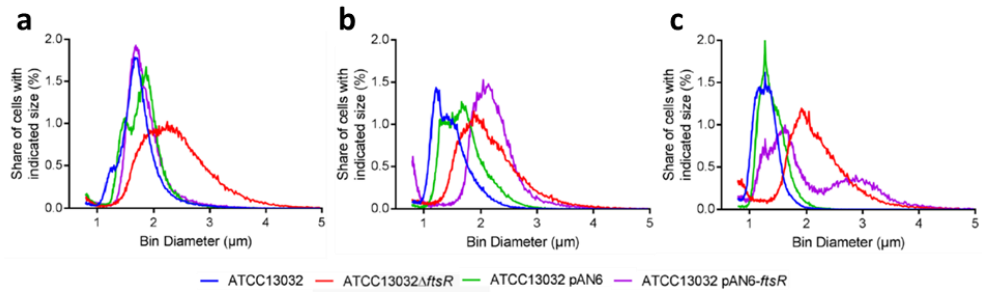


**Figure 11. Coulter counter measurements in the exponential phase at 3 h (a) and 6 h (b) and in the stationary phase at 24 h (c).** The cells were diluted to an $OD_{600}$ of ~0.1 and analyzed in the volumetric measurement mode. The cells were assigned to bins according to their size. The bin diameter is proportional to the cell size. Plotted are mean values of two technical replicates.

## 4.5. Transcriptome comparison of the Δ*ftsR* mutant with its parent wild type

In order to elucidate whether *odhI* is transcriptionally controlled by the regulator FtsR and to investigate global gene expression in general to get an impression of the FtsR regulon, transcriptome analysis of the ATCC13032Δ*ftsR* mutant and the parent wild type was performed using DNA microarrays and RNA isolated from cells cultivated in glucose minimal medium and harvested in the exponential growth phase. In total, 52 genes had an at least two-fold altered mRNA level, of which 34 genes showed a ≥ 2-fold increased mRNA level and 18 genes a ≥ 2-fold decreased mRNA level in the Δ*ftsR* mutant. However, expression of *odhI*, *secA2*, cg1632, and cg1633 was not significantly altered in the Δ*ftsR* mutant (Table 5), argueing against transcriptional regulation of *odhI* by FtsR.

**Table 5: mRNA ratios of the *secA2* operon in a Δ*ftsR* deletion mutant**. The transcriptome analysis of ATCC13032Δ*ftsR* versus ATCC13032 (three biological replicates) of the genes located together in an operon with *odhI* using DNA microarrays are shown.

| locus tag | gene name | annotated function | mRNA ratio | p-value |
|---|---|---|---|---|
| cg1629 | *secA2* | preprotein translocase subunit SecA2 | 0.59 | 0.073 |
| cg1630 | *odhI* | oxoglutarate dehydrogenase inhibitor protein | 1.09 | 0.332 |
| cg1631 | *ftsR* | putative transcriptional regulator, MerR family | 0.02 | 0.004 |
| cg1632 | --- | putative secreted protein | 0.52 | 0.101 |
| cg1633 | --- | putative transcriptional regulator, MerR family | 1.03 | 0.434 |

Both the upregulated and the downregulated genes covered a broad and heterogeneous range of cellular functions (Table 6). Within the group of genes showing a decreased mRNA level, the *ftsZ* gene with an mRNA ratio of 0.35 was the most prominent one. The group of upregulated genes included *oppC* and *oppD* encoding components of a putative ABC-type peptide transport system, four *prp* genes involved in propionate or propionyl-CoA catabolism, seven genes located in the CGP3 prophage region, which in total extends from cg1890 to cg2071, and a cluster of eight neighboring genes (cg0830-cg0838) including those for an ABC-type trehalose uptake system.

**Table 6: Transcriptome analysis of the *C. glutamicum* strains ATCC13032Δ*ftsR* and ATCC13032 using DNA microarrays.** Three biological replicates of the experiment were performed, and genes are listed whose average mRNA ratio was increased or decreased at least 2-fold and a p-value ≤0.05.

| Locus tag | Gene name | Annotated function | mRNA ratio | p-value |
|---|---|---|---|---|
| cg0027 | | putative transcriptional regulator, MarR-family | 2.39 | 0.034 |
| cg0078 | | putative membrane protein | 2.06 | 0.029 |
| cg0256 | | putative protein, conserved | 2.32 | 0.047 |
| cg0274 | *maoA* | putative oxidoreductase, possibly involved in oxidative stress response | 2.51 | 0.048 |
| cg0292 | *tnp16a* | transposase | 2.00 | 0.032 |
| cg0661 | | hypothetical protein, conserved | 2.33 | 0.040 |
| cg0760 | *prpB2* | 2-methylisocitrate lyase, propionate catabolism | 4.20 | 0.017 |
| cg0762 | *prpC2* | 2-methylcitrate synthase, propionate catabolism | 4.22 | 0.007 |
| cg0797 | *prpB1* | 2-methylisocitrate lyase | 2.03 | 0.018 |
| cg0798 | *prpC1* | 2-methycitrate synthase | 2.01 | 0.007 |
| cg0824 | *tnp5a* | transposase | 2.44 | 0.003 |
| cg0830 | | putative membrane protein | 3.22 | 0.045 |
| cg0831 | *tusG* | ABC-type trehalose uptake system, permease | 2.89 | 0.029 |
| cg0832 | *tusF* | ABC-type trehalose uptake system, permease | 2.90 | 0.026 |
| cg0833 | | putative membrane protein involved in trehalose uptake | 2.63 | 0.030 |
| cg0834 | *tusE* | ABC-type trehalose uptake system, binding protein | 2.98 | 0.039 |
| cg0836 | | hypothetical protein | 3.30 | 0.027 |

*(Continued)*

**Table 6.** *Continued.*

| Locus tag | Gene name | Annotated function | mRNA ratio | p-value |
|---|---|---|---|---|
| cg0837 | | hypothetical protein | 3.28 | 0.021 |
| cg0838 | | putative helicase | 4.61 | 0.026 |
| cg1942 | | putative secreted protein CGP3 region | 2.05 | 0.015 |
| cg1969 | | hypothetical protein CGP3 region | 2.03 | 0.026 |
| cg1971 | | hypothetical protein CGP3 region | 2.41 | 0.025 |
| cg1995 | | hypothetical protein CGP3 region | 2.23 | 0.042 |
| cg2009 | | putative CLP-family ATP-binding protease, CGP3 region | 2.22 | 0.047 |
| cg2065 | | putative superfamily II DNA or RNA helicase, CGP3 region | 2.83 | 0.021 |
| cg2066 | | putative low-complexity protein | 2.02 | 0.036 |
| cg2183 | *oppC* | ABC-type peptide transport system, permease component | 8.82 | 0.015 |
| cg2184 | *oppD* | ABC-type peptide transport system, ATPase component | 17.99 | 0.005 |
| cg2461 | *tnp4a* | transposase | 2.23 | 0.031 |
| cg2570 | *dctP* | C4-dicarboxylate-binding protein, TRAP-family | 2.10 | 0.018 |
| cg2644 | *clpP2* | ATP-dependent Clp protease proteolytic subunit | 2.14 | 0.006 |
| cg2915 | | hypothetical protein | 2.61 | 0.021 |
| cg3181 | | putative secreted protein | 2.30 | 0.046 |
| cg3266 | *tnp5c* | transposase | 2.13 | 0.001 |
| cg0370 | | putative ATP-dependent RNA helicase, DEAD/DEAH box-family | 0.50 | 0.015 |
| cg0789 | *amiA* | putative N-acyl-L-amino acid amidohydrolase | 0.48 | 0.003 |
| cg0812 | *dtsR1 (accD1)* | acetyl/propionyl-CoA carboxylase, β chain, mycolic acid biosynthesis | 0.47 | 0.025 |
| cg0896 | | putative membrane protein | 0.20 | 0.032 |
| cg0980 | *mepB* | putative secreted protein related to metalloendopeptidase | 0.49 | 0.001 |
| cg1037 | *rpf2* | resuscitation promoting factor, secreted protein | 0.42 | 0.015 |
| cg1076 | *glmU* | putative UDP-N-acetylglucosamine pyrophosphorylase | 0.49 | 0.014 |
| cg1290 | *metE* | 5-methyltetrahydropteroyltriglutamate-homocysteine methyltransferase, essential for methionine biosynthesis | 0.39 | 0.036 |
| cg1336 | | putative secreted protein | 0.46 | 0.037 |
| cg1370 | | hypothetical protein, conserved | 0.39 | 0.026 |
| cg1631 | *ftsR* | transcriptional activator of *ftsZ*, MerR-family | 0.02 | 0.004 |
| cg2118 | *fruR* | transcriptional regulator of sugar metabolism, presumably fructose responsive, DeoR-family | 0.36 | 0.002 |
| cg2366 | *ftsZ* | cell division protein FtsZ | 0.35 | 0.019 |
| cg2477 | | hypothetical protein, conserved | 0.24 | 0.007 |
| cg2519 | | hypothetical protein, conserved | 0.49 | 0.02 |
| cg2853 | | putative protein fragment, conserved | 0.45 | 0.006 |
| cg3186 | *cmt2* | trehalose corynomycolyl transferase | 0.49 | 0.049 |
| cg3335 | *malE (mez)* | malic enzyme ($NADP^+$) | 0.49 | 0.002 |

## 4.6. Genome re-sequencing of the *ftsR* deletion mutant and amplification of the trehalose cluster

To investigate whether the phenotype of the Δ*ftsR* mutant and the inability to fully complement it is solely caused by the respective deletion and not partially the result of secondary mutations, genome re-sequencing of three individual clones and comparison with the ATCC13032 wild type strain (reference genome published under accession number BX927147) was performed. Only four prominent single nucleotide polymorphisms (SNPs) could be detected (Table 7): a silent mutation each in cg1158 and cg2704, a mutation in the intergenic region between cg2057 and cg2058 (which are located in the CGP3 region), and a mutation in cg2030 (also located in the CGP3 region), causing a change from methionine to threonine. Presumably, these SNPs are not responsible for causing the abovementioned effects.

**Table 7. Single nucleotide polymorphisms in ATCC13032Δ*ftsR* strains.** The table shows the four SNPs discovered by genome re-sequencing of three individual ATCC13032Δ*ftsR* mutants.

| position | locus tag | annotated function | original base | new base |
|---|---|---|---|---|
| 1074171 | cg1158 | putative secreted protein | T | C |
| 1921443 | cg2030 | hypothetical protein in CGP3 region | A | G |
| 1947024 | cg2057-cg2058 | intergenic region in CGP3 region | C | T |
| 2577235 | cg2704 | putative ABC-type sugar transporter, permease subunit | C | T |

The transcriptome comparison of ATCC13032Δ*ftsR* with ATCC13032 revealed 2.6- to 4.6-fold increased mRNA levels of the genomic region encompassing cg0830-cg0838 in the Δ*ftsR* mutant (Table 8). Interestingly, two of the nine genes annotated in this region are oriented in the opposite direction than the other seven, but nevertheless also showed an increased mRNA level. Although this could be a consequence of a similar regulation of the nine genes, it might also result from an amplification event leading to an increased DNA copy number and therefore increased mRNA levels. We therefore analyzed the sequenced genome of the three clones of strain ATCC13032Δ*ftsR* in this respect. For all three clones, this analysis indeed revealed an amplification event. As shown in Table 8, the sequence coverage of the DNA region from cg0828 to cg0840 was 5- to 7-fold (mean value 6.36 ± 0.57) higher than that of the residual genome in all three clones. When looking at the DNA microarray data, it becomes evident that the mRNA levels of cg0828, cg0829, cg0839, and cg0840 were also 2.5- to 3.4-fold increased in the Δ*ftsR* mutant, but since the p-value was above 0.05, they were not included in Table 6. The amplified DNA region includes the genes cg0831 and cg0835, which enocde the trehalose uptake system TusFGK$_2$-E (Henrich, 2011). Trehalose is a component of mycolates, which are important building blocks of the cell envelope of the Corynebacteriales (Tropis *et al.*, 2005).

**Table 8. Amplification of the DNA region encompassing cg0828-cg0840 in the ATCC13032Δ*ftsR* mutants.** Gene coverage values obtained from genome re-sequencing as well as data from the abovementioned transcriptome analysis are presented.

| Locus tag | Gene name | Annotated function | Gene coverage ATCC 13032 | Gene coverage ATCC13032Δ*ftsR* | | | mRNA ratio Δ*ftsR*/ WT | p-value |
|---|---|---|---|---|---|---|---|---|
| | | | | clone 1 | clone 2 | clone 3 | | |
| cg0819 | --- | hypothetical protein | 0.99 | 1.07 | 1.14 | 1.01 | 0.97 | 0.45 |
| cg0820 | *purE* | phosphoribosyl-aminoimidazole carboxylase, catalytic subunit | 1.1 | 1.08 | 1.2 | 1.03 | 0.93 | 0.39 |
| cg0821 | --- | hypothetical protein, conserved | 1.07 | 1.07 | 0.92 | 1.01 | 0.90 | <0.01 |
| cg0822 | --- | hypothetical protein, conserved | 1.02 | 1.03 | 0.94 | 0.99 | 1.38 | 0.02 |
| cg0823 | *ntaA* | nitrilotriacetate mono-oxygenase component A | 1.06 | 0.89 | 0.99 | 0.93 | 0.85 | 0.32 |
| cg0824 | --- | tnp5a, transposase | 0.98 | 1.5 | 1.57 | 1.5 | 2.44 | <0.01 |
| cg0825 | *fabG* | 3-ketoacyl-acyl-carrier-protein reductase | 0.9 | 0.91 | 0.95 | 0.98 | 1.08 | 0.22 |
| cg0826 | --- | putative membrane protein | 1.1 | 1.32 | 1.34 | 1.21 | 0.91 | 0.33 |
| cg0827 | --- | hypothetical protein | 0.99 | 1.07 | 1.14 | 1.01 | --- | --- |
| **cg0828** | --- | putative dihydrofolate reductase | 0.97 | 5.24 | 6.49 | 6.22 | 3.41 | 0.05 |
| **cg0829** | --- | putative lactoylglutathione lyase or related lyase, glyoxylase-family, conserved | 0.94 | 5.95 | 7 | 7.09 | 2.91 | 0.06 |
| **cg0830** | --- | putative membrane protein | 0.99 | 5.6 | 6.42 | 6.48 | 3.22 | 0.05 |
| **cg0831** | *tusG* | trehalose uptake system, ABC-type, permease protein | 1.03 | 5.42 | 5.93 | 6.23 | 2.89 | 0.03 |
| **cg0832** | *tusF* | trehalose uptake system, ABC-type, membrane spanning protein | 0.96 | 5.46 | 5.68 | 6.18 | 2.90 | 0.02 |
| **cg0833** | --- | putative membrane protein, involved in trehalose uptake, conserved | 1.01 | 6.18 | 6.74 | 7.34 | 2.63 | 0.03 |
| **cg0834** | *tusE* | trehalose uptake system, ABC-type, bacterial extracellular solute-binding protein | 1.1 | 5.9 | 6.35 | 7.02 | 2.98 | 0.04 |
| **cg0835** | *tusK* (*msiK2*) | trehalose uptake system, ABC-type component | 1.03 | 5.51 | 6.28 | 6.72 | 2.27 | 0.06 |
| **cg0836** | --- | hypothetical protein | 0.98 | 5.72 | 6.4 | 6.74 | 3.30 | 0.03 |
| **cg0837** | --- | hypothetical protein | 1.03 | 6.12 | 6.28 | 6.73 | 3.28 | 0.02 |
| **cg0838** | --- | putative helicase | 1.05 | 6.4 | 7.1 | 7.28 | 4.61 | 0.03 |
| **cg0839** | --- | hypothetical protein | 1.12 | 6.46 | 7.04 | 7.33 | 2.45 | 0.16 |
| **cg0840** | --- | hypothetical protein, conserved | 1.04 | 5.67 | 6.79 | 6.64 | 2.45 | 0.19 |
| cg0841 | --- | hypothetical protein, conserved | 0.98 | 1.02 | 0.98 | 0.93 | 1.36 | 0.05 |
| cg0842 | --- | putative DNA helicase | 1.02 | 1.01 | 0.98 | 1.01 | 1.11 | 0.21 |
| cg0843 | --- | putative helicase | 0.98 | 0.95 | 0.99 | 0.95 | 1.10 | 0.21 |
| cg0844 | --- | putative type II restriction enzyme, methylase subunit | 1.06 | 1.03 | 1 | 0.96 | 1.57 | 0.05 |

*(Continued)*

**Table 8.** *Continued.*

| Locus tag | Gene name | Annotated function | Gene coverage ATCC 13032 | Gene coverage ATCC13032Δ*ftsR* clone 1 | clone 2 | clone 3 | mRNA ratio Δ*ftsR*/ WT | p-value |
|---|---|---|---|---|---|---|---|---|
| cg0845 | --- | putative superfamily II DNA/RNA helicase, SNF2-family | 0.97 | 0.94 | 1.03 | 0.89 | 0.61 | 0.06 |
| cg0847 | --- | putative transcriptional regulator, conserved | 0.82 | 0.97 | 0.93 | 0.86 | 0.64 | <0.01 |
| cg0848 | *wbbL* | putative rhamnosyl transferase WbbL | 0.85 | 0.92 | 0.95 | 0.84 | 0.53 | 0.02 |
| cg0849 | *rmlA2* | GDP-mannose pyrophosphorylase, mannose-1-phosphate guanylyltransferase | 0.98 | 1.02 | 1.02 | 0.96 | 0.61 | 0.14 |
| cg0850 | *whcD* (*whiB2*) | transcription factor, *whmD* homolg, not involved in oxidative stress | 1.09 | 1 | 1.05 | 1.2 | 0.68 | 0.01 |

## 4.7. DNA affinity purification for unraveling transcriptional regulation of *odhI*

Another approach for analyzing transcriptional regulation of *odhI* was to identify potential regulatory proteins which bind to the *odhI* promoter region by DNA affinity chromatography, using a 590-bp DNA fragment covering the *odhI* promoter region and the first 84 bp of the *odhI*-coding region. The immobilized DNA fragment was incubated with crude protein extract of *C. glutamicum* wild type cells grown in glucose minimal medium. The proteins eluting after several washing steps were separated by SDS-PAGE and stained with Coomassie (Figure 12). Subsequent MALDI-ToF-MS analysis resulted in the identification of seven proteins. They represent proteins that are often found in DNA affinity purifications with *C. glutamicum* cell extracts independent of the promoter region used. Unfortunately, neither FtsR nor any other transcriptional regulator which might be involved in the regulation of *odhI* was identified.

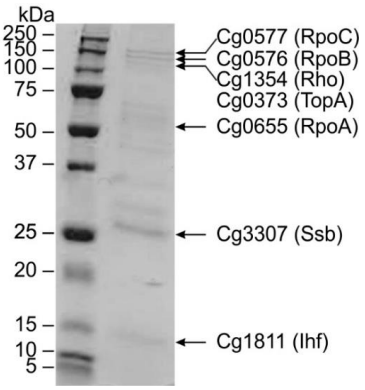


**Figure 12. DNA affinity purification with the *odhI* promoter region and crude cell extract of *C. glutamicum* ATCC13032.** Proteins binding to the *odhI* promoter were separated by SDS-PAGE, stained with Coomassie and analyzed by peptide mass fingerprinting using MALD-ToF-MS. Identified proteins are marked with arrows and labeled with names and corresponding Cg numbers. The protein ladder used (left lane) is the Precision Plus Protein™ Dual Xtra (Bio-Rad Laboratories, Inc., CA, USA).

Kim *et al.* (2010) have described that addition of penicillin for induction of glutamate production leads to a ten-fold increased expression of *odhI*, which suggests that inhibition of OdhA by OdhI might take place under these conditions. Based on this report, an additional DNA affinity purification experiment was performed with the following alterations: the culture volume for preparation of the crude protein extract was increased to five liters, glutamate production was induced at an $OD_{600}$ of about five by addition of 10 µM penicillin G and the cells were harvested after seven hours at an $OD_{600}$ of about seven. The DNA affinity purification was performed as described above. Again, identification of proteins typically found in these kind of experiments (polymerases, topoisomerase, helicase, etc.) confirmed that the experiment *per se* was successful (Figure 13). Unfortunately, it was once more not possible to identify FtsR or any other transcriptional regulator which might be potentially involved in the regulation of *odhI.* Growth monitoring during this experiment and subsequent HPLC analysis revealed that induction with penicillin was successful due to stagnated growth and detection of an increased glutamate secretion (for additional data, see protocol of the practical course of master student Michele Reindl).

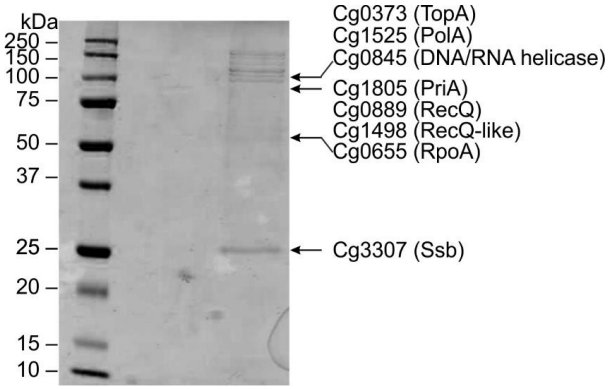


**Figure 13. DNA affinity purification with the *odhI* promoter and crude cell extract of *C. glutamicum* ATCC13032 cells induced for glutamate secretion by penicillin addition.** Proteins binding to the *odhI* promoter were separated by SDS-PAGE, stained with Coomassie and subjected to peptide mass fingerprinting using MALD-ToF-MS. Identified proteins are marked with arrows and labeled with names and corresponding Cg numbers. The protein ladder used (left lane) is the Precision Plus Protein™ Dual Xtra (Bio-Rad Laboratories, Inc., CA, USA).

## 4.8. Focusing on investigation of the uncharacterized regulator FtsR

The results shown so far did not support our hypothesis that FtsR or another transcriptional regulator is involved in the regulation of *odhI*, which was initially one major goal of this doctoral thesis. Since deletion of *ftsR* led to a severe growth defect under standard conditions and strong morphological changes, indicating an important function of FtsR, it seemed reasonable to shift the focus of this work on the investigation of this yet uncharactarized protein. As

described above, the *ftsR* gene and its immediate genomic vicinity were found to be highly conserved within the Actinobacteria (Figure 4) and an amino acid sequence alignment of FtsR homologs of different actinobacterial species revealed that especially the N-terminal part is highly conserved (Figure 5). Since the microscopy and microarray data presented led to the strong suspicion that FtsR might be involved in the regulation of *ftsZ* and no transcriptional regulator of this gene was known to date in *C. glutamicum*, it was considered worthwile to investigate this protein in more depth. Thenceforward, we decided to name it FtsR, standing for regulator of *ftsZ*. Moreover, we decided to switch from the ATCC13032 wild type to the MB001 strain for some of the upcoming experiments, because it cannot be excluded that the amplification of the trehalose cluster might provoke secondary effects, which makes interpreting the experimental data more difficult.

### 4.9. Deletion and overexpression of the *ftsR* gene in the MB001 background

MB001 differs from ATCC13032 by the deletion of the three prophage regions CGP1 (13.5 kb), CGP2 (3.9 kb), and CGP3 (187.3 kb) (Baumgart *et al.*, 2013b). It has been reported previously that the MB001 strain behaved like its parent wild type in the majority of conditions tested but showed improved growth and fitness under SOS response-inducing conditions that trigger CGP3 induction in the wild type. Thus, MB001 is a useful strain background for the analysis of deletions causing stressed cells, as secondary effects resulting from prophage induction can be excluded. In the context of this thesis, working with MB001 makes it even more feasible to distinguish between effects primarily caused by the *ftsR* deletion and secondary effects. Therefore, the strain background was changed for some of the following experiments from ATCC13032 to MB001. The in-frame deletion mutant MB001Δ*ftsR* as well as an *ftsR*-overexpressing strain constructed in this background were analyzed with respect to their growth behaviour and the moprohological phenotype. Both, growth behavior (Figure 14a) and cell morphology of MB001Δ*ftsR* (Figure 15) were comparable to those of ATCC13032Δ*ftsR*. Overexpression of *ftsR* in MB001 also caused similar effects as in ATCC13032 (Figure 14b). Thus, the absence of the prophages CGP1, CGP2, and CGP3 had no obvious influence on the effects of *ftsR* deletion and overexpression on growth and cell morphology.

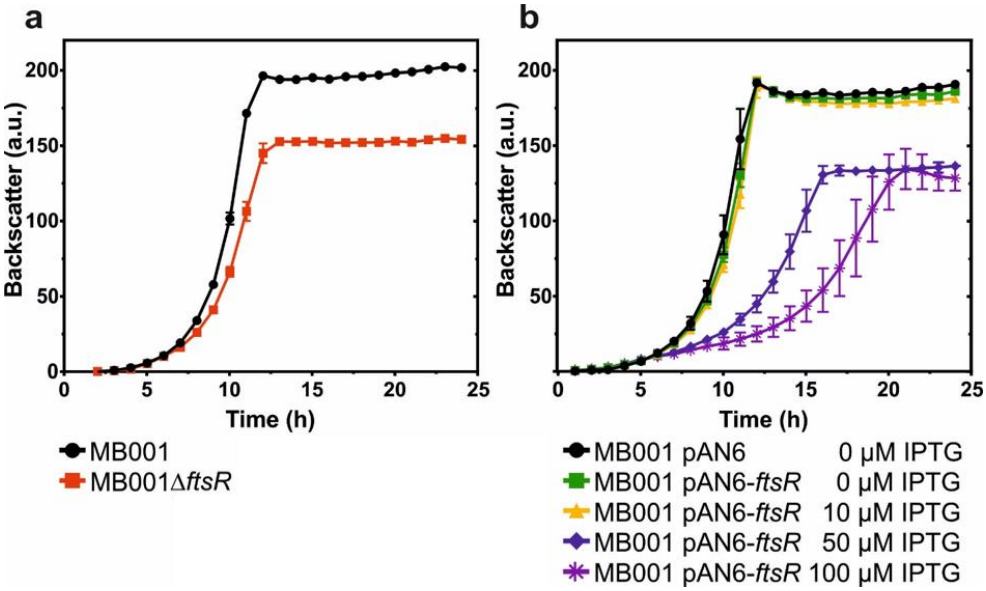


**Figure 14. Growth behavior of *C. glutamicum* MB001 with deleted (a) or (over)expressed (b) *ftsR*.** The cells were first cultivated in BHI medium followed by two consecutive cultivations in CGXII minimal medium with 2% (w/v) glucose as carbon source. For the plasmid-based (over)expression, kanamycin (25 µg/mL) and IPTG was added as indicated. Means and standard deviations of three biological replicates of the second CGXII culture are presented.

## 4.10. Complementation of the MB001Δ*ftsR* phenotype with native FtsR and homologs of *C. diphtheriae* and *M. tuberculosis*

In the complementation experiments performed with strain MB001Δ*ftsR*, a full reversal of the growth defect and of the morphological changes was observed for MB001Δ*ftsR* pAN6-*ftsR* without IPTG induction (Figure 15). These results confirm that *ftsR* deletion causes the growth defect and the morphological changes of the corresponding mutants. Due to the conservation of the *ftsR* locus in different actinobacterial species, we assumed a similar function of the homologous genes and proteins. To test this hypothesis, we expressed *ftsR* homologs of two pathogenic relatives, CDC7B_1201 of *Corynebacterium diphtheriae* C7 and Rv1828 of *Mycobacterium tuberculosis* H37Rv, in the *C. glutamicum* MB001Δ*ftsR* strain using pAN6-based expression plasmids and monitored growth and cell morphology. While this thesis was in preparation, initial biochemical and structural studies of Rv1828 were published (Singh *et al.*, 2018), which will be discussed alongside our results. With pAN6-CDC7B_1201, almost full reversal of the growth defect and of the morphological changes was achieved by basal expression without IPTG induction (Figure 15). As previously observed for overexpression of *C. glutamicum ftsR*, stronger induction of CDC7B_1201 gene expression had a negative effect on growth (data not shown). With pAN6-rv1828, the best complementation was achieved in the presence of 100 µM IPTG (Figure 15). Whereas a full

reversal to wild type morphology was observed, growth was improved with pAN6-rv1828 but did not reach the wild type characteristics. These results strongly suggest that the FtsR homologs of Actinobacteria have similar or identical functions and target genes.

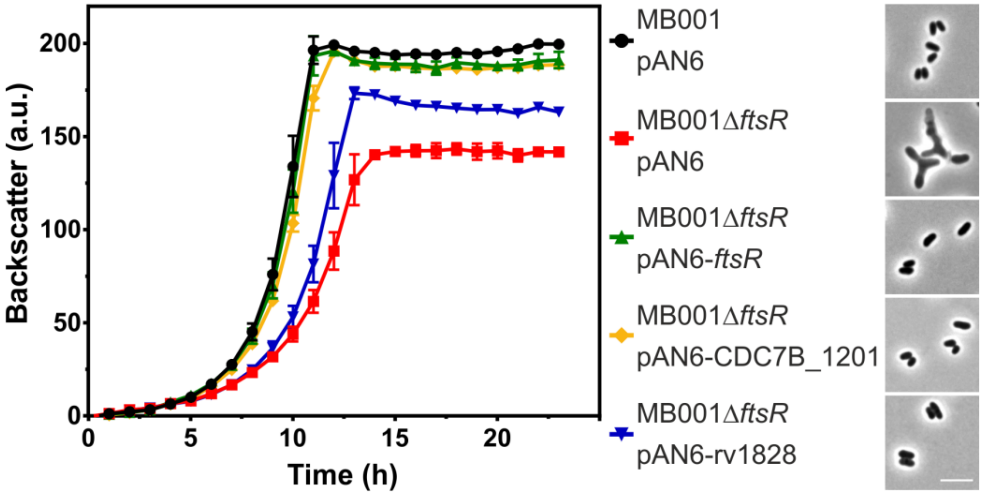


**Figure 15. Complementation of the growth defect (left panel) and the morphological phenotype (right panel) of the MB001Δ*ftsR* mutant by plasmid-encoded FtsR and homologous proteins of related species.** The cells were first cultivated in BHI medium with kanamycin (25 µg/mL) followed by two consecutive cultivations in CGXII minimal medium with kanamycin (25 µg/mL) and 2% (w/v) glucose as carbon source. MB001Δ*ftsR* was transformed with pAN6 encoding *ftsR*, CDC7B_1201, or rv1828 under control of the leaky *tac* promoter. IPTG was only added for expression of rv1828, where 100 µM were required to obtain the best complementation from the tested conditions. Means and standard deviations of three biological replicates of the second CGXII culture are presented. Microscopy was performed with stationary cells. The white scale bar represents 5 µm.

## 4.11. Quantitative PCR to further investigate trehalose cluter amplification

A qPCR experiment was performed to confirm the amplification of the trehalose cluster in ATCC13032Δ*ftsR* with an alternative method and to investigate whether this amplification did also occur in MB001Δ*ftsR*. To do so, the genomic DNA of three independent clones of ATCC13032Δ*ftsR,* four independent clones of MB001Δ*ftsR*, and the respective wild type strains was isolated and used as templates. Two primer pairs were designed to specifically amplify two genes located in the trehalose cluster, cg0834 and cg0840. With a third primer pair, the reference gene *recF* was specifically amplified, serving as a control fragment. The results of the genome resequencing of ATCC13032Δ*ftsR* were confirmed by qPCR, which revealed a ≥5-fold increased DNA level for cg0834 and cg0840 compared to the reference gene *recF* (cg0005) (Figure 16). The amplification mechanism of this cluster is unknown and the exact genomic structure of the amplification cannot be deduced from the short sequencing reads. In MB001Δ*ftsR*, qPCR did not reveal an increased DNA level of cg0834 and cg0840,

indicating that the amplification event only occurred in ATCC13032Δ*ftsR*, but not in the prophage-free strain MB001Δ*ftsR*. Since *ftsR* deletion mutants were constructed only once for each strain, firm conclusions on a functional correlation between the observed amplification event and the presence of the prophages cannot be drawn. However, the amplification could be responsible for the observed differences in the complementation studies between the wild type and the MB001 strain.

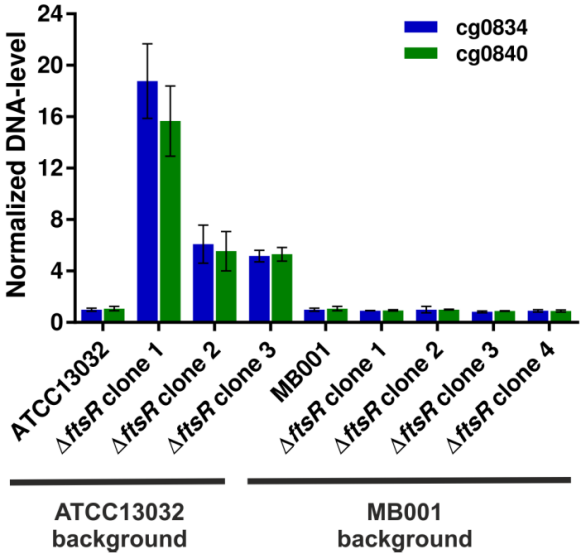


**Figure 16. Normalized DNA levels of cg0834 and cg0840 in different *ftsR* deletion strains and the corresponding reference strains.** Chromosomal DNA of three independent clones of ATCC13032Δ*ftsR*, four independent clones of MB001Δ*ftsR*, and the respective wild type strains was isolated and the relative copy numbers of were determined. Means and standard deviations of two technical replicates of each clone are presented. The DNA level of *recF* was used as reference and was set to 1. Illustrated are the normalized DNA levels of the genes cg0834 and cg0840 determined by qPCR and calculated using the ΔΔCt quantification method with the program qPCRsoft 3.1.

## 4.12. Effect of *ftsR* deletion on *ftsZ* promoter activity and FtsZ distribution

To investigate a transcriptional activation of *ftsZ* expression by FtsR *in vivo*, a transcriptional fusion of the *ftsZ* promoter to a reporter gene encoding the mVenus protein was constructed resulting in plasmid pJC1-$P_{ftsZ}$-*venus*. The reporter plasmid and the parent plasmid pJC1-*venus*-term that served as negative control were transformed into strains MB001 and MB001Δ*ftsR*. Subsequently, *ftsZ* promoter activity was measured as cell-specific fluorescence (defined as ratio of fluorescence and backscatter) in a BioLector® growth experiment. As shown in Figure 17, the lack of *ftsR* caused a significantly lower specific fluorescence, supporting an activation of *ftsZ* expression by FtsR. Comparable results were obtained with the strains ATCC13032 and ATCC13032Δ*ftsR* carrying pJC1-$P_{ftsZ}$-*venus* (Figure 18).

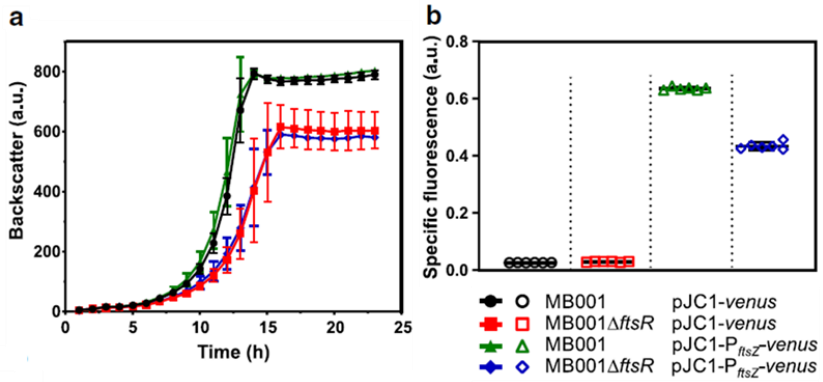


**Figure 17. Influence of the *ftsR* deletion in *C. glutamicum* MB001 on the expression of the *venus* reporter gene under control of the *ftsZ* promoter.** The indicated strains were cultivated in CGXII medium with 2% (w/v) glucose and 25 µg/mL kanamycin in a BioLector® system with automated measurement of cell density as backscatter and of Venus fluorescence. (**a**) For measurement of backscatter, mean values and standard deviations of three biological replicates are shown. (**b**) Specific fluorescence is shown as ratio of fluorescence and backscatter after 20 h of cultivation. The results of six individual biological replicates is represented as scatter dot plot with the black lines indicating the mean value and the error bars depicting the standard deviation.

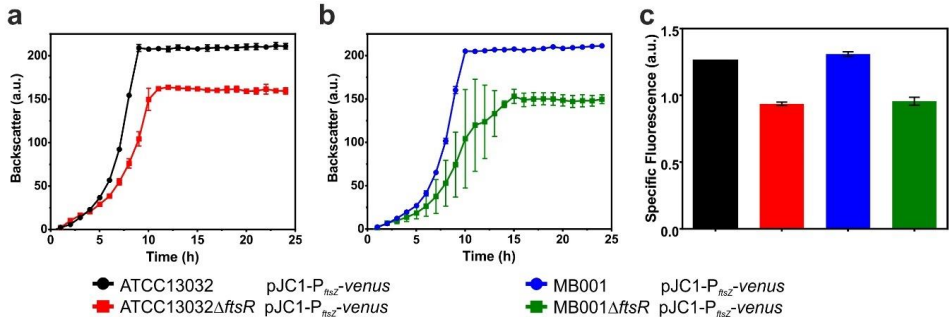


**Figure 18. Influence of the *ftsR* deletion on the expression of the *venus* reporter gene under control of the *ftsZ* promoter.** The indicated strains were cultivated in CGXII medium with 1% (w/v) glucose and 25 µg/mL kanamycin in a BioLector® system with automated measurement of cell density as backscatter at 620 nm and fluorescence (excitation at 510 nm, emission at 532 nm). Specific fluorescence represents the ratio of fluorescence and backscatter. (**a**) Growth data for the ATCC13032 background. (**b**) Growth data for the MB001 background. (**c**) Comparison of the specific fluorescence of all strains after 24 h. Means and standard deviations of three biological replicates are shown.

To test whether the lack of FtsR influences the distribution of FtsZ within the cell, we generated derivatives of ATCC13032 and ATCC13032Δ*ftsR* with a chromosomal insertion of a second copy of *ftsZ* fused in-frame to the coding sequence of the fluorescent protein mVenus under control of the native *ftsZ* promoter. Both strains were cultivated in CGXII minimal medium with glucose as carbon source and analyzed by fluorescence microscopy (Figure 19). In the strain lacking FtsR, the frequency as well as the intensity of the FtsZ rings was reduced. This may be caused by a reduced availability of FtsZ within the cells, which likely contributes to the morphological phenotype of the *ftsR* deletion mutant.

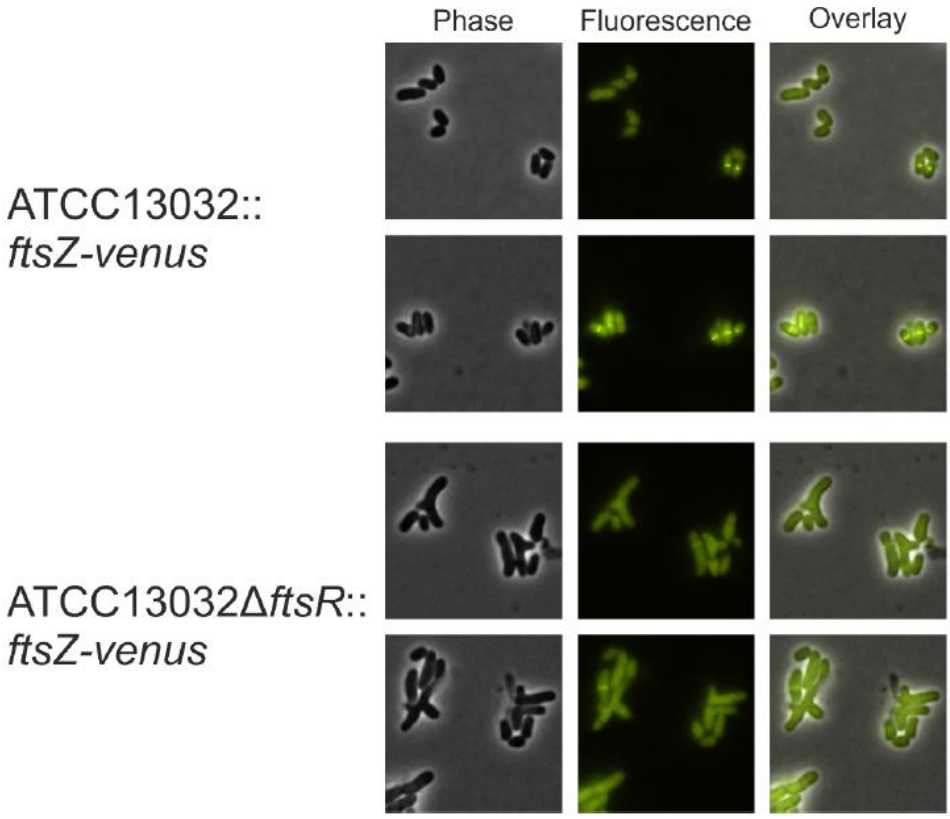


**Figure 19. Fluorescence microscopy of the *C. glutamicum* strains ATCC13032::*ftsZ-venus* and ATCC13032Δ*ftsR*::*ftsZ-venus* carrying a second chromosomal copy of *ftsZ* fused in-frame to the coding sequence of the fluorescent protein Venus.** The cells were first cultivated in BHI + 2% (w/v) glucose and afterwards transferred to CGXII + 2% (w/v) glucose, both with 25 µg/mL kanamycin. Samples for microscopy were taken after about 6 h of cultivation of the main culture, which is approximately in the middle of the exponential growth phase. Two representative pictures for each culture are shown. The experiment was performed with two biological replicates each.

### 4.13. Genome-wide profiling of *in vivo* FtsR binding sites

Transcriptional regulators usually bind to specific DNA sequences within the promoter regions of their target genes. With the aim to identify the *in vivo* binding site of FtsR in the *ftsZ* promoter region and to identify further target genes of FtsR, a ChAP-Seq experiment was performed. For this purpose, *in vivo* formaldehyde-crosslinked FtsR-Strep-DNA complexes were purified by StrepTactin affinity chromatography and the isolated DNA fragments were sequenced. Nine peaks with a sequencing coverage above 2000 were detected, which is at least 50-fold higher than the background noise signal observed for the entire genome with a 40-fold coverage (Figure 20, Figure 21, Table 9). The nine peaks were analyzed with respect to their chromosomal location and the mRNA level of the neighboring genes (Table 9). Based on the mRNA ratios observed in the transcriptome comparison of *C. glutamicum* ATCC13032Δ*ftsR*

*versus* ATCC13032, three potentially FtsR-activated genes (*ftsZ*, cg0852, cg2477) and five potentially FtsR-repressed genes (*cop1*-cg3181-cg3180, *phoC*, cg0838) were identified using mRNA ratio (Δ*ftsR*/wild type) cutoffs of 1.5 and 0.75. Indeed, the peak with the third highest coverage value was located in the promoter region of the *ftsZ* gene (for a separate picture of this peak, see Figure 21). A repetition of the ChAP-Seq experiment confirmed the results of the first one except that the overall coverage was lower, and the order of the peaks varied slightly (Table 9).

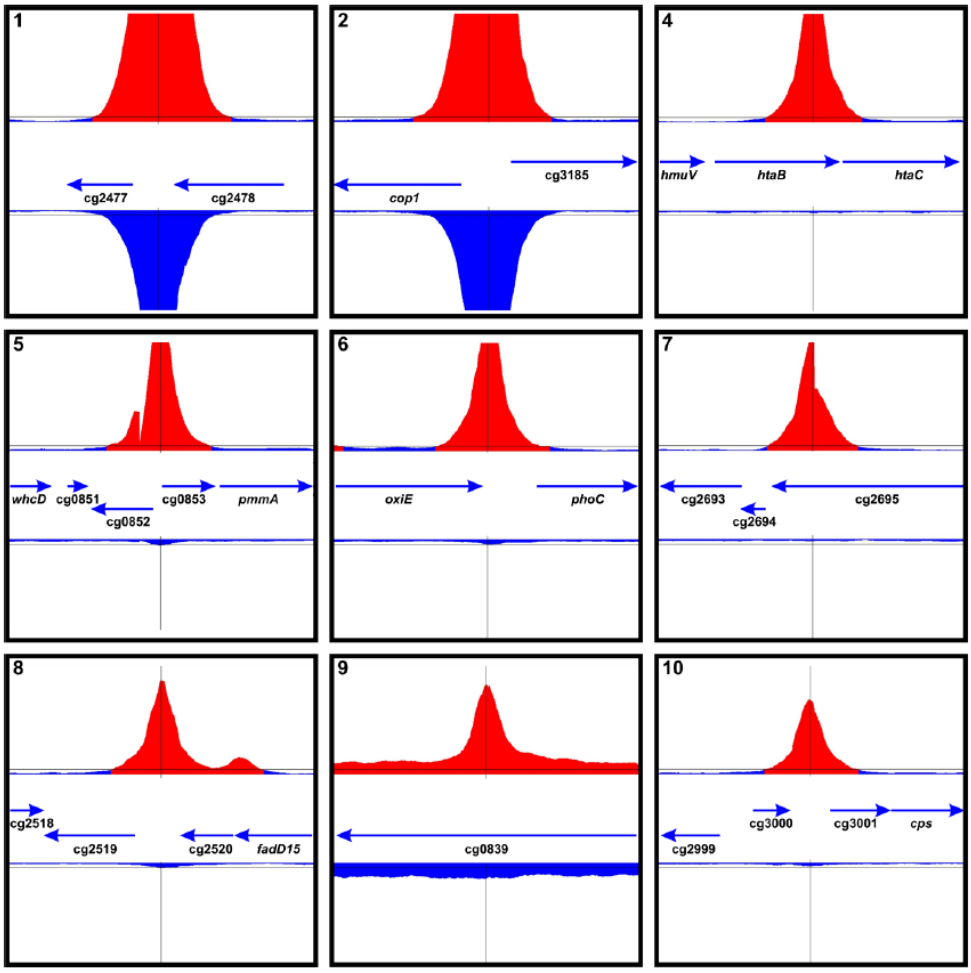


**Figure 20. DNA regions showing the highest coverage (red peaks) in the ChAP-Seq experiment with FtsR-Strep (strain *C. glutamicum* Δ*ftsR* pAN6-ftsR-Strep).** As negative control, the DNA enriched by StrepTactin affinity chromatography from strain *C. glutamicum* Δ*ftsR* pAN6 was used (blue background). The red peak in the *ftsZ* promoter region (between cg2365 and cg2366), which had the 3rd highest coverage, is depicted in Figure 21. Due to the high peaks in the negative control of sample peaks 1 and 2, an independent ChAP-Seq experiment was performed, which confirmed binding of FtsR between cg2477 and cg2478 and between *cop1* and cg3185 (see Table 9) without the high background peaks in the negative control.

**Table 9. Results of ChAP-Seq analysis with *C. glutamicum* ATCC13032Δ*ftsR* pAN6-*ftsR*-Strep.** The nine DNA regions that showed a ≥50-fold higher coverage than the entire genome (coverage 40) in the ChAP-Seq analysis with FtsR-Strep were analyzed with respect to the location of the peak within the genome and the mRNA levels of the genes in this region. Based on that, a prediction was made which genes could be potential FtsR targets. The arrows indicate whether the genes are encoded on the leading (→) or lagging strand (←) within the genome. Graphical representations of selected peaks as derived from the ChAP-Seq analysis are shown in Figure 20.

| No[a] | Coverage[a] | Peak position | | | DNA microarray 13032Δ*ftsR*/13032 | | | Potential *ftsR* target genes |
|---|---|---|---|---|---|---|---|---|
| | | in gene | downstream 3'-end of | upstream of | Gene | mRNA ratio | p-value | |
| **1 (1)** | 28,811 (4781) | - | cg2478 (NCgl2178, penicillin binding protein) ← | cg2477 (NCgl2177, conserved hyp. protein) ← | cg2478 | 0.75 | 0.11 | cg2477 potentially activated by FtsR |
| | | | | | cg2477 | 0.24 | 0.01 | |
| **2 (5)** | 22,757 (934) | - | - | cg3182 (NCgl2777, *cop1*, trehalose corynomycolyl transferase) ← | cg3182 | 1.70 | 0.20 | *cop1*-cg3181-cg3180 potentially repressed by FtsR |
| | | | | cg3181 (NCgl2776, putative secreted protein) ← | cg3181 | 2.30 | 0.05 | |
| | | | | cg3180 (NCgl2775, putative secreted protein) ← | cg3180 | 1.91 | 0.05 | |
| | | | | cg3183 (NCgl2778, putative transposase) → | cg3183 | n.a. | n.a. | |
| **3 (2)** | 4437 (1556) | - | cg2367 (NCgl2076, *ftsQ*, cell division septal protein) ← | cg2366 (NCgl2075, *ftsZ*, cell division GTPase) ← | cg2367 | 1.20 | 0.02 | *ftsZ* activated by FtsR |
| | | | | | cg2366 | 0.35 | 0.02 | |
| **4 (11)** | 3899 (373) | cg0470 (NCgl0381, *htaB*, heme transport-associated protein) → | cg0469 (NCgl0380, *hmuV*) → | cg0471 (NCgl0382, *htaC*, heme-transport associated protein) → | cg0469 | 1.41 | < 0.01 | - |
| | | | | | cg0470 | 1.45 | 0.09 | |
| | | | | | cg0471 | 1.55 | 0.03 | |
| **5 (12)** | 3836 (365) | - | - | cg0852 (NCgl0712, conserved hypothetical protein) ← | cg0852 | 0.62 | 0.01 | cg0852 potentially activated by FtsR |
| | | | | cg0853 (NCgl0713, conserved hypothetical protein) → | cg0853 | 1.03 | 0.29 | |

(*Continued*)

**Table 9.** *Continued.*

| No[a] | Coverage[a] | Peak position | | | DNA microarray 13032Δ*ftsR*/13032 | | | Potential *ftsR* target genes |
|---|---|---|---|---|---|---|---|---|
| | | in gene | downstream 3'-end of | upstream of | Gene | mRNA ratio | p-value | |
| | | | | cg0854 (NCgl0714, *pmmA*, phospho-manno-mutase) → | cg0854 | 0.89 | 0.25 | |
| | | | | cg0855 (NCgl0715, conserved hypothetical protein) → | cg0855 | 1.18 | 0.08 | |
| | | | | cg0856 (NCgl0716, mannose-6-phosphate isomerase) → | cg0856 | 1.09 | 0.03 | |
| **6 (3)** | 3630 (1529) | - | cg3392 (*oxiE*, *idhA2*, NCgl2958) → (myo-inositol 2-dehydro-genase) | cg3393 (NCgl2959, *phoC*, secreted cell wall-ass. phos-phatase) → | cg3392 | 1.25 | 0.03 | *phoC* potentially repressed by FtsR |
| | | | | | cg3393 | 1.60 | 0.03 | |
| **7 (15)** | 2871 (315) | cg2695 (NCgl2368, ATPase of ABC trans-porter) ← | cg2697 (*ssb*, NCgl2370, single-stranded DNA-binding protein) ← | cg2694 (NCgl2367, putative phospho-diesterase, nucleotide pyrophos-phatase) ← | cg2693 | 1.31 | 0.03 | – |
| | | | | cg2693 (NCgl2366, putative phospho-diesterase, nucleotide pyrophos-phatase) ← | cg2694 | 1.29 | 0.05 | |
| | | | | | cg2695 | 1.06 | 0.42 | |
| | | | | | cg2697 | 1.04 | 0.24 | |
| **8 (6)** | 2355 (858) | - | cg2518 (NCgl2213, put. secreted protein) → | - | cg2518 | 0.81 | 0.18 | – |
| | | | cg2519 (NCgl2214, conserved hyp. protein) ← | | cg2519 | 0.49 | 0.03 | |
| | | | cg2520 (NCgl2215, hyp. protein) ← | | cg2520 | 0.92 | 0.45 | |
| | | | cg2521 (NCgl2216, *fadD15*, long chain fatty acid CoA ligase) ← | | cg2521 | 0.91 | 0.43 | |
| **9 (8)** | 2248 | cg0839 (NCgl0701) ← (hyp. protein) | cg0840 (NCgl0702, conserved hyp. protein) ← | cg0838 (NCgl0700, ATP-dep. helicase) ← | cg0838 | 4.61 | 0.03 | cg0838 potentially repressed by FtsR |
| | | | | | cg0839 | 2.45 | 0.16 | |
| | | | | | cg0840 | 2.45 | 0.19 | |

The genes cg0852 and cg2477 encode conserved proteins of unknown function. The putative operon *cop1*-cg3181-cg3180 encodes three secreted proteins (Brand *et al.*, 2003). The Cop1 protein (also termed Csp1) was shown to function as mycolyltransferase involved in the conversion of trehalose monocorynomycolate to trehalose dicorynomycolate (Brand *et al.*, 2003, Puech *et al.*, 2000). The protein encoded by *phoC* was proposed to function as cell-wall-associated phosphatase (Schaaf & Bott, 2007, Wendisch & Bott, 2005) and is induced under phosphate-limiting conditions (Ishige *et al.*, 2003). The cg0838 gene is part of the DNA region found to be amplified in the ATCC13032Δ*ftsR* mutant but had a higher mRNA ratio than the neighboring genes that were also amplified (Table 8), pointing to a possible repression by FtsR. The large Cg0838 protein (179 kDa) is proposed to function as an ATP-dependent helicase and contains a unique C-terminal domain including a metal-binding cysteine cluster.

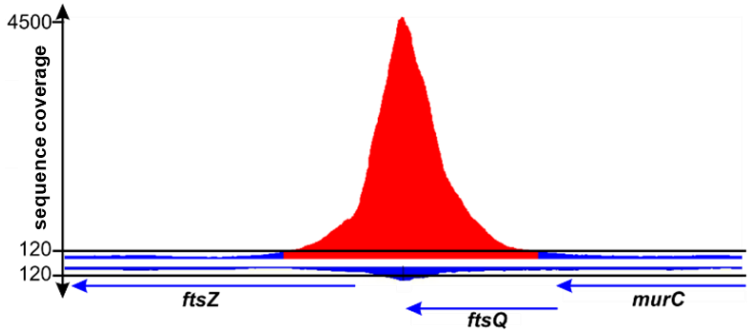


**Figure 21. Binding of the *ftsZ* promoter region by FtsR.** Sequencing coverage of the *ftsZ* promoter after ChAP-Seq with FtsR-Strep. The threshold was set at a sequence coverage value of 120, which corresponds approximately to 3 times above background level. Blue arrows represent the coding regions of the respective genes. The negative control is presented below the red peak in blue and points downwards.

The search for a common DNA sequence motif in the nine sequences with a coverage above 2000 using the MEME software (Bailey *et al.*, 2009) revealed the motif shown in Figure 22. The motif was identified in eight of the nine sequences except for the sequence with a coverage of 2871. When looking at the corresponding motif in the *ftsZ* promoter region, it forms an imperfect 25-bp inverted repeat: AACCCTAAAGTAAAGGTTGAGGGTA.

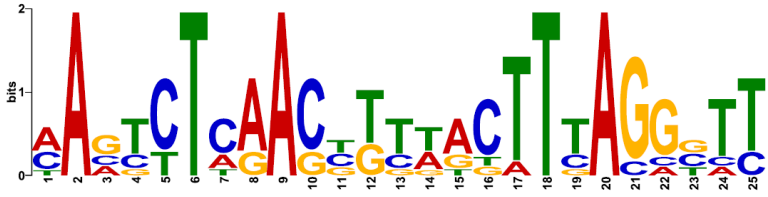


**Figure 22. FtsR consensus DNA-binding motif.** The motif was identified by the MEME software (Bailey *et al.*, 2009) using the nine DNA regions with the highest coverage in the ChAP-Seq experiment with FtsR-Strep.

The center of this motif was located at position -73 with respect to the transcriptional start site of *ftsZ* as determined by RNA-Seq (Pfeifer-Sancar *et al.*, 2013). This position is compatible with an activating function of FtsR for *ftsZ* expression (Figure 23). It should be mentioned that in *C. glutamicum* strain ATCC13689, five transcriptional start sites were identified for *ftsZ* by primer extension and RACE studies (Letek *et al.*, 2007), none of which corresponds to the one identified by RNA-Seq for strain ATCC13032 (Pfeifer-Sancar *et al.*, 2013).

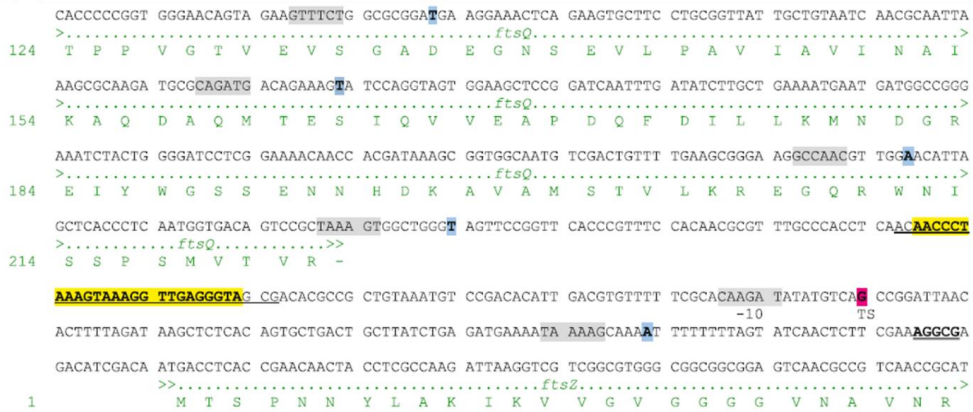


**Figure 23. DNA sequence of the *ftsZ* promoter region including parts of the coding regions of *ftsQ* and *ftsZ* and the corresponding amino acid sequences.** The ribosome binding site of *ftsZ* is double underlined. The transcriptional start site identified by RNA-Seq (Pfeifer-Sancar *et al.*, 2013) in strain ATCC13032 is highlighted in magenta, the transcriptional start sites identified by primer extension and RACE in strain ATCC13689 (Letek *et al.*, 2007) are indicated in blue. The deduced -10 regions are shown in grey boxes. The FtsR-binding site identified in this work is highlighted in yellow. The 30-bp region used for EMSAs with purified FtsR-Strep (Figure 26) is underlined.

The DNA-binding motif shown above was used to search for similar motifs in the *ftsZ* promoter regions of other actinobacterial species possessing FtsR homologs using Clustal Omega (Sievers *et al.*, 2011). All analyzed promoters contained a similar motif (Figure 24a), supporting the assumption that regulation of *ftsZ* expression by FtsR homologs is a conserved mechanism in FtsR-containing *Actinobacteria*. The motif generated from the proposed binding sites also represents a 25-bp inverted repeat (Figure 24b), which is very similar to the one derived from the *C. glutamicum* sequences enriched by ChAP-Seq with FtsR (Figure 22).

**a**

| | | |
|---|---|---|
| *C. glutamicum* | CAAC**AACCCTAAAGTAAAGGTTGAGGGTA**GCGA-162bp-CGACA**ATG** | cg2366 |
| *C. diphtheriae* | TCAA**AACCCTAAAGTAAAGGTTTAGGGTC**TAGA-163bp-TCTTA**ATG** | DIP1595 |
| *M. tuberculosis* | CTCT**AAGCCTATGGTTGAGGTTGAGAGTT**TGCC -42bp-GAACG**ATG** | rv2150 |
| *R. erythropolis* | CTCT**AACCCTGTGGTTGAGGTTTAGAGTT**TATC-102bp-AGCCG**ATG** | RER_35490 |
| *N. farcinica* | CGCT**AACCCTATGGTTGAGGTTCAGGGTT**TTCC -32bp-AGCCC**ATG** | NFA_17690 |
| *T. paurometabola* | CTTT**AAGCCTGTGGTTGAGGTTTAGGGTT**CTGG -35bp-GAAAC**ATG** | Tpau_2643 |
| *S. coelicolor* | TGGT**AACCCTAAACTTCAGCGTTAGGGTT**CGGG -98bp-TCGAC**GTG** | SCO2082 |
| *N. multipartita* | CTAT**AACCGTATGGTTGAGGTTGAGGGTT**CGAC-115bp-GGCGA**ATG** | Namu_3798 |
| *P. acnes* | TGAG**TAGTCTCAAGCTACGGTTGAGGGTC**AAGG -87bp-CTCCA**GTG** | PPA0761 |
| *A. cellulolyticus* | CTAT**AAGCCTCTAGTTGAGGGTGAGGGTT**GCGA -34bp-TGCAG**ATG** | Acel_1012 |
| *A. mirum* | ACAC**AACTCTTGACCCAGCGTCGAGGGTT**TCAA -65bp-GACCG**ATG** | amir_5760 |
| *M. luteus* | CTTG**GAGCCTCACGTGAAGGTTGATGCGG**AGGC-184bp-ACACC**GTG** | mlut_13570 |

**b**

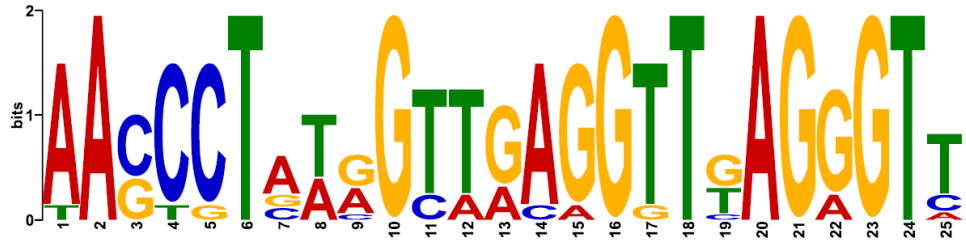


**Figure 24. Putative FtsR binding sites in the *ftsZ* promoters of various actinobacteria.** **a** Proposed FtsR binding sites in the *ftsZ* promoters of several actinobacterial species identified by sequence alignment with the FtsR binding site in the *C. glutamicum ftsZ* promoter. The respective *ftsZ* locus tags are given on the right. The proposed binding motifs are shown as colored letters. The annotated start codons of the FtsZ proteins are indicated by bold letters. The distance between the proposed FtsR binding site and the start codon varies from 41 to 193 bp. **b** Consensus DNA binding motif generated by MEME from the sequences shown in **a** using default parameters.

## 4.14. *in vitro* binding of purified FtsR to the proposed binding motif in the *ftsZ* promoter region

To test whether purified FtsR is able to bind to the proposed binding motif in the *ftsZ* promoter region, FtsR-Strep was overproduced in *C. glutamicum* ATCC13032Δ*ftsR* using plasmid pAN6-*ftsR*-Strep and purified using StrepTactin-Sepharose (Figure 25a). As described above, FtsR-Strep could complement the growth defect of the ATCC13032Δ*ftsR* mutant to the same extent as native FtsR, indicating that the Strep-tag did not negatively influence FtsR activity. Size-exclusion chromatography of affinity-purified FtsR-Strep (calculated mass 28.5 kDa) and comparison to standard proteins indicated that the protein forms a dimer (Figure 25b). This is in line with the dimeric state of the homologous protein Rv1828 (Singh *et al.*, 2018).

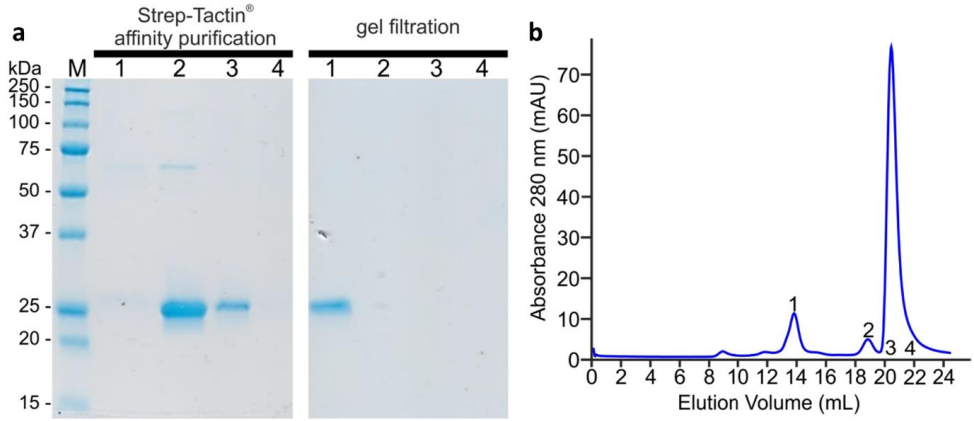


**Figure 25. Purification of FtsR-Strep.** (**a**) SDS-PAGE and Coomassie staining of purified FtsR-Strep. On the left side, the elution fractions 1-4 of the Strep-Tactin® affinity purification are shown. The second elution fraction was subjected to gel filtration for further purification (see Materials and Methods for details) and the analyzed fractions marked in the elution profile of the gel filtration (**b**) are shown on the right side of the gel. Gel filtration was performed using a Superdex™ 200 Increase 10/300 GL column integrated into an ÄKTA™ Pure25 system at a flow rate of 0.6 mL/minute (GE Healthcare Bio-Sciences AB, Uppsala, Sweden) and a buffer composed of 50 mM Tris-HCl, 250 mM NaCl, pH 7.5. The molecular mass of FtsR was estimated by comparison with standard proteins of known molecular mass and elution volume, which were cytochrome *c* (12.4 kDa, 18,82 mL), carbonic anhydrase (29 kDa, 16.15 mL), albumin (66.0 kDa, 13.73 mL), alcohol dehydrogenase (150.0 kDa, 12.53 mL), and β-amylase (200.0 kDa, 11.58 mL). FtsR-Strep eluted at 13.70 mL.

Purified FtsR-Strep was able to completely shift a 30-bp double-stranded oligonucleotide covering the predicted FtsR-binding site in the *ftsZ* promoter region at a 2-fold molar excess of the dimeric protein (Figure 26). In contrast, a control 30-bp double-strand-oligonucleotide derived from the promoter region of cg1081 was incompletely shifted even at an 8.5-fold molar excess of dimeric FtsR-Strep.

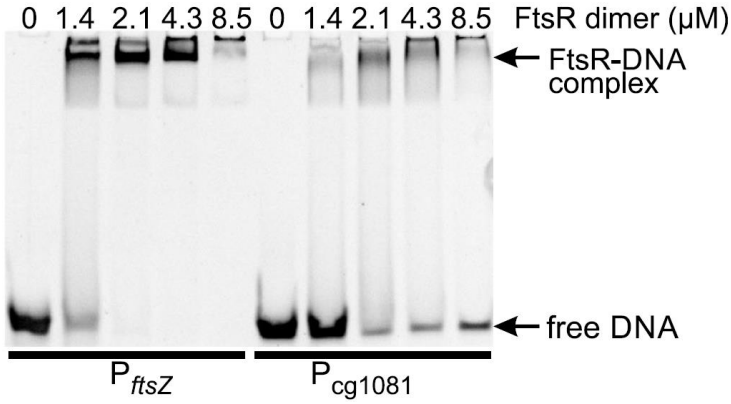


**Figure 26. *in vitro* DNA binding studies with FtsR-Strep.** Purified FtsR-Strep was incubated in the indicated concentrations with a constant concentration (1 μM) of a 30-bp double-stranded oligonucleotide covering the predicted FtsR-binding site in the *ftsZ*-promoter region. The mixture was then analyzed by electrophoresis using a non-denaturing 15% (w/v) polyacrylamide gel. As negative control, a DNA fragment of the promoter region of cg1081 was used (1 μM).

The specificity of this interaction was further tested using a competition-EMSA (Figure 27). A Cy3-labelled 271-bp DNA fragment covering the *ftsZ* promoter region including the FtsR binding site was incubated with FtsR protein and increasing concentrations of either specific (same fragment as above) or unspecific unlabeled competitor DNA. Only the specific competitor DNA reversed the shift of the labelled DNA fragment by FtsR, supporting its specific binding to the *ftsZ* promoter region.

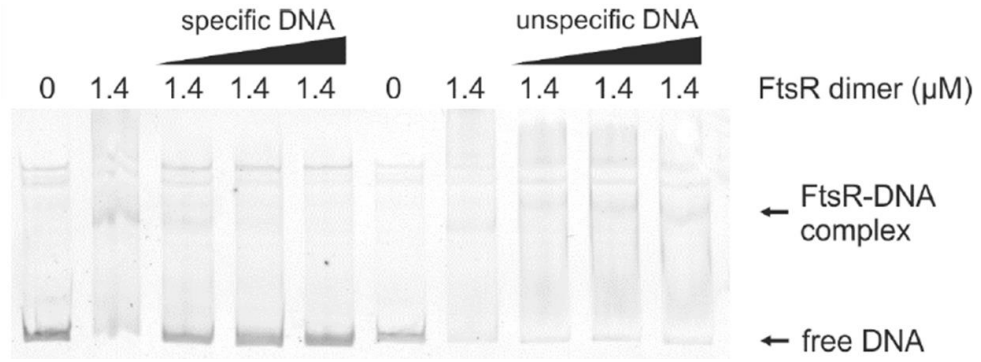


**Figure 27. EMSA competition experiment with FtsR and the *ftsZ* promoter region.** 2 nM Cy3-labeled *ftsZ* promoter DNA (271 bp) was incubated with 0 or 1.4 µM FtsR dimer and increasing concentrations (0.47 µM, 0.94 µM, 1.86 µM) of either unlabeled specific competitor DNA (same DNA fragment as above) or unlabeled unspecific competitor DNA (260-bp DNA fragment further upstream in the *ftsZ* promoter).

### 4.15. DNA affinity chromatography with the *ftsZ* promoter

As a complementary approach to show transcriptional control of *ftsZ* by binding of FtsR to the *ftsZ* promoter region, DNA affinity purification was performed using a 417-bp DNA fragment covering the 3′-end of the *ftsQ* coding region (36 bp), the intergenic region between *ftsQ* and *ftsZ*, and the first 96 bp of the *ftsZ* coding region. The immobilized DNA fragment was incubated with crude protein extract of *C. glutamicum* wild type cells grown in glucose minimal medium and harvested in the exponential growth phase. The proteins eluting after several washing steps were separated by SDS-PAGE and stained with Coomassie. Subsequent peptide mass fingerprinting using MALDI-ToF-MS resulted in the identification of eight proteins (Figure 28, Table 10). Six of them represent proteins that are often found in DNA affinity purifications with *C. glutamicum* cell extracts independent of the promoter region used. These are the single-stranded DNA-binding protein Ssb (Cg3307), the restriction endonucleases CglIR (Cg1997) and CglIIR (Cg1998), the ε-subunit of DNA polymerase III (Cg2321), DNA polymerase I (Cg1525), and the transcription termination factor Rho (Cg1354). Most interesting were the remaining two proteins, both of which are annotated as transcriptional regulators, Cg0444 (RamB) and Cg1631 (FtsR). The identity of these two proteins was further verified by MS/MS analysis of selected peptides (Table 10).

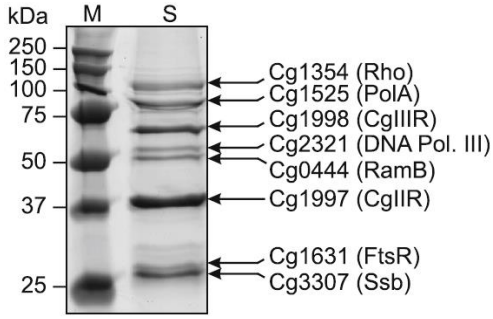


**Figure 28. DNA affinity chromatography with the *ftsZ* promoter region.** Crude cell extract of *C. glutamicum* ATCC13032 cultivated in glucose minimal medium to the mid-exponential growth phase was incubated with an immobilized 417-bp DNA fragment covering the *ftsZ* promoter region and strongly binding proteins were eluted with a high-salt buffer. Proteins enriched with the *ftsZ* promoter were separated by SDS-PAGE, stained with colloidal Coomassie, and identified by peptide-mass fingerprinting using MALDI-ToF-MS analysis (Table 10). The band with an apparent mass of about 27 kDa was identified as FtsR (M: marker; S: sample).

**Table 10. MALDI-TOF-MS analysis of the proteins enriched by DNA affinity chromatography with the *ftsZ* promoter region.** [a]The following parameters were used for the database search using the in-house database of *C. glutamicum* ATCC13032 proteins based on the genome sequence: missed cleavages, 1; global modifications, carbamidomethyl (C); variable modifications: oxidation (M), mass tolerance: 80 ppm; MS/MS tolerance, 0.5 Da. [b]Given are the masses of the peptides identified by MS/MS and the corresponding ion scores.

| Protein | Annotated function | Calculated mass (Da) | Mascot score[a] | Number of peptides matched | MS/MS[b] (ion score) | Sequence coverage |
|---|---|---|---|---|---|---|
| Cg1354 | transcription termination factor Rho | 83985 | 161 | 19 | | 39% |
| Cg1525 | DNA polymerase I | 96769 | 248 | 30 | | 44% |
| Cg1998 | restriction endonuclease CglIIR | 71053 | 181 | 23 | | 43% |
| Cg2321 | DNA polymerase III epsilon subunit | 51383 | 68 | 10 | | 24% |
| Cg0444 | transcriptional regulator RamB | 54117 | 202 | 23 | 1400.7 (35)<br>1559.7 (37)<br>1774.8 (31) | 52% |
| Cg1997 | type II restriction endonuclease CglIR | 39915 | 104 | 12 | | 47% |
| Cg1631 | transcriptional regulator FtsR | 27267 | 52 | 7 | 1103.5 (21)<br>1389.6 (23)<br>1566.8 (47) | 30% |
| Cg3307 | single-stranded DNA-binding protein Ssb | 23287 | 46 | 4 | | 30% |

The regulator of acetate metabolism RamB (Cg0444) has already been studied quite extensively and represses genes involved in acetate metabolism and alleviates glucose and sucrose uptake (Gerstmeir *et al.*, 2004, Auchter *et al.*, 2011). A function in *ftsZ* regulation has not been described for RamB and a well conserved RamB-binding site (AA/GAACTTTGCAAA (Auchter *et al.*, 2011)) is absent from the *ftsZ* promoter region. Analogous to the experiment described in chaper 4.12 and Figure 17, *ftsZ* promoter activity was additionally tested in a

Δ*ramB* background, but it was only very slightly altered in comparison to the wild type (data not shown). Enrichment of the second transcriptional regulator FtsR with the *ftsZ* promoter fragment supports its role in *ftsZ* regulation.

## 4.16. Analysis of the transcriptome of a Δ*ftsR* mutant in the MB001 background

The transcriptome of a Δ*ftsR* mutant has already been analyzed in the ATCC13032 background. 52 genes were regulated, with 34 genes showing a ≥two-fold increased and 18 genes a ≥two-fold decreased mRNA level in the Δ*ftsZ* mutant (mean value of 3 biological replicates, p-value ≤0.05). To reduce the complexity of the results and to be able to distinguish between effects primarily caused by the *ftsR* deletion and secondary effects (e.g. phage related effects), a second DNA microarray experiment was performed with the *C. glutamicum* MB001 strain and the corresponding deletion mutant MB001Δ*ftsR*. Here, the number of regulated genes was reduced to a set of eight (Table 12), with three genes showing a ≥two-fold increased and five genes a ≥two-fold decreased mRNA level in the Δ*ftsR* mutant (mean value of four biological replicates, p-value ≤0.05).

**Table 11: Transcriptome analysis of the Δ*ftsR* mutant**. Genes with a ≥two-fold increased or a ≥two-fold decreased mRNA ratio in the comparison MB001Δ*ftsR*/MB001 and a p-value of ≤0.05 are shown. The results shown are mean values of four biological replicates. Additionally, the result for *ftsZ* is shown in the last row.

| Locus tag | Gene name | Annotated function | mRNA ratio (MB001Δ*ftsR*/ MB001) | p-value |
|---|---|---|---|---|
| cg1631 | *ftsR* | transcriptional regulator, MerR-family | 0.003 | 0.0027 |
| cg2477 | --- | hypothetical protein, conserved | 0.055 | 0.0143 |
| cg2080 | --- | hypothetical protein, conserved | 0.471 | 0.0003 |
| cg0470 | *htaB* | secreted heme transport-associated protein | 0.494 | 0.0002 |
| cg2893 | --- | putative cadaverine transporter, multidrug efflux permease, MFS-type | 0.498 | 0.0185 |
| cg3181 | --- | putative secreted protein | 2.066 | 0.0042 |
| cg3182 | *cop1* | trehalose corynomycolyl transferase | 2.118 | 0.0028 |
| cg2378 | *mraZ* | putative MraZ protein | 2.195 | 0.0014 |
| cg2366 | *ftsZ* | cell division protein FtsZ | 0.755 | 0.0023 |

The downregulated genes include, besides the deleted cg1631 (*ftsR*) itself, the two conserved hypothetical protein-encoding genes cg2477 and cg2080, the secreted heme transport-associated protein-encoding gene cg0470 (*htaB*), and the putative cadaverin transporter-encoding gene cg2839. Among the upregulated genes are cg3181 and cg3182 (*cop1*), which

code for a putative secreted protein and a trehalose corynomycolyl transferase, respectively. The strongest upregulation was observed for cg2378 (*mraZ*). In the promoter regions of the genes cg2477 and cg3182, also peaks have been detected during the ChAP-Seq experiment (Figure 20 and Table 9). Compared to the transcriptome analysis of the Δ*ftsR* mutant in the wild type background (significantly decreased *ftsZ* mRNA ratio of 0.35, Table 6), the mRNA ratio of the *ftsZ* gene did not fulfil the set criteria (≥two-fold increased or ≥two-fold decreased mRNA level, p-value≤0.05) in the MB001 background. However, it showed 25% decreased expression with a p-value of 0.002 in the Δ*ftsR* mutant, which is in the same range as observed in the reporter gene studies (Figure 17) and might be sufficient for causing the specified phenotype because of the particular importance of FtsZ for cell division processes.

### 4.17. FtsR-independent expression of FtsZ

Previous studies showed that differences in *ftsZ* expression cause aberrant cell morphology and FtsZ localization in *C. glutamicum* (Letek *et al.*, 2006). In order to test whether the altered cell morphology and the growth defect of the Δ*ftsR* mutant are solely caused by the differences in *ftsZ* expression, strains were constructed in which the expression of *ftsZ* is independent of FtsR and controlled by the gluconate-inducible *gntK* promoter of *C. glutamicum* (Letek *et al.*, 2006, Frunzke *et al.*, 2008). A DNA fragment containing a terminator sequence and the *gntK* promoter was inserted between the native *ftsZ* promoter and the ribosome binding site of *ftsZ* within the chromosomes of *C. glutamicum* MB001 and MB001Δ*ftsR* by double homologous recombination (Figure 29).

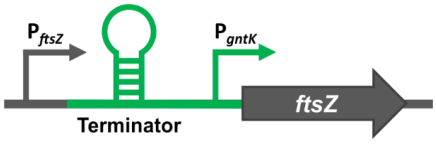


**Figure 29. Promoter exchange of *ftsZ*.** Strains with FtsR-independent *ftsZ*-expression were constructed using a DNA fragment with a terminator sequence and the gluconate-inducible *gntK*-promoter, which was inserted between the native *ftsZ* promoter and the ribosome binding site of *ftsZ* on the chromosome of MB001 and the MB001Δ*ftsR* mutant.

The promoter exchange strains MB001::$P_{gntK}$-*ftsZ* and MB001Δ*ftsR*::$P_{gntK}$-*ftsZ* showed no growth in presence of sucrose (repressive conditions, Figure 30a), confirming that the terminator prevented sufficient transcription of *ftsZ* from its native promoter. Under standard conditions with 2% (w/v) glucose as carbon source (Figure 30b), also no growth was observed, which was inconsistent with the results of similar experiments previously performed by Letek *et al.* (2006). The difference might be caused by residual *ftsZ* expression due to readthrough from the original promoter in the previous studies, which is absent in our strains due to an

efficient terminator inserted behind the native promoter. With gluconate as carbon source (inducing conditions, Figure 30c) the promoter exchange strains were able to grow, however, the wild type background and Δ*ftsR* background strains showed strong growth differences, which was a first hint that FtsR must have additional targets besides *ftsZ*.

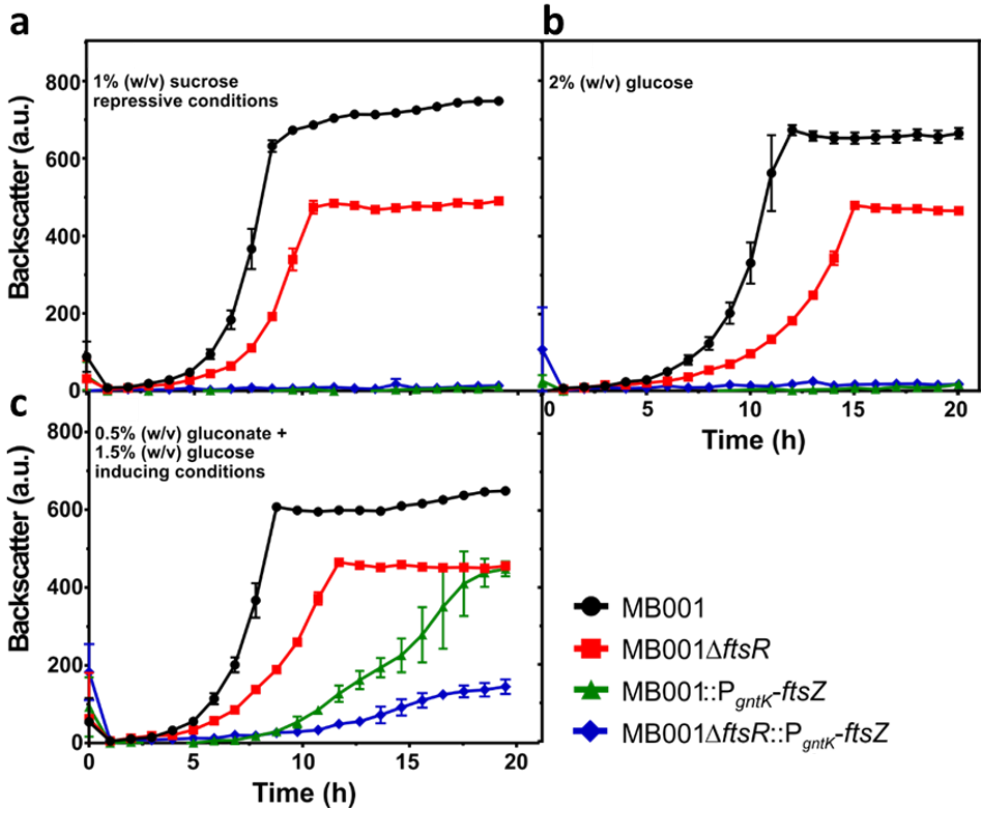


**Figure 30. Growth of promoter exchange strains and their parental strains.** The growth of the promoter exchange strains was tested in comparison to strains with the native *ftsZ* promoter using either sucrose (**a**), glucose (**b**), or glucose plus gluconate (**c**) as carbon source(s). Cells were pre-cultivated in either BHI medium (**a** and **b**) or BHI medium supplemented with 0.1% (w/v) gluconate for $P_{gntK}$ induction when gluconate was also used as carbon source in the main culture (**c**), followed by two consecutive cultivations in CGXII minimal medium supplemented with the indicated carbon sources. Means and standard deviations of three biological replicates are presented.

In order to analyze the consequences of different *ftsZ* expression levels on growth and morphology and to find conditions where both MB001 and MB001Δ*ftsR* with *ftsZ* under control of $P_{gntK}$ show similar growth behavior, cells were cultivated in CGXII medium with 2% (w/v) glucose supplemented with 0.005, 0.01, 0.05, and 0.1% (w/v) gluconate (Figure 31). The changes in growth and morphology observed in this experiment nicely demonstrated the potential of fine-tuning of gene expression with the $P_{gntK}$-system.

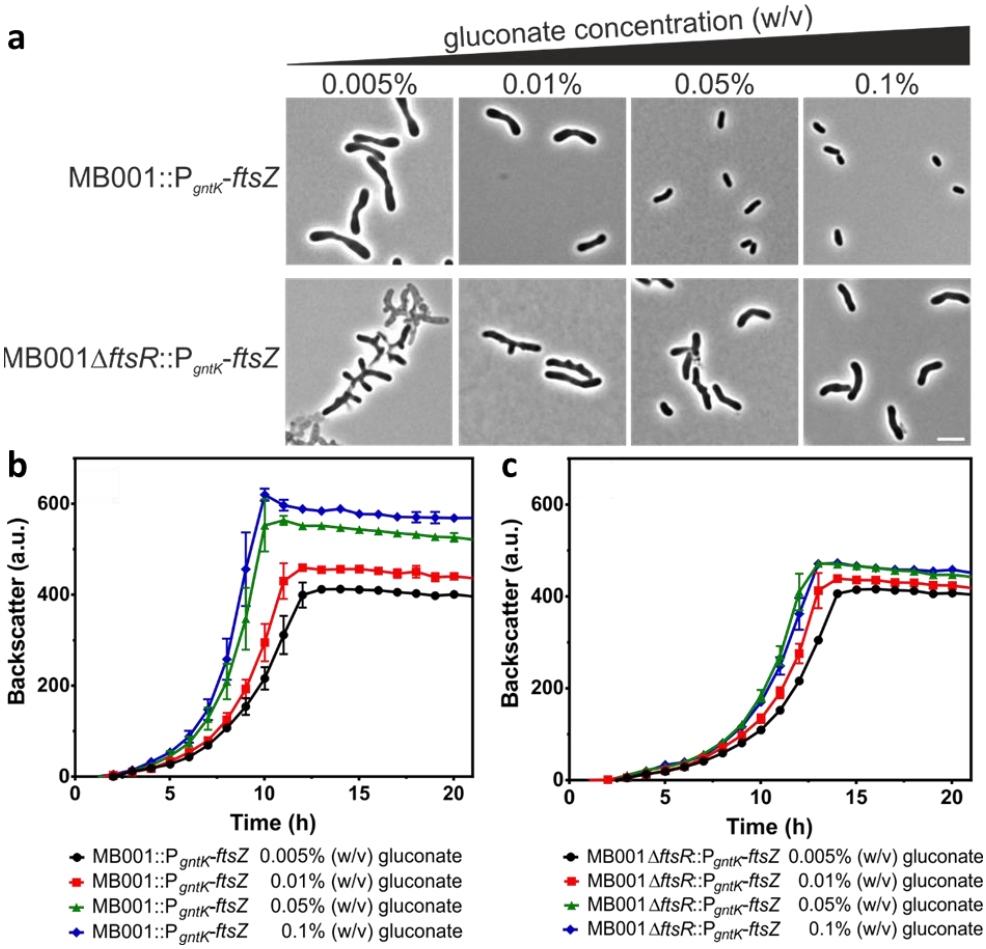


**Figure 31. Effect of different gluconate concentrations on cell morphology (a) and growth (b, c) of the promoter exchange strains MB001::P$_{gntK}$-*ftsZ* and MB001Δ*ftsR*::P$_{gntK}$-*ftsZ*.** The two strains were first pre-cultivated in BHI medium supplemented with 0.1% (w/v) gluconate to induce *ftsZ* expression by P$_{gntK}$. The second pre-cultivation was performed in CGXII medium with 2% (w/v) glucose supplemented with the indicated gluconate concentrations. The main cultures were then performed in media having the same composition as the ones for the second pre-cultivation. (**a**) Microscopic pictures of cells from the stationary phase. The white scale bar represents 5 µm. (**b, c**) The growth experiments show mean values and standard deviations of three biological replicates.

Strain MB001::P$_{gntK}$-*ftsZ* showed enlarged cells with thickened poles at the lowest gluconate concentrations. This phenotype was reverted to wild type morphology at 0.1% (w/v) gluconate (Figure 31a). Strain MB001Δ*ftsR*::P$_{gntK}$-*ftsZ* displayed strongly branched cells at the two lowest gluconate concentrations and even at 0.1% (w/v) gluconate the cells were still enlarged compared to the *ftsR*-positive strain (Figure 31a). With respect to growth, the two strains showed a quite similar behavior at the lowest gluconate concentration. Increased gluconate concentrations strongly improved growth of the *ftsR*-positive strain (Figure 31b), whereas growth of the *ftsR*-negative strain was only marginally increased (Figure 31c).

The most similar growth of the two promoter exchange strains was achieved with a pre-cultivation in BHI complex medium supplemented with 0.1% gluconate (w/v) and a main culture in CGXII medium supplemented with 0.01% gluconate and 1.99% glucose (Figure 32). Under these conditions, the influence of growth differences is strongly reduced, and it should be possible to distinguish between effects resulting directly from the deletion of *ftsR* and those that occur due to altered levels of FtsZ. Therefore, these strains are suitable for subsequent experiments such as reporter gene studies.

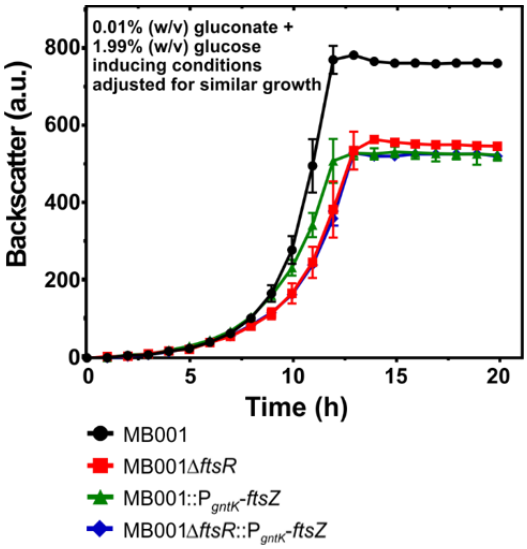


**Figure 32. Growth conditions enabling comparable growth of the promoter exchange strains.** The growth of the promoter exchange strains was tested in comparison to the corresponding strains with the native *ftsZ* promoter. Cells were pre-cultivated in BHI medium supplemented with 0.1% (w/v) gluconate for $P_{gntK}$ induction, followed by two consecutive cultivations in CGXII minimal medium supplemented with 0.1% (w/v) gluconate and 1.99% (w/v) glucose. Means and standard deviations for three biological replicates of the second CGXII culture are presented.

Overall, these results demonstrate the importance of an appropriate FtsZ level for normal cell morphology and growth, but they also show that the branched cells of the Δ*ftsR* mutant are not solely caused by reduced *ftsZ* expression, but presumably also by altered expression of other genes as a consequence of the *ftsR* deletion. Similarly, the growth defect of the Δ*ftsR* mutant cannot be rescued simply by increased expression of *ftsZ* and thus involves further genes. These could either be direct target genes of FtsR or genes whose expression is indirectly influenced by the absence of FtsR.

## 4.18. Influence of FtsR on *ftsZ* promoter activity in strains with FtsR-independent *ftsZ*-expression

The *ftsR* deletion in *C. glutamicum* MB001 led to a significant reduction of *ftsZ* promoter activity (Figure 17). In order to confirm that the observed activation of the *ftsZ* promoter by FtsR is independent of the actual *ftsZ* expression, the strains MB001::$P_{gntK}$-*ftsZ* and MB001Δ*ftsR*::$P_{gntK}$-*ftsZ* were transformed with the reporter plasmid pJC1-$P_{ftsZ}$-*venus* and either pEC-*ftsR* or pEC-XC99E as empty plasmid control (Figure 33). With *ftsZ* being under control of $P_{gntK}$ and addition of the same gluconate concentration to the medium, expression of the chromosomal *ftsZ* should be identical for all strains. In plasmid pEC-*ftsR*, the *ftsR* gene is expressed under control of the IPTG-inducible but leaky *trc* promoter (Figure 33). The growth conditions were chosen according to the previous experiment where the mixture of 0.01% (w/v) gluconate and 1.99% (w/v) glucose led to comparable growth of strains MB001::$P_{gntK}$-*ftsZ* and MB001Δ*ftsR*::$P_{gntK}$-*ftsZ*. The latter strain carrying pJC1-$P_{ftsZ}$-*venus* and the vector pEC-XC99E showed a significant growth defect in comparison to the other strains tested (Figure 33a, red curve). This defect must be due to altered expression of genes besides *ftsZ* that are regulated directly or indirectly by FtsR. Accordingly, the growth defect was reversed in the presence of the *ftsR* expression plasmid (Figure 33a, blue curve). The activity of the native *ftsZ* promoter on plasmid pJC1-$P_{ftsZ}$-*venus* was much lower in the strain lacking FtsR (Figure 33b, red curve) and was strongly increased when *ftsR* was expressed *via* pEC-*ftsR* (Figure 33b, blue curve). Growth and specific fluorescence were comparable for the two strains with chromosomal *ftsR* expression (Figure 33, black and green curves). These results confirm transcriptional activation of *ftsZ* expression by FtsR and that the phenotype of *ftsR* deletion mutants is not solely caused by a reduced *ftsZ* expression.

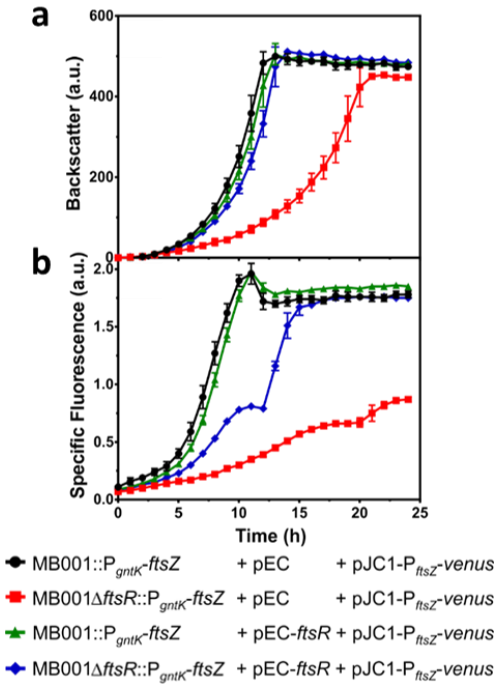


**Figure 33. Influence of *ftsR* expression on (a) growth and (b) plasmid-based *ftsZ* promoter activity in the *ftsZ* promoter exchange strains MB001::P$_{gntK}$-*ftsZ* and MB001Δ*ftsR*::P$_{gntK}$-*ftsZ*.** The strains were transformed with pJC1-P$_{ftsZ}$-*venus* for monitoring *ftsZ* promoter activity and either with the *ftsR* expression plasmid pEC-*ftsR* or the vector pEC-XC99E. Cells were cultivated first in BHI complex medium supplemented with 0.1% (w/v) gluconate followed by a second pre-culture and the main culture in CGXII minimal medium containing 0.01% (w/v) gluconate and 1.99% (w/v) glucose as carbon source. Kanamycin (25 µg/mL) and chloramphenicol (10 µg/mL) were added to all cultures. Means and standard deviations for three biological replicates of the second CGXII culture are presented.

# 5. Discussion

## 5.1. Regulation of OdhI in *C. glutamicum*

In the last decades, it was shown that the regulation of the 2-oxoglutarate dehydrogenase complex (ODHC) plays a pivotal role in glutamate production, as its activity is strongly reduced during cultivation of *C. gutamicum* under glutamate-producing *versus* non-producing conditions (Kataoka *et al.*, 2006, Shirai *et al.*, 2005, Shimizu *et al.*, 2003, Kawahara *et al.*, 1997). Furthermore, it was demonstrated that ODHC, which marks a very important branch point in the metabolism of *C. glutamicum*, is regulated by the small inhibitor protein OdhI in order to control the flux of 2-oxoglutarate towards efficient glutamate production (Bott, 2007). Regulation of OdhI itself as inhibitor of ODHC by phosphorylation or succinylation of the lysine-132-residue has been reported previously (Komine-Abe *et al.*, 2017). The initial aim of this doctoral thesis was to analyze whether OdhI is not only controlled at the posttranslational level, but also at the transcriptional level. The chance that *odhI* might be transcriptionally regulated seemed reasonable due to its location upstream of the two genes cg1631 (*ftsR*) and cg1633, which are both annotated to encode putative MerR-type transcriptional regulators. Since these two genes were suspected to regulate *odhI* expression, they were investigated in more detail. Growth studies revealed that the absence of cg1631 (later designated as *ftsR*) caused a severe growth defect under standard conditions and an even stronger growth defect was observed when this gene was overexpressed. Microscopy revealed a strong morphological phenotype with cells containing multiple septa both for the *ftsR* deletion mutant and for the overexpressing strain. This showed that the FtsR level is highly critical in *C. glutamicum* and hinted towards a possible function of FtsR in the regulation of cell division. No growth defect or altered phenotype was observed for the ∆cg1633 mutant under these conditions. In fact, cg1633 had already been investigated in more detail during a practical course of Graziella Bosco. Her studies suggested that cg1633 is most likely involved in metal homostasis and no evidence was found that *odhI* expression is affected by Cg1633 (Bosco, 2007). Therefore, cg1633 was no longer investigated within this doctoral thesis.

An alignment with FtsR homologs of different bacterial species revealed that most of the other sequences are considerably shorter than *C. glutamicum* FtsR, implicating that maybe the annotated start codon is incorrect. However, complementation studies with the annotated FtsR protein and with the shortened variant indicated that the annotation is correct since the shorter variant complemented the phenotype to a lower degree. Nevertheless, the growth defect of the ∆*ftsR* mutant was not fully restored even with the presumably correct FtsR variant, as it showed a longer lag phase and did not reach the final backscatter values obtained with the wild type, indicating that there might be secondary effects of the *ftsR* deletion which are eventually responsible for this effect.

FtsR was further investigated regarding a possible regulation of *odhI*. However, neither transcriptome analysis with DNA microarrays of the Δ*ftsR* mutant nor DNA affinity purification with the *odhI* promoter region did provide any support for the idea that FtsR might be involved in transcriptional regulation of *odhI*. Also, no other potential proteins which might regulate *odhI* expression were identified by DNA affinity purification, although the experiment *per se* was reliable, since proteins that bind DNA unspecifically and are often found in DNA affinity purifications (e.g. Ssb, polymerase subunits, topoisomerase etc.) were enriched. The results of this thesis indicate that *odhI* is not regulated on a transcriptional level. However, the experimental set-up concerning cultivation or reaction conditions might not have been optimal for the identification of a transcriptional regulator of *odhI*. Thus further experiments should be performed to confim this preliminary assumption.

## 5.2. Do secondary effects contribute to the Δ*ftsR* mutant phenotype?

The DNA microarray experiment with *C. glutamicum* ATCC13032Δ*ftsR versus* the wild type revealed a total of 52 genes which showed an at least two-fold altered mRNA ratio. It cannot be excluded that the deletion of *ftsR* might have downstream effects on other genes which secondarily cause or contribute to the Δ*ftsR* phenotype. One striking difference in the transcriptome of the *C. glutamicum* ATCC13032Δ*ftsR* mutant was the increased mRNA level of a set of genes, ranging from cg0828 to cg0840, which is referred to as “trehalose cluster”. This cluster harbors the genes cg0831-cg0835 encoding the trehalose uptake system TusFGK$_2$-E. Intriguingly, trehalose is a component of mycolates, which are important building blocks of the cell envelope of *Corynebacteriales* (Tropis *et al.*, 2005). Moreover, the disaccharide is known as a reserve carbohydrate and for its function as a stress protectant in many organisms and has also been reported to be associated with several more biological processes like sporulation, germination, virulence, and morphogenesis (Tournu *et al.*, 2013). It is known that trehalose synthesis can occur *via* different pathways. Besides the abovementioned TusFGK$_2$-E that allows uptake of exogenous trehalose, three major pathways involved in trehalose synthesis, OtsAB, TreYZ, and TreS, have been described for *C. glutamicum* (Ruhal *et al.*, 2013, Tzvetkov *et al.*, 2003, Wolf *et al.*, 2003). Trehalose synthesis varies in utilization of the metabolic routes in different bacterial species. However, severe growth defects as a result of impairment of trehalose production appear to be universal (Tournu *et al.*, 2013).

Moreover, it cannot be excluded that the increased expression of the genes of the trehalose cluster might influence the expression of other genes. To further pursue any possible secondary mutations, genome re-sequencing of three independent *C. glutamicum* ATCC13032Δ*ftsR* mutants was performed. The four detected prominent SNPs are presumably

not responsible for causing the abovementioned effects because they led to silent mutations or are located in an intergenic region or a hypothetical CGP3 region. However, the genome re-sequencing revealed that the trehalose cluster was present in an increased copy number in all three independent Δ*ftsR* mutants, which was additionally shown in a qPCR experiment. This strongly suggests that the increased mRNA level of the trehalose cluster revealed by transcriptome analysis is likely caused by a gene dosis effect and not by an upregulation on the transcriptional level. It remains unclear what may have triggered the amplification of the trehalose gene cluster. However, *tnp5a* (cg0824) which is located upstream in close proximity of the cluster, encodes a transposase that could have been involved in the process. In the Δ*ftsR* background, *tnp5a* showed a significantly increased coverage in genome resequencing and a significantly elevated mRNA ratio in transcriptome analysis, indicating an amplification or increased activity of the transposase. The three transposases *tnp16a* (cg0292), *tnp4a* (cg2461), and *tnp5c* (cg3266) are not in the immediate vicinity of the cluster, but also show a significantly elevated mRNA ratio in transcriptome analysis. The causal relationship between transposable elements (TEs) and adaptation to several environmental stresses has been reported previously for a variety of prokaryotes and eukaryotes. The molecular mechanisms underlying TE-induced mutations as well as the consequences of TE activation are highly diverse (Casacuberta & González, 2013). In the context of this doctoral thesis, it can be speculated whether the transposase *tnp5a* or one of the other transposases confers the trehalose cluster the ability to respond to stress through its amplification. However, the amplification could also have occured for other reasons or purely by chance and has not occurred in the MB001 background.

For trehalose being known as stress protectant and due to its role in cell envelope biosynthesis, the increased copy number of *tusFGK$_2$-E* observed for *C. glutamicum* ATCC13032Δ*ftsR* could indicate a stress response to counteract the morphological phenotype of the Δ*ftsR* mutant. An imaginable consequence of the amplification is that the increased expression of *tusFGK$_2$-E* leads to an increased trehalose uptake capacity. However, the absorbed trehalose could only result from the degradation of for example trehalose mycolates of the cell envelope, since trehalose was not added to the medium. This increased uptake capacity could possibly allow a more efficient recycling of the trehalose split off from cell wall components. Additionally, the significantly decreased mRNA ratio of the trehalose corynomycolyl transferase encoding gene *cmt2* (cg3186) in the Δ*ftsR* mutant observed by transcriptome analysis could support this hypothesis, as Cmt2 is involved in trehalose dicorynomycolate synthesis.

### 5.3. The switch to MB001 as background strain

In addition to the abovementioned possibilities of secondary downstream effects of a *ftsR* deletion, it seemed reasonable that also phage-related effects might be triggered by stress induced by the *ftsR* deletion. Due to this, the background strain was switched from the ATCC13032 type strain to the MB001 strain for some experiments with the purpose to make it more feasible to distinguish between effects primarily caused by the *ftsR* deletion and secondary effects. The deletion and the overexpression of *ftsR* in the MB001 background led to the same severe growth defect and morphological phenotype as in the ATCC13032 background strain. Transcriptome analysis and the qPCR experiment to investigate the amplification of the trehalose cluster has also been performed with strain MB001Δ*ftsR*. Neither increased expression nor amplification of the trehalose gene cluster were detected in the DNA microarray and in the qPCR experiment. This vitiated the previously elaborated “trehalose cluster hypothesis”, since the same phenotype as for the ATCC13032 background was observed. So, it could no longer be assumed that the elevated copy number of the trehalose gene cluster is responsible for the observed phenotype, or it is at least not the main cause for the phenotype in the ATCC13032 background. Overall, the set of significantly regulated genes in DNA microarray experiments with deleted *ftsR* was strongly reduced in the MB001 background compared to the ATCC13032 strain, most likely due to the elimination of trehalose cluster amplification and abolished phage-related effects, which facilitates the analysis of FtsR in this strain. Moreover, in contrast to the ATCC13032 background, the complementation experiment worked readily in the MB001 background, as the growth as well as the morphology was completely restored by plasmid-based *ftsR* expression. This indicates once more that potential secondary effects of a *ftsR* deletion were strongly reduced or were no longer present in MB001Δ*ftsR*.

### 5.4. FtsR, the first transcriptional regulator of FtsZ identified for the C*orynebacteriales* order

As already mentioned, the severe growth defect and drastic morphological changes caused by *ftsR* deletion and overexpression hinted to the encoded regulator playing a pivotal role in cell division. Because there is hitherto no transcriptional regulator of FtsZ known for *C. glutamicum* and the regulation of cell division in the *Corynebacteriales* order itself is largely unknown, the main focus of this work was shifted towards the investigation of this previously uncharacterized protein, FtsR. The obtained results revealed that FtsR is a transcriptional regulator of the tubulin-like GTPase FtsZ in *C. glutamicum* and the first transcriptional regulator of the key player of cell division discovered in this organism. Moreover, the conserved genomic locus in different *Corynebacteriales* species and successful complementation experiments of

the Δ*ftsR* phenotype with FtsR homologs of *C. diphtheriae* and *M. tuberculosis* support the assumption that FtsR fulfils a similar function in related organisms. Antibiotics research in recent years has shown that the inhibition of bacterial cell division is a promising strategy against human pathogens, with particular focus on FtsZ itself. Most compounds identified so far mainly aim at its GTPase activity, leading to an impaired assembly of the Z-ring and therefore to cell death (Sass & Brötz-Oesterhelt, 2013). However, this antibiotic class is already subject to the emergence of resistance mechanisms. Contributing to this is the fact that most new antibiotics are merely variants of substances already in use, so that bacteria can adapt to them rapidly, which highlights the urgent need for antimicrobial therapies that follow new mechanisms or attack novel targets (Lock & Harry, 2008). The newly identified regulator FtsR could therefore serve as an interesting candidate for the development of new antimicrobial drugs against these pathogenic relatives of *C. glutamicum*.

## 5.5. The importance of fine-tuning

The overexpression experiments with increasing amounts of IPTG as well as the experiments with varying gluconate concentrations when *ftsZ* is under control of the *gntK* promoter showed strikingly the importance of accurate *ftsZ* expression for the maintanence of normal growth and morphology of *C. glutamicum*. Furthermore, evidence for the activation of *ftsZ* expression by FtsR came from transcriptome analysis, where the *ftsZ* mRNA level was reduced in the Δ*ftsR* mutant, and reporter gene studies showing reduced activity of the *ftsZ* promoter in the Δ*ftsR* background, representing a novel control mechanism of actinobacterial cytokinesis. In ATCC13032Δ*ftsR* and MB001Δ*ftsR*, the *ftsZ* mRNA level was decreased by 65% and 25%, respectively. The latter reduction by a fourth seems to be minor, however, this slightly altered *ftsZ* expression might still be responsible for the impaired growth and severe morphological phenotype due to the particular importance of FtsZ concerning the cell division process.

## 5.6. FtsR's mode of action and binding site

Bioinformatic analyses revealed that FtsR belongs to the MerR superfamily of transcriptional regulators, which mostly function as activators, responding to a vast diversity of stimuli including oxidative stress, xenobiotics, and metal ion excess, with the latter forming a particular subgroup in this family of regulators (McEwan *et al.*, 2011, Brown *et al.*, 2003). Structures of already characterized MerR-type regulators show that they have very similar conformations, usually consisting of an N-terminal DNA-binding helix-turn-helix domain and a structurally more diverse effector-binding domain located in the C-terminus, which are linked by a helical domain forming an antiparallel coiled-coil required for dimerization (Kumaraswami *et al.*, 2010, Newberry & Brennan, 2004). MerR-type regulators typically bind as homodimers to inverted

repeats in the promoter region of their target genes. The binding sites are often located in the spacer regions between the -10 and -35 elements (Brown *et al.*, 2003). However, there are also other cases reported where for example the recognition site is located upstream of the -35 region or where a C-terminal effector-binding region is missing or larger than usual, such as for the Gram-positive Lactobacilli, Clostridia, and *Bacillus subtilis* or for members of the Gram-negative genus *Neisseria* (Counago *et al.*, 2016, Kidd *et al.*, 2005, Ahmed *et al.*, 1995). The spacer regions of MerR target promoters are often elongated, consisting of 19-20 bp instead of 16-18 bp, which hampers transcription because the -10 and -35 regions are located on opposite sides of the DNA strand (Brown *et al.*, 2003). A well-described mechanism of transcriptional activation by regulators of the MerR superfamily is assumed to rely on a conformational change of the N-terminal DNA-binding region of the protein after recognition of a stimulus by the C-terminal effector binding domain, which causes a twist of the bound DNA molecule in a manner that the -10 and -35 regions are rearranged, enabling RNA polymerase to bind and initiate transcription (Philips *et al.*, 2015, Newberry & Brennan, 2004, Ansari *et al.*, 1992, Frantz & O'Halloran, 1990). FtsR eluted as dimer during gel filtration and the binding site identified in the *ftsZ* promoter region was found to be an inverted repeat, which was located at position -61 to -85 upstream of the *ftsZ* transcriptional start site identified by RNA-Seq (Pfeifer-Sancar *et al.*, 2013) rather than between the -10 and -35 regions. This position is compatible with an activating function of FtsR but might involve a different mechanism of transcriptional activation than the one described above. Binding of FtsR to the *ftsZ* promoter was further confirmed by DNA affinity chromatography with the *ftsZ* promoter region. *In vivo* binding of FtsR to the *ftsZ* promoter was confirmed by ChAP-Seq experiments and purified FtsR was shown to bind to a 30 bp-DNA fragment covering the proposed DNA binding site of FtsR in EMSAs, which represents an imperfect 25-bp inverted repeat.

It should be mentioned that in the *C. glutamicum* strain ATCC13689 five transcriptional start sites were identified for *ftsZ* by RACE and primer extension experiments (Letek *et al.*, 2007), none of which corresponds to the one identified by RNA-Seq for the strain ATCC13032 (Pfeifer-Sancar *et al.*, 2013). Further studies are required to test for the presence of additional transcriptional start sites of the *ftsZ* gene in strain ATCC13032, in which the FtsR binding site might be located between the -10 and -35 regions. Multiple promoters contributing to *ftsZ* expression appear to be present in various bacteria such as *M. tuberculosis* (Roy & Ajitkumar, 2005, Kiran *et al.*, 2009), *E. coli* (Flardh *et al.*, 1997), *Streptomyces coelicolor* (Hajduk *et al.*, 2016, Flardh *et al.*, 2000), or *Streptomyces griseus* (Kwak *et al.*, 2001). They allow a dynamic adjustment of the FtsZ levels according to different stimuli and probably make the cells more robust with respect to spontaneous mutations in the *ftsZ* promoter region. Hitherto, an effector molecule which might trigger binding of FtsR remains to be discovered, as attempts for its identification by different GC-MS approaches were unsuccessful ((i) analysis after extraction

of fatty acid methyl esters from purified FtsR to detect a fatty acid as putative effector molecule, (ii) analysis after trypsin digestion of FtsR to detect a released effector molecule); data not shown.

FtsR was found to be conserved in many different families of Actinobacteria, including the genus *Mycobacterium*. In a ChIP-Seq experiment with the FtsR homolog Rv1828 of *M. tuberculosis*, the promoter region of the *ftsZ* gene was the top target (Galagan *et al.*, 2010, Minch *et al.*, 2015, Reddy *et al.*, 2009). Using the proposed binding motif of FtsR (AACCCTAAAGTAAAGGTTGAGGGTA) as template, we identified a very similar sequence (AACtCTAAgcctAtGGTTGAGGtTt) in the *ftsZ* promoter of *M. tuberculosis*, the region which also showed by far the highest coverage in the ChIP-Seq experiment (Minch *et al.*, 2015). Here, the motif was located exactly between the -10 and -35 regions of the transcriptional start site P1, which is located at position -43 relative to the *ftsZ* translational start (Kiran *et al.*, 2009). The binding motif proposed for Rv1828 in a recent study is different but overlaps partially with the motif proposed in this thesis (Singh *et al.*, 2018). Mutational analysis of this binding motif by EMSAs revealed that binding of Rv1828 is not influenced when the specific part of the motif is altered that does not overlap with our proposed binding motif (Singh *et al.*, 2018). This, together with the strong conservation among many species, suggests that the motif proposed in this thesis is more likely to be correct. The results obtained for FtsR taken together with the earlier findings for and recently published characterization of Rv1828 (Singh *et al.*, 2018) strongly support the notion that FtsR and its actinobacterial homologs are involved in transcriptional regulation of *ftsZ*. In line with this, the *ftsZ* promoter regions of various actinobacterial genera were found to contain DNA sequence motifs similar to the ones determined for FtsR and Rv1828.

## 5.7. FtsR must have additional targets besides FtsZ

The studies with the promoter exchange strains in which *ftsZ* expression was controlled by the gluconate-inducible *gntK* promoter revealed that growth behavior and morphology of the Δ*ftsR* mutant are not solely caused by altered *ftsZ* expression. Despite comparable *ftsZ* expression, the Δ*ftsR* strain grew much worse than the *ftsR*-positive reference strain and the morphology of the Δ*ftsR* strain differed from that of the *ftsR*-positive reference strain, in particular by the formation of branched cells. This suggests that (i) FtsZ alone is not responsible for the branched cell morphology, and (ii) that there must be some other, FtsR-regulated gene(s) that cause(s) enlarged cells even when FtsZ expression is fine-tuned by sufficient gluconate concentrations.

Potential further target genes of FtsR were deduced by combining ChAP-Seq and transcriptome results. The target with the most obvious relation to the altered cell morphology

of the Δ*ftsR* mutant was the *cop1*-cg3181-cg3182 gene cluster. These three genes encode two secreted proteins and Cop1 (Csp1), a mycolyltransferase converting trehalose monocorynomycolate to trehalose dicorynomycolate. This could possibly be linked to the morphological phenotype of Δ*ftsR* because of corynomycolic acids being important building blocks of the corynebacterial cell wall (Dover *et al.*, 2004). Together with the genera *Mycobacteria* and *Norcadia, Corynebacteria* belong to the mycolata group, whose cell envelope differs from other Gram-positive bacteria, as it additionally contains (coryno)mycolic acids, which are covalently linked to the peptidoglycan layer by arabinogalactan, surrounding the cell wall like an outer membrane, which provides resistance to antimicrobial compounds and other stress conditions (Favrot & Ronning, 2012, Hett & Rubin, 2008, Dover *et al.*, 2004).

The mycolyl transferase function was assigned to the N-terminal portion of Cop1 (Puech *et al.*, 2000). A *C. glutamicum cop1* deletion mutant had an altered cell morphology characterized by enlarged, club-shaped cells and it was speculated that the C-terminal part of Cop1 plays a role in cell shape formation (Brand *et al.*, 2003). In the case of *cop1*, the FtsR-binding site (AAGTCTAAAGTTGAACTTAAGATTG) starts downstream of the -35 region and ends downstream of the -10 region (TAAGAT). The transcriptome analysis data from DNA microarray experiments with MB001Δ*ftsR* suggest a repression of *cop1* by FtsR and the morphology of the cells overexpressing *ftsR* resemble that of cells lacking functional *cop1* (Brand *et al.*, 2003). The peak located in the promoter region of *cop1* had the second highest coverage value in the ChAP-Seq experiment. The highest coverage value was obtained for the peak in the promoter region of cg2477, which encodes a putative protein that has not been characterized so far. The expression of cg2477 was significantly altered in ATCC13032Δ*ftsR*, which makes both genes noticeable putative candidates for FtsR targets. DNA affinity purification experiments with promoter regions of *cop1* and cg2477 could be performed to further investigate this hypothesis.

Another interesting gene with significantly altered expression in the DNA microarray experiments with the MB001Δ*ftsR* strain is *mraZ*. It was shown in previous studies that the encoded protein is a transcriptional repressor of *ftsEX* in *C. glutamicum* and that its overproduction causes an elongated cell shape (Maeda *et al.*, 2016, Eraso *et al.*, 2014). FtsEX are components of the early divisome forming an ATP-binding cassette transporter, with FtsE representing the ATPase and FtsX the membrane domain of the complex (Donovan & Bramkamp, 2014). The genomes of *C. glutamicum* and *M. tuberculosis* contain homologs of FtsEX, but relatively little is understood regarding their function. Different functions of FtsEX are proposed for different organisms: in *E. coli*, FtsEX regulates peptidoglycan hydrolases and location of FtsX in the middle of the cell is achieved by interaction of FtsE with FtsA and FtsQ, whereas FtsX interacts directly with FtsZ (Corbin *et al.*, 2007, Schmidt *et al.*, 2004); in *B. subtilis*, FtsEX is involved in spatio-temporal regulation of sporulation and is located around

the cell membrane (Garti-Levi *et al.*, 2008); in *B. subtilis* and *Streptococcus pneumonia*, FtsEX mediates coupling of peptidoglycan hydrolysis and cell division and it was shown to regulate the activity of a cell wall hydrolytic enzyme, CwlO (Domínguez-Cuevas *et al.*, 2013, Meisner *et al.*, 2013, Sham *et al.*, 2013); in *C. crescentus*, FtsEX is speculated to play a role in tethering of Z-rings to the membrane, because it is recruited to the nascent division site prior to FtsA, which is involved in membrane association of the Z-rings (Goley *et al.*, 2011). With the knowledge previously generated for these other bacteria and considering that for *C. glutamicum* and *M. tuberculosis* FtsA has not been described so far (Donovan & Bramkamp, 2014), it can be speculated that FtsEX plays a role in the formation of the Z-ring and the stabilization of the future cell division site, which in turn is regulated by MraZ-mediated repression. In the Δ*ftsR* mutant, the mRNA level of *mraZ* was elevated, which suggests that FtsR not only directly regulates FtsZ, but is also involved in the complex process of cell division by repressing MraZ and thus controlling FtsEX. However, in the DNA microarray experiments with the Δ*ftsR* mutant, no significantly altered expression of *ftsEX* was observed, suggesting that an effector may be needed to activate the repressive function of MraZ.

The presented results of the ChAP-Seq and transcriptome analysis as well as the proposed binding motif for FtsR suggest a direct influence of the regulator on the expression of the genes *cop1* and *mraZ*. However, further studies are required to investigate the exact mode of regulation by FtsR on these targets and to identify further candidate genes and their functions. Beyond that, it might also be possible that FtsR does not only play a role in cell division, but also in other yet undiscovered processes, which do not necessarily have to contribute to the described phenotype.

## 5.8. The physiological function of FtsR

Regarding the physiological function of FtsR, a possible role could be to serve as a regulatory mechanism that controls cell division in response to the nutritional status of the cell. In recent years, several studies have revealed metabolic enzymes to directly influence cell division by modulating the activity of FtsZ (Monahan & Harry, 2016). Transcriptional regulation, as shown here for FtsR, is another means to influence FtsZ activity. The fact that FtsR activates *ftsZ* expression suggests that FtsR signals favorable nutritional conditions with a high cell division rate and thus a high FtsZ demand. As the *ftsR* gene and its homologs in other Actinobacteria are always located downstream of the *odhI/garA* gene, a functional link to OdhI/GarA might exist. OdhI/GarA controls the metabolic flux at the 2-oxoglutarate node of the central metabolism, which is particularly relevant for nitrogen assimilation. Our preliminary attempts to find a potential ligand of FtsR were not successful and the identification of the stimulus controlling FtsR activity is ultimately required to understand the function of this regulator.

## 6. References

**Adams, D.W., and Errington, J.** (2009) Bacterial cell division: assembly, maintenance and disassembly of the Z ring. Nat Rev Microbiol 7: 642-653.

**Ahmed, M., Lyass, L., Markham, P.N., Taylor, S.S., Vazquez-Laslop, N., and Neyfakh, A.A.** (1995) Two highly similar multidrug transporters of *Bacillus subtilis* whose expression is differentially regulated. J Bacteriol 177: 3904-3910.

**Alm, E.J., Huang, K.H., Price, M.N., Koche, R.P., Keller, K., Dubchak, I.L., and Arkin, A.P.** (2005) The MicrobesOnline Web site for comparative genomics. Genome Res 15: 1015-1022.

**Altschul, S.F., Gish, W., Miller, W., Myers, E.W., and Lipman, D.J.** (1990) Basic local alignment search tool. J Mol Biol 215: 403-410.

**Ansari, A.Z., Chael, M.L., and O'Halloran, T.V.** (1992) Allosteric underwinding of DNA is a critical step in positive control of transcription by Hg-MerR. Nature 355: 87-89.

**Auchter, M., Cramer, A., Huser, A., Ruckert, C., Emer, D., Schwarz, P., Arndt, A., Lange, C., Kalinowski, J., Wendisch, V.F., and Eikmanns, B.J.** (2011) RamA and RamB are global transcriptional regulators in *Corynebacterium glutamicum* and control genes for enzymes of the central metabolism. J Biotechnol 154: 126-139.

**Bailey, T.L., Boden, M., Buske, F.A., Frith, M., Grant, C.E., Clementi, L., Ren, J., Li, W.W., and Noble, W.S.** (2009) MEME SUITE: tools for motif discovery and searching. Nucleic Acids Res 37: W202-208.

**Baumgart, M., Luder, K., Grover, S., Gätgens, C., Besra, G.S., and Frunzke, J.** (2013a) IpsA, a novel LacI-type regulator, is required for inositol-derived lipid formation in Corynebacteria and Mycobacteria. BMC Biol. 11: 122.

**Baumgart, M., Schubert, K., Bramkamp, M., and Frunzke, J.** (2016) Impact of LytR-CpsA-Psr proteins on cell wall biosynthesis in *Corynebacterium glutamicum*. J Bacteriol 198: 3045-3059.

**Baumgart, M., Unthan, S., Ruckert, C., Sivalingam, J., Grunberger, A., Kalinowski, J., Bott, M., Noack, S., and Frunzke, J.** (2013b) Construction of a prophage-free variant of *Corynebacterium glutamicum* ATCC 13032 for use as a platform strain for basic research and industrial biotechnology. Appl Environ Microbiol 79: 6006-6015.

**Beall, B., and Lutkenhaus, J.** (1992) Impaired cell division and sporulation of a *Bacillus subtilis* strain with the *ftsA* gene deleted. J Bacteriol 174: 2398-2403.

**Becker, J., and Wittmann, C.** (2020) Pathways at work: metabolic flux analysis of the industrial cell factory *Corynebacterium glutamicum*. In: *Corynebacterium glutamicum*: Biology and Biotechnology. M. Inui & K. Toyoda (eds). Cham: Springer International Publishing, pp. 227-265.

**Bernhardt, T.G., and de Boer, P.A.** (2003) The *Escherichia coli* amidase AmiC is a periplasmic septal ring component exported via the twin-arginine transport pathway. Mol Microbiol 48: 1171-1182.

**Bi, E., and Lutkenhaus, J.** (1993) Cell division inhibitors SulA and MinCD prevent formation of the FtsZ ring. J Bacteriol 175: 1118-1125.

**Börmann, E.R., Eikmanns, B.J., and Sahm, H.** (1992) Molecular analysis of the *Corynebacterium glutamicum gdh* gene encoding glutamate dehydrogenase. Mol. Microbiol. 6: 317-326.

**Bosco, G.** (2007) Untersuchungen zum putativen Transkriptionsregulator Cg1633 aus *Corynebacterium glutamicum*. Praktikum Mikrobiologie III. IBT-1. Forschungszentrum Jülich.

**Bosco, G.** (2011) Charakterisierung von Proteinen einer neuartigen Signaltransduktionskaskade in *Corynebacterium glutamicum*. Schriften des Forschungszentrums Jülich Reihe Gesundheit / Health 45.

**Bott, M.** (2007) Offering surprises: TCA cycle regulation in *Corynebacterium glutamicum*. Trends Microbiol. 15: 417-425.

**Bramkamp, M., Emmins, R., Weston, L., Donovan, C., Daniel, R.A., and Errington, J.** (2008) A novel component of the division-site selection system of *Bacillus subtilis* and a new mode of action for the division inhibitor MinCD. Mol Microbiol 70: 1556-1569.

**Brand, S., Niehaus, K., Puhler, A., and Kalinowski, J.** (2003) Identification and functional analysis of six mycolyltransferase genes of *Corynebacterium glutamicum* ATCC 13032: the genes *cop1*, *cmt1*, and *cmt2* can replace each other in the synthesis of trehalose dicorynomycolate, a component of the mycolic acid layer of the cell envelope. Arch Microbiol 180: 33-44.

**Brinkrolf, K., Brune, I., and Tauch, A.** (2007) The transcriptional regulatory network of the amino acid producer *Corynebacterium glutamicum*. J. Biotechnol. 129: 191-211.

**Brown, N.L., Stoyanov, J.V., Kidd, S.P., and Hobman, J.L.** (2003) The MerR family of transcriptional regulators. FEMS Microbiol Rev 27: 145-163.

**Casacuberta, E., and González, J.** (2013) The impact of transposable elements in environmental adaptation. Mol Ecol 22: 1503-1517.

**CDC** (2014) Diphtheria, http://www.cdc.gov/diphtheria/clinicians.html

**Chomczynski, P., and Sacchi, N.** (2006) The single-step method of RNA isolation by acid guanidinium thiocyanate-phenol-chloroform extraction: twenty-something years on. Nat Protoc 1: 581-585.

**Corbin, B.D., Wang, Y., Beuria, T.K., and Margolin, W.** (2007) Interaction between cell division proteins FtsE and FtsZ. J Bacteriol 189: 3026-3035.

**Counago, R.M., Chen, N.H., Chang, C.W., Djoko, K.Y., McEwan, A.G., and Kobe, B.** (2016) Structural basis of thiol-based regulation of formaldehyde detoxification in *H. influenzae* by a MerR regulator with no sensor region. Nucleic Acids Res 44: 6981-6993.

**Cure, G., and Keddie, R.** (1973) Methods for the morphological examination of aerobic coryneform bacteria. In: Sampling – Microbiological Monitoring of Environments. R. Board & D. Lovelock (eds). London: Academic Press, pp. 123-135.

**Daniel, R.A., and Errington, J.** (2003) Control of cell morphogenesis in bacteria: two distinct ways to make a rod-shaped cell. Cell 113: 767-776.

**de Boer, P.A., Crossley, R.E., and Rothfield, L.I.** (1989) A division inhibitor and a topological specificity factor coded for by the minicell locus determine proper placement of the division septum in *E. coli*. Cell 56: 641-649.

**Delaunay, S., Gourdon, P., Lapujade, P., Mailly, E., Oriol, E., Engasser, J.M., Lindley, N.D., and Goergen, J.L.** (1999) An improved temperature-triggered process for glutamate production with *Corynebacterium glutamicum*. Enzyme Microb. Technol. 25: 762-768.

**Domínguez-Cuevas, P., Porcelli, I., Daniel, R.A., and Errington, J.** (2013) Differentiated roles for MreB-actin isologues and autolytic enzymes in *Bacillus subtilis* morphogenesis. Mol Microbiol 89: 1084-1098.

**Donovan, C., and Bramkamp, M.** (2014) Cell division in *Corynebacterineae*. Front Microbiol 5: 132.

**Dover, L.G., Cerdeno-Tarraga, A.M., Pallen, M.J., Parkhill, J., and Besra, G.S.** (2004) Comparative cell wall core biosynthesis in the mycolated pathogens, *Mycobacterium tuberculosis* and *Corynebacterium diphtheriae*. FEMS Microbiol Rev 28: 225-250.

**Du, S., and Lutkenhaus, J.** (2017) Assembly and activation of the *Escherichia coli* divisome. Mol Microbiol 105: 177-187.

**Duperray, F., Jezequel, D., Ghazi, A., Letellier, L., and Shechter, E.** (1992) Excretion of glutamate from Corynebacterium glutamicum triggered by amine surfactants. Biochim Biophys Acta 1103: 250-258.

**Dziadek, J., Rutherford, S.A., Madiraju, M.V., Atkinson, M.A., and Rajagopalan, M.** (2003) Conditional expression of *Mycobacterium smegmatis ftsZ*, an essential cell division gene. Microbiology 149: 1593-1603.

**Eggeling, L., and Bott, M.** (2005) Handbook of *Corynebacterium glutamicum*. In. Boca Raton, Florida, USA: CRC Press, Taylor & Francis Group, pp.

**Eggeling, L., and Bott, M.** (2015) A giant market and a powerful metabolism: L-lysine provided by *Corynebacterium glutamicum*. Appl. Microbiol. Biotechnol. 99: 3387-3394.

**Eggeling, L., Krumbach, K., and Sahm, H.** (2001) L-Glutamate efflux with *Corynebacterium glutamicum*: why is penicillin treatment or Tween addition doing the same? J Mol Microbiol Biotechnol 3: 67-68.

**Eraso, J.M., Markillie, L.M., Mitchell, H.D., Taylor, R.C., Orr, G., and Margolin, W.** (2014) The highly conserved MraZ protein is a transcriptional regulator in *Escherichia coli*. J Bacteriol 196: 2053-2066.

**Favrot, L., and Ronning, D.R.** (2012) Targeting the mycobacterial envelope for tuberculosis drug development. Expert Rev Anti Infect Ther 10: 1023-1036.

**Figge, R.M., Divakaruni, A.V., and Gober, J.W.** (2004) MreB, the cell shape-determining bacterial actin homologue, co-ordinates cell wall morphogenesis in *Caulobacter crescentus*. Mol Microbiol 51: 1321-1332.

**Flardh, K.** (2003) Essential role of DivIVA in polar growth and morphogenesis in *Streptomyces coelicolor* A3(2). Mol Microbiol 49: 1523-1536.

**Flardh, K., Garrido, T., and Vicente, M.** (1997) Contribution of individual promoters in the *ddlB-ftsZ* region to the transcription of the essential cell-division gene *ftsZ* in *Escherichia coli*. Mol Microbiol 24: 927-936.

**Flardh, K., Leibovitz, E., Buttner, M.J., and Chater, K.F.** (2000) Generation of a non-sporulating strain of *Streptomyces coelicolor* A3(2) by the manipulation of a developmentally controlled *ftsZ* promoter. Mol Microbiol 38: 737-749.

**Frantz, B., and O'Halloran, T.V.** (1990) DNA distortion accompanies transcriptional activation by the metal-responsive gene-regulatory protein MerR. Biochemistry 29: 4747-4751.

**Frunzke, J., Engels, V., Hasenbein, S., Gatgens, C., and Bott, M.** (2008) Co-ordinated regulation of gluconate catabolism and glucose uptake in *Corynebacterium glutamicum* by two functionally equivalent transcriptional regulators, GntR1 and GntR2. Mol Microbiol 67: 305-322.

**Galagan, J.E., Sisk, P., Stolte, C., Weiner, B., Koehrsen, M., Wymore, F., Reddy, T.B., Zucker, J.D., Engels, R., Gellesch, M., Hubble, J., Jin, H., Larson, L., Mao, M., Nitzberg, M., White, J., Zachariah, Z.K., Sherlock, G., Ball, C.A., and Schoolnik, G.K.** (2010) TB database 2010: overview and update. Tuberculosis (Edinb) 90: 225-235.

**Garcia-Nafria, J., Baumgart, M., Turkenburg, J.P., Wilkinson, A.J., Bott, M., and Wilson, K.S.** (2013) Crystal and solution studies reveal that the transcriptional regulator AcnR of

*Corynebacterium glutamicum* is regulated by citrate-$Mg^{2+}$ binding to a non-canonical pocket. J Biol Chem 288: 15800-15812.

**Garti-Levi, S., Hazan, R., Kain, J., Fujita, M., and Ben-Yehuda, S.** (2008) The FtsEX ABC transporter directs cellular differentiation in *Bacillus subtilis*. Mol Microbiol 69: 1018-1028.

**Gebel, L.** (2006) Untersuchungen zur Funktion der Proteine PknG, GlnH und GlnX aus *Corynebacterium glutamicum*. Mathematisch-Naturwissenschaftliche Fakultät. Heinrich-Heine-Universität Düsseldorf.

**Gerstmeir, R., Cramer, A., Dangel, P., Schaffer, S., and Eikmanns, B.J.** (2004) RamB, a novel transcriptional regulator of genes involved in acetate metabolism of *Corynebacterium glutamicum*. J Bacteriol 186: 2798-2809.

**Gibson, D.G.** (2011) Chapter fifteen - Enzymatic Assembly of Overlapping DNA Fragments. In: Methods in Enzymology. V. Christopher (ed). Academic Press, pp. 349-361.

**Goley, E.D., Yeh, Y.-C., Hong, S.-H., Fero, M.J., Abeliuk, E., McAdams, H.H., and Shapiro, L.** (2011) Assembly of the *Caulobacter* cell division machine. Mol Microbiol 80: 1680-1698.

**Gonzy-Treboul, G., Karmazyn-Campelli, C., and Stragier, P.** (1992) Developmental regulation of transcription of the *Bacillus subtilis ftsAZ* operon. J Mol Biol 224: 967-979.

**Gueiros-Filho, F.J., and Losick, R.** (2002) A widely conserved bacterial cell division protein that promotes assembly of the tubulin-like protein FtsZ. Genes Dev 16: 2544-2556.

**Hadfield, T.L., McEvoy, P., Polotsky, Y., Tzinserling, V.A., and Yakovlev, A.A.** (2000) The pathology of diphtheria. J Infect Dis 181 Suppl 1: S116-120.

**Haeusser, D.P., Schwartz, R.L., Smith, A.M., Oates, M.E., and Levin, P.A.** (2004) EzrA prevents aberrant cell division by modulating assembly of the cytoskeletal protein FtsZ. Mol Microbiol 52: 801-814.

**Hajduk, I.V., Rodrigues, C.D., and Harry, E.J.** (2016) Connecting the dots of the bacterial cell cycle: Coordinating chromosome replication and segregation with cell division. Semin Cell Dev Biol 53: 2-9.

**Hale, C.A., and de Boer, P.A.** (1997) Direct binding of FtsZ to ZipA, an essential component of the septal ring structure that mediates cell division in *E. coli*. Cell 88: 175-185.

**Hanahan, D.** (1983) Studies on transformation of *Escherichia coli* with plasmids. J. Mol. Biol. 166: 557-580.

**Henrich, A.W.** (2011) Characterization of maltose and trehalose transport in *Corynebacterium glutamicum*. Dissertation. Mathematisch-Naturwissenschaftliche Fakultät. Universität zu Köln.

**Hett, E.C., and Rubin, E.J.** (2008) Bacterial growth and cell division: a mycobacterial perspective. Microbiol Mol Biol Rev 72: 126-156, table of contents.

**Huisman, O., D'Ari, R., and Gottesman, S.** (1984) Cell-division control in *Escherichia coli*: specific induction of the SOS function SfiA protein is sufficient to block septation. Proc Natl Acad Sci USA 81: 4490-4494.

**Ikeda, M., and Nakagawa, S.** (2003) The *Corynebacterium glutamicum* genome: features and impacts on biotechnological processes. Appl. Microbiol. Biotechnol. 62: 99-109.

**Ishige, T., Krause, M., Bott, M., Wendisch, V.F., and Sahm, H.** (2003) The phosphate starvation stimulon of *Corynebacterium glutamicum* determined by DNA microarray analyses. J Bacteriol 185: 4519-4529.

**Jakoby, M., Tesch, M., Sahm, H., Krämer, R., and Burkovski, A.** (1997) Isolation of the *Corynebacterium glutamicum glnA* gene encoding glutamine synthetase I. FEMS Microbiol. Lett. 154: 81-88.

**Jones, L.J., Carballido-Lopez, R., and Errington, J.** (2001) Control of cell shape in bacteria: helical, actin-like filaments in *Bacillus subtilis*. Cell 104: 913-922.

**Kalinowski, J., Bathe, B., Bartels, D., Bischoff, N., Bott, M., Burkovski, A., Dusch, N., Eggeling, L., Eikmanns, B.J., Gaigalat, L., Goesmann, A., Hartmann, M., Huthmacher, K., Krämer, R., Linke, B., McHardy, A.C., Meyer, F., Möckel, B., Pfefferle, W., Pühler, A., Rey, D.A., Rückert, C., Rupp, O., Sahm, H., Wendisch, V.F., Wiegrabe, I., and Tauch, A.** (2003) The complete *Corynebacterium glutamicum* ATCC 13032 genome sequence and its impact on the production of L-aspartate-derived amino acids and vitamins. J. Biotechnol. 104: 5-25.

**Kanzaki, T., Isobe, K., Okazaki, H., Motizuki, K., and Fukuda, H.** (1967) L-Glutamic acid fermentation. Part I. Selection of an oleic acid-requiring mutant and its properties. Agricultural and Biological Chemistry 31: 1307-1317.

**Kataoka, M., Hashimoto, K.I., Yoshida, M., Nakamatsu, T., Horinouchi, S., and Kawasaki, H.** (2006) Gene expression of *Corynebacterium glutamicum* in response to the conditions inducing glutamate overproduction. Lett. Appl. Microbiol. 42: 471-476.

**Kawahara, Y., Takahashi-Fuke, K., Shimizu, E., Nakamatsu, T., and Nakamori, S.** (1997) Relationship between the glutamate production and the activity of 2-oxoglutarate dehydrogenase in *Brevibacterium lactofermentum*. Biosci. Biotechnol. Biochem. 61: 1109-1112.

**Kelly, A.J., Sackett, M.J., Din, N., Quardokus, E., and Brun, Y.V.** (1998) Cell cycle-dependent transcriptional and proteolytic regulation of FtsZ in Caulobacter. Genes Dev 12: 880-893.

**Kensy, F., Zang, E., Faulhammer, C., Tan, R.K., and Buchs, J.** (2009) Validation of a high-throughput fermentation system based on online monitoring of biomass and fluorescence in continuously shaken microtiter plates. Microb Cell Fact 8: 31.

**Kidd, S.P., Potter, A.J., Apicella, M.A., Jennings, M.P., and McEwan, A.G.** (2005) NmlR of *Neisseria gonorrhoeae*: a novel redox responsive transcription factor from the MerR family. Mol Microbiol 57: 1676-1689.

**Kim, J., Fukuda, H., Hirasawa, T., Nagahisa, K., Nagai, K., Wachi, M., and Shimizu, H.** (2010) Requirement of *de novo* synthesis of the OdhI protein in penicillin-induced glutamate production by *Corynebacterium glutamicum*. Appl. Microbiol. Biotechnol. 86: 911-920.

**Kimura, E.** (2002) Triggering mechanism of L-glutamate overproduction by DtsR1 in coryneform bacteria. J. Biosci. Bioeng. 94: 545-551.

**Kimura, E., Abe, C., Kawahara, Y., Nakamatsu, T., and Tokuda, H.** (1997) A dtsR gene-disrupted mutant of Brevibacterium lactofermentum requires fatty acids for growth and efficiently produces L-glutamate in the presence of an excess of biotin. Biochem Biophys Res Commun 234: 157-161.

**Kinoshita, S., Udaka, S., and Shimono, M.** (1957) Studies on amino acid fermentation. Part I. Production of L-glutamic acid by various microorganisms. J. Gen. Appl. Microbiol. 3: 193-205.

**Kiran, M., Maloney, E., Lofton, H., Chauhan, A., Jensen, R., Dziedzic, R., Madiraju, M., and Rajagopalan, M.** (2009) *Mycobacterium tuberculosis ftsZ* expression and minimal promoter activity. Tuberculosis (Edinb) 89 Suppl 1: S60-64.

**Kirchner, O., and Tauch, A.** (2003) Tools for genetic engineering in the amino acid-producing bacterium *Corynebacterium glutamicum*. J. Biotechnol. 104: 287-299.

**Koch-Koerfges, A., Kabus, A., Ochrombel, I., Marin, K., and Bott, M.** (2012) Physiology and global gene expression of a *Corynebacterium glutamicum* ΔF(1)F(O)-ATP synthase mutant devoid of oxidative phosphorylation. Biochim Biophys Acta 1817: 370-380.

**Komine-Abe, A., Nagano-Shoji, M., Kubo, S., Kawasaki, H., Yoshida, M., Nishiyama, M., and Kosono, S.** (2017) Effect of lysine succinylation on the regulation of 2-oxoglutarate dehydrogenase inhibitor, OdhI, involved in glutamate production in *Corynebacterium glutamicum*. Biosci Biotech Bioch 81: 2130-2138.

**Kortmann, M., Kuhl, V., Klaffl, S., and Bott, M.** (2015) A chromosomally encoded T7 RNA polymerase-dependent gene expression system for *Corynebacterium glutamicum*: construction and comparative evaluation at the single-cell level. Microb Biotechnol 8: 253-265.

**Krawczyk, S., Raasch, K., Schultz, C., Hoffelder, M., Eggeling, L., and Bott, M.** (2010) The FHA domain of OdhI interacts with the carboxyterminal 2-oxoglutarate dehydrogenase domain of OdhA in *Corynebacterium glutamicum*. FEBS Lett 584: 1463-1468.

**Kruse, T., Bork-Jensen, J., and Gerdes, K.** (2005) The morphogenetic MreBCD proteins of *Escherichia coli* form an essential membrane-bound complex. Mol Microbiol 55: 78-89.

**Kumaraswami, M., Newberry, K.J., and Brennan, R.G.** (2010) Conformational plasticity of the coiled-coil domain of BmrR is required for *bmr* operator binding: the structure of unliganded BmrR. J Mol Biol 398: 264-275.

**Kwak, J., Dharmatilake, A.J., Jiang, H., and Kendrick, K.E.** (2001) Differential regulation of *ftsZ* transcription during septation of *Streptomyces griseus*. J Bacteriol 183: 5092-5101.

**Laemmli, U.K.** (1970) Cleavage of structural proteins during the assembly of the head of bacteriophage T4. Nature 227: 680-685.

**Lawn, S.D., and Zumla, A.I.** (2011) Tuberculosis. Lancet 378: 57-72.

**Lee, D.S., Kim, P., Kim, E.S., Kim, Y., and Lee, H.S.** (2018) *Corynebacterium glutamicum* WhcD interacts with WhiA to exert a regulatory effect on cell division genes. Antonie Van Leeuwenhoek 111: 641-648.

**Letek, M., Fiuza, M., Ordonez, E., Villadangos, A.F., Ramos, A., Mateos, L.M., and Gil, J.A.** (2008) Cell growth and cell division in the rod-shaped actinomycete *Corynebacterium glutamicum*. Antonie Van Leeuwenhoek International Journal of General and Molecular Microbiology 94: 99-109.

**Letek, M., Ordonez, E., Fiuza, M., Honrubia-Marcos, P., Vaquera, J., Gil, J.A., Castro, D., and Mateos, L.M.** (2007) Characterization of the promoter region of *ftsZ* from *Corynebacterium glutamicum* and controlled overexpression of FtsZ. Int Microbiol 10: 271-282.

**Letek, M., Valbuena, N., Ramos, A., Ordonez, E., Gil, J.A., and Mateos, L.M.** (2006) Characterization and use of catabolite-repressed promoters from gluconate genes in *Corynebacterium glutamicum*. J. Bacteriol. 188: 409-423.

**Levin, P.A., Kurtser, I.G., and Grossman, A.D.** (1999) Identification and characterization of a negative regulator of FtsZ ring formation in *Bacillus subtilis*. Proc Natl Acad Sci USA 96: 9642-9647.

**Levin, P.A., Margolis, P.S., Setlow, P., Losick, R., and Sun, D.** (1992) Identification of *Bacillus subtilis* genes for septum placement and shape determination. J Bacteriol 174: 6717-6728.

**Lindemann, B., Ogiwara, Y., and Ninomiya, Y.** (2002) The discovery of umami. Chem Senses 27: 843-844.

**Livak, K.J., and Schmittgen, T.D.** (2001) Analysis of relative gene expression data using real-time quantitative PCR and the $2^{-\Delta\Delta CT}$ method. Methods 25: 402-408.

**Lock, R.L., and Harry, E.J.** (2008) Cell-division inhibitors: new insights for future antibiotics. Nat Rev Drug Discov 7: 324-338.

**Maeda, T., Tanaka, Y., Takemoto, N., Hamamoto, N., and Inui, M.** (2016) RNase III mediated cleavage of the coding region of *mraZ* mRNA is required for efficient cell division in *Corynebacterium glutamicum*. Mol Microbiol 99: 1149-1166.

**Margolin, W.** (2005) FtsZ and the division of prokaryotic cells and organelles. Nat Rev Mol Cell Biol 6: 862-871.

**McEwan, A.G., Djoko, K.Y., Chen, N.H., Counago, R.L., Kidd, S.P., Potter, A.J., and Jennings, M.P.** (2011) Novel bacterial MerR-like regulators their role in the response to carbonyl and nitrosative stress. Adv Microb Physiol 58: 1-22.

**Meisner, J., Montero Llopis, P., Sham, L.-T., Garner, E., Bernhardt, T.G., and Rudner, D.Z.** (2013) FtsEX is required for CwlO peptidoglycan hydrolase activity during cell wall elongation in *Bacillus subtilis*. Mol Microbiol 89: 1069-1083.

**Minch, K.J., Rustad, T.R., Peterson, E.J., Winkler, J., Reiss, D.J., Ma, S., Hickey, M., Brabant, W., Morrison, B., Turkarslan, S., Mawhinney, C., Galagan, J.E., Price, N.D., Baliga, N.S., and Sherman, D.R.** (2015) The DNA-binding network of Mycobacterium tuberculosis. Nat Commun 6: 5829.

**Mingorance, J., Tamames, J., and Vicente, M.** (2004) Genomic channeling in bacterial cell division. J Mol Recognit 17: 481-487.

**Momose, H., and Takagi, T.** (1978) Glutamic acid production in biotin-rich media by temperatureresensitive mutants of *Brevibacterium lactofermentum*, a novel fermentation process. Agr Biol Chem 42: 1911-1917.

**Monahan, L.G., and Harry, E.J.** (2016) You Are What You Eat: Metabolic Control of Bacterial Division. Trends Microbiol 24: 181-189.

**Mouritsen, O.G.** (2012) Umami flavour as a means of regulating food intake and improving nutrition and health. Nutr Health 21: 56-75.

**Nakamura, J., Hirano, S., Ito, H., and Wachi, M.** (2007) Mutations of the *Corynebacterium glutamicum* NCgl1221 gene, encoding a mechanosensitive channel homolog, induce L-glutamic acid production. Appl. environm. Microbiol. 73: 4491-4498.

**Nakao, Y., Kikuchi, M., Suzuki, M., and Doi, M.** (1972) Microbial production of L-glutamic acid by glycerol auxotrophs. Agr Biol Chem 36: 490-496.

**Newberry, K.J., and Brennan, R.G.** (2004) The structural mechanism for transcription activation by MerR family member multidrug transporter activation, N terminus. J Biol Chem 279: 20356-20362.

**Niebisch, A., and Bott, M.** (2001) Molecular analysis of the cytochrome $bc_1$-$aa_3$ branch of the *Corynebacterium glutamicum* respiratory chain containing an unusual diheme cytochrome $c_1$. Arch. Microbiol. 175: 282-294.

**Niebisch, A., Kabus, A., Schultz, C., Weil, B., and Bott, M.** (2006) Corynebacterial protein kinase G controls 2-oxoglutarate dehydrogenase activity via the phosphorylation status of the OdhI protein. J Biol Chem 281: 12300-12307.

**Nunheimer, T.D., Birnbaum, J., Ihnen, E.D., and Demain, A.L.** (1970) Product inhibition of the fermentative formation of glutamic acid. Appl Microbiol 20: 215-217.

**Okazaki, H., Kanzaki, T., Doi, M., Sumino, Y., and Fukuda, H.** (1967) L-Glutamic acid fermentation. Part II. The production of L-glutamic acid by an oleic acid-requiring mutant. Agr Biol Chem 31: 1314-1317.

**Overbeek, R., Larsen, N., Walunas, T., D'Souza, M., Pusch, G., Selkov, E., Jr., Liolios, K., Joukov, V., Kaznadzey, D., Anderson, I., Bhattacharyya, A., Burd, H., Gardner, W., Hanke, P., Kapatral, V., Mikhailova, N., Vasieva, O., Osterman, A., Vonstein, V., Fonstein,**

**M., Ivanova, N., and Kyrpides, N.** (2003) The ERGO genome analysis and discovery system. Nucleic Acids Res 31: 164-171.

**Pfeifer-Sancar, K., Mentz, A., Ruckert, C., and Kalinowski, J.** (2013) Comprehensive analysis of the *Corynebacterium glutamicum* transcriptome using an improved RNAseq technique. BMC Genomics 14: 888.

**Pfeifer, E., Gatgens, C., Polen, T., and Frunzke, J.** (2017) Adaptive laboratory evolution of *Corynebacterium glutamicum* towards higher growth rates on glucose minimal medium. Sci Rep 7: 16780.

**Pfeifer, E., Hunnefeld, M., Popa, O., Polen, T., Kohlheyer, D., Baumgart, M., and Frunzke, J.** (2016) Silencing of cryptic prophages in *Corynebacterium glutamicum*. Nucleic Acids Res.

**Philips, S.J., Canalizo-Hernandez, M., Yildirim, I., Schatz, G.C., Mondragon, A., and O'Halloran, T.V.** (2015) TRANSCRIPTION. Allosteric transcriptional regulation via changes in the overall topology of the core promoter. Science 349: 877-881.

**Pichoff, S., and Lutkenhaus, J.** (2005) Tethering the Z ring to the membrane through a conserved membrane targeting sequence in FtsA. Mol Microbiol 55: 1722-1734.

**Puech, V., Bayan, N., Salim, K., Leblon, G., and Daffe, M.** (2000) Characterization of the *in vivo* acceptors of the mycoloyl residues transferred by the corynebacterial PS1 and the related mycobacterial antigens 85. Mol Microbiol 35: 1026-1041.

**Raasch, K., Bocola, M., Labahn, J., Leitner, A., Eggeling, L., and Bott, M.** (2014) Interaction of 2-oxoglutarate dehydrogenase OdhA with its inhibitor OdhI in *Corynebacterium glutamicum*: mutants and a model. J Biotechnol 191: 99-105.

**Radmacher, E., Stansen, K.C., Besra, G.S., Alderwick, L.J., Maughan, W.N., Hollweg, G., Sahm, H., Wendisch, V.F., and Eggeling, L.** (2005) Ethambutol, a cell wall inhibitor of *Mycobacterium tuberculosis*, elicits L-glutamate efflux of *Corynebacterium glutamicum*. Microbiology 151: 1359-1368.

**Ramos, A., Honrubia, M.P., Valbuena, N., Vaquera, J., Mateos, L.M., and Gil, J.A.** (2003) Involvement of DivIVA in the morphology of the rod-shaped actinomycete *Brevibacterium lactofermentum*. Microbiology 149: 3531-3542.

**Ramos, A., Letek, M., Campelo, A.B., Vaquera, J., Mateos, L.M., and Gil, J.A.** (2005) Altered morphology produced by *ftsZ* expression in *Corynebacterium glutamicum* ATCC 13869. Microbiology 151: 2563-2572.

**Raskin, D.M., and de Boer, P.A.** (1999) MinDE-dependent pole-to-pole oscillation of division inhibitor MinC in *Escherichia coli*. J Bacteriol 181: 6419-6424.

**Reddy, T.B., Riley, R., Wymore, F., Montgomery, P., DeCaprio, D., Engels, R., Gellesch, M., Hubble, J., Jen, D., Jin, H., Koehrsen, M., Larson, L., Mao, M., Nitzberg, M., Sisk, P., Stolte, C., Weiner, B., White, J., Zachariah, Z.K., Sherlock, G., Galagan, J.E., Ball, C.A., and Schoolnik, G.K.** (2009) TB database: an integrated platform for tuberculosis research. Nucleic Acids Res 37: D499-508.

**Robert, X., and Gouet, P.** (2014) Deciphering key features in protein structures with the new ENDscript server. Nucleic Acids Res. 42: W320-324.

**Roy, S., and Ajitkumar, P.** (2005) Transcriptional analysis of the principal cell division gene, *ftsZ*, of *Mycobacterium tuberculosis*. J Bacteriol 187: 2540-2550.

**Ruhal, R., Kataria, R., and Choudhury, B.** (2013) Trends in bacterial trehalose metabolism and significant nodes of metabolic pathway in the direction of trehalose accumulation. Microb Biotechnol 6: 493-502.

**Sambrook, J., and Russell, D.** (2001) *Molecular Cloning. A Laboratory Manual*. Cold Spring Harbor Laboratory Press, Cold Spring Harbor, New York.

**Sano, C.** (2009) History of glutamate production. Am J Clin Nutr 90: 728s-732s.

**Sass, P., and Brötz-Oesterhelt, H.** (2013) Bacterial cell division as a target for new antibiotics. Curr Opin Microbiol 16: 522-530.

**Schaaf, S., and Bott, M.** (2007) Target genes and DNA-binding sites of the response regulator PhoR from *Corynebacterium glutamicum*. J Bacteriol 189: 5002-5011.

**Schäfer, A., Tauch, A., Jäger, W., Kalinowski, J., Thierbach, G., and Pühler, A.** (1994) Small mobilizable multipurpose cloning vectors derived from the *Escherichia coli* plasmids pK18 and pK19 - Selection of defined deletions in the chromosome of *Corynebacterium glutamicum*. Gene 145: 69-73.

**Schaffer, S., Weil, B., Nguyen, V.D., Dongmann, G., Gunther, K., Nickolaus, M., Hermann, T., and Bott, M.** (2001) A high-resolution reference map for cytoplasmic and membrane-associated proteins of *Corynebacterium glutamicum*. Electrophoresis 22: 4404-4422.

**Schmidt, K.L., Peterson, N.D., Kustusch, R.J., Wissel, M.C., Graham, B., Phillips, G.J., and Weiss, D.S.** (2004) A predicted ABC transporter, FtsEX, is needed for cell division in *Escherichia coli*. J Bacteriol 186: 785-793.

**Schröder, J., and Tauch, A.** (2010) Transcriptional regulation of gene expression in *Corynebacterium glutamicum*: the role of global, master and local regulators in the modular and hierarchical gene regulatory network. FEMS Microbiol. Rev. 34: 685-737.

**Schultz, C., Niebisch, A., Gebel, L., and Bott, M.** (2007) Glutamate production by *Corynebacterium glutamicum*: dependence on the oxoglutarate dehydrogenase inhibitor protein OdhI and protein kinase PknG. Appl Microbiol Biotechnol 76: 691-700.

**Schultz, C., Niebisch, A., Schwaiger, A., Viets, U., Metzger, S., Bramkamp, M., and Bott, M.** (2009) Genetic and biochemical analysis of the serine/threonine protein kinases PknA, PknB, PknG and PknL of *Corynebacterium glutamicum*: evidence for non-essentiality and for phosphorylation of OdhI and FtsZ by multiple kinases. Mol Microbiol 74: 724-741.

**Schwinde, J.W., Hertz, P.F., Sahm, H., Eikmanns, B.J., and Guyonvarch, A.** (2001) Lipoamide dehydrogenase from *Corynebacterium glutamicum*: molecular and physiological analysis of the *lpd* gene and characterization of the enzyme. Microbiology 147: 2223-2231.

**Sham, L.-T., Jensen, K.R., Bruce, K.E., and Winkler, M.E.** (2013) Involvement of FtsE ATPase and FtsX extracellular loops 1 and 2 in FtsEX-PcsB complex function in cell division of *Streptococcus pneumoniae* D39. mBio 4: e00431-00413.

**Shiio, I., Otsuka, S.I., and Katsuya, N.** (1962) Effect of biotin on the bacterial formation of glutamic acid. II. Metabolism of glucose. J Biochem 52: 108-116.

**Shiio, I., and Ozaki, H.** (1970) Regulation of nicotinamide adenine dinucleotide phosphate-specific glutamate dehydrogenase from *Brevibacterium flavum*, a glutamate-producing bacterium. J. Biochem. 68: 633-647.

**Shimizu, H., Tanaka, H., Nakato, A., Nagahisa, K., Kimura, E., and Shioya, S.** (2003) Effects of the changes in enzyme activities on metabolic flux redistribution around the 2-oxoglutarate branch in glutamate production by *Corynebacterium glutamicum*. Bioproc. Biosys. Eng. 25: 291-298.

**Shirai, T., Nakato, A., Izutani, N., Nagahisa, K., Shioya, S., Kimura, E., Kawarabayasi, Y., Yamagishi, A., Gojobori, T., and Shimizu, H.** (2005) Comparative study of flux redistribution of metabolic pathway in glutamate production by two coryneform bacteria. Metab. Eng. 7: 59-69.

**Sievers, F., Wilm, A., Dineen, D., Gibson, T.J., Karplus, K., Li, W., Lopez, R., McWilliam, H., Remmert, M., Soding, J., Thompson, J.D., and Higgins, D.G.** (2011) Fast, scalable generation of high-quality protein multiple sequence alignments using Clustal Omega. Mol Syst Biol 7: 539.

**Singh, S., Sevalkar, R.R., Sarkar, D., and Karthikeyan, S.** (2018) Characteristics of the essential pathogenicity factor Rv1828, a MerR family transcription regulator from *Mycobacterium tuberculosis*. Febs j 285: 4424-4444.

**Slayden, R.A., Knudson, D.L., and Belisle, J.T.** (2006) Identification of cell cycle regulators in *Mycobacterium tuberculosis* by inhibition of septum formation and global transcriptional analysis. Microbiology 152: 1789-1797.

**Takinami, K., Yoshii, H., Tsura, H., and Okada, H.** (1966) Biochemical effects of fatty acid and its derivatives on L-glutamic Acid fermentation. Agr Biol Chem 30: 674-682.

**Tamames, J., Gonzalez-Moreno, M., Mingorance, J., Valencia, A., and Vicente, M.** (2001) Bringing gene order into bacterial shape. Trends Genet 17: 124-126.

**Tournu, H., Fiori, A., and Van Dijck, P.** (2013) Relevance of trehalose in pathogenicity: some general rules, yet many exceptions. PLoS Pathog 9: e1003447.

**Tropis, M., Meniche, X., Wolf, A., Gebhardt, H., Strelkov, S., Chami, M., Schomburg, D., Kramer, R., Morbach, S., and Daffe, M.** (2005) The crucial role of trehalose and structurally related oligosaccharides in the biosynthesis and transfer of mycolic acids in *Corynebacterineae*. J. Biol. Chem. 280: 26573-26585.

**Tzvetkov, M., Klopprogge, C., Zelder, O., and Liebl, W.** (2003) Genetic dissection of trehalose biosynthesis in *Corynebacterium glutamicum*: inactivation of trehalose production leads to impaired growth and an altered cell wall lipid composition. Microbiology 149: 1659-1673.

**Untergasser, A., Cutcutache, I., Koressaar, T., Ye, J., Faircloth, B.C., Remm, M., and Rozen, S.G.** (2012) Primer3—new capabilities and interfaces. Nucleic Acids Res 40: e115-e115.

**Usuda, Y., Tujimoto, N., Abe, C., Asakura, Y., Kimura, E., Kawahara, Y., Kurahashi, O., and Matsui, H.** (1996) Molecular cloning of the *Corynebacterium glutamicum* ('*Brevibacterium lactofermentum*' AJ12036) *odhA* gene encoding a novel type of 2-oxoglutarate dehydrogenase. Microbiology 142: 3347-3354.

**van der Rest, M.E., Lange, C., and Molenaar, D.** (1999) A heat shock following electroporation induces highly efficient transformation of *Corynebacterium glutamicum* with xenogeneic plasmid DNA. Appl. Microbiol. Biotechnol. 52: 541-545.

**Ventura, M., Rieck, B., Boldrin, F., Degiacomi, G., Bellinzoni, M., Barilone, N., Alzaidi, F., Alzari, P.M., Manganelli, R., and O'Hare, H.M.** (2013) GarA is an essential regulator of metabolism in *Mycobacterium tuberculosis*. Mol Microbiol 90: 356-366.

**Vogt, M., Haas, S., Klaffl, S., Polen, T., Eggeling, L., van Ooyen, J., and Bott, M.** (2014) Pushing product formation to its limit: Metabolic engineering of *Corynebacterium glutamicum* for L-leucine overproduction. Metab. Eng. 22: 40-52.

**Wendisch, V.F., and Bott, M.** (2005) Phosphorus metabolism of *Corynebacterium glutamicum*. In: Handbook of *Corynebacterium glutamicum.* L. Eggeling & M. Bott (eds). Boca Raton, USA: CRC Press, pp. 377-396.

**Wendisch, V.F., Jorge, J.M., Perez-Garcia, F., and Sgobba, E.** (2016) Updates on industrial production of amino acids using *Corynebacterium glutamicum*. World J. Microbiol. Biotechnol. 32: 105.

**WHO** (2015) Tuberculosis fact sheet, http://www.who.int/mediacentre/factsheets/fs104/en/

**Wolf, A., Krämer, R., and Morbach, S.** (2003) Three pathways for trehalose metabolism in *Corynebacterium glutamicum* ATCC13032 and their significance in response to osmotic stress. Mol Microbiol 49: 1119-1134.

**Wu, L.J., and Errington, J.** (2004) Coordination of cell division and chromosome segregation by a nucleoid occlusion protein in *Bacillus subtilis*. Cell 117: 915-925.

**Zacharia, V.M., Manzanillo, P.S., Nair, V.R., Marciano, D.K., Kinch, L.N., Grishin, N.V., Cox, J.S., and Shiloh, M.U.** (2013) *cor*, a novel carbon monoxide resistance gene, is essential for *Mycobacterium tuberculosis* pathogenesis. mBio 4: e00721-00713.

## Danksagung

Die vorliegende Arbeit wurde am Institut für Bio- und Geowissenschaften 1 des Forschungszentrums Jülich unter der Leitung von Prof. Dr. Michael Bott angefertigt. Ich danke ihm für die Möglichkeit, meine Promotion an seinem Institut durchführen zu dürfen sowie für die Übernahme des Erstgutachtens und das stete Interesse an meiner Arbeit. Gedankt sei außerdem Prof. Dr. Martina Pohl für die Übernahme des Zweitgutachtens.

Mein ganz besonderer Dank gilt Dr. Meike Baumgart für die ausgezeichnete Betreuung sowie für die stetige Diskussionsbereitschaft. Sie hatte immer ein offenes Ohr und zahlreiche wertvolle Ratschläge und Antworten auf alle Fragen. Bei ihr sowie allen weiteren Mitarbeitern des IBG-1 möchte ich mich außerdem für die angenehme Arbeitsatmosphäre und die gute, kollegiale Unterstützung bedanken. Vor allem Andi, Maike und Julia – ohne euch wäre es nicht Dasselbe gewesen.

Besonders möchte ich meinen Eltern und meiner Oma danken, die mich während der gesamten Zeit meines Studiums moralisch unterstützt und mich stets in meinen Zielen bestärkt haben, wodurch sie entscheidend zum Gelingen dieser Arbeit beigetragen haben. Ein außerordentlicher Dank gilt außerdem Benedikt, der mich sowohl in guten als auch in schwierigen Phasen ausgehalten und mir immer Mut gemacht hat.

## Eidesstattliche Versicherung

Ich versichere an Eides Statt, dass die Dissertation von mir selbständig und ohne unzulässige fremde Hilfe unter Beachtung der „Grundsätze zur Sicherung guter wissenschaftlicher Praxis an der Heinrich-Heine-Universität Düsseldorf“ erstellt worden ist.

_____ _____

Ort, Datum Unterschrift

Band / Volume 227
**Strain and Tool Development for the Production of Industrially Relevant Compounds with *Corynebacterium glutamicum***
M. Kortmann (2021), II, 138 pp
ISBN: 978-3-95806-522-2

Band / Volume 228
**Complex magnetism of nanostructures on surfaces: from orbital magnetism to spin excitations**
S. Brinker (2021), III, 208 pp
ISBN: 978-3-95806-525-3

Band / Volume 229
**High-throughput All-Electron Density Functional Theory Simulations for a Data-driven Chemical Interpretation of X-ray Photoelectron Spectra**
J. Bröder (2021), viii, 169, XL pp
ISBN: 978-3-95806-526-0

Band / Volume 230
**Molecular tools for genome engineering of *Corynebacterium glutamicum***
C. K. Sonntag (2021), VIII, 111 pp
ISBN: 978-3-95806-532-1

Band / Volume 231
**Interface Functionalization of Magnetic Oxide $Fe_3O_4$/$SrTiO_3$ Heterostructures**
M. H. A. Hamed (2021), xvii, 151 pp
ISBN: 978-3-95806-535-2

Band / Volume 232
**Optically induced magnetization reversal in Co/Pt multilayers**
Role of domain wall dynamics
U. Parlak (2021), ix, 162, XII pp
ISBN: 978-3-95806-536-9

Band / Volume 233
**Application of Silicon Photomultipliers in Neutron Detectors**
S. Kumar (2021), xxvi, 157 pp
ISBN: 978-3-95806-537-6

Band / Volume 234
**Towards Magneto-Elastomeric Nanocomposites with Supramolecular Activity**
L. S. Fruhner (2021), XVI, 213 pp
ISBN: 978-3-95806-538-3

Band / Volume 235
**Geometric and Electronic Properties of Heteromolecular Organic Monolayers on Noble Metal Substrates Studied by Photoemission Spectroscopy and X-ray Standing Waves**
G. van Straaten (2021), vii, 115 pp
ISBN: 978-3-95806-539-0

Band / Volume 236
**Nanoparticle assemblies: Order by self-organization and collective magnetism**
A. Qdemat (2021), xix, 282 pp
ISBN: 978-3-95806-542-0

Band / Volume 237
**γ-Aminobutyrate as carbon and nitrogen source for *Corynebacterium glutamicum* and regulation of the catabolic genes by GabR**
L. Zhu (2021), 111 pp
ISBN: 978-3-95806-543-7

Band / Volume 238
**Single-Trap Phenomena in Nanowire Biosensors**
Y. Kutovyi (2021), 171 pp
ISBN: 978-3-95806-544-4

Band / Volume 239
**Single crystal growth and neutron scattering studies of novel quantum materials**
X. Wang (2021), VI, 145 pp
ISBN: 978-3-95806-546-8

Band / Volume 240
**Structure and Dynamics of Magnetocaloric Materials**
N. A. Maraytta (2021), vii, 146 pp
ISBN: 978-3-95806-557-4

Band / Volume 241
**Novel insights into the transcriptional regulation of cell division in *Corynebacterium glutamicum***
K. J. Kraxner (2021), V, 83 pp
ISBN: 978-3-95806-560-4

Weitere ***Schriften des Verlags im Forschungszentrum Jülich*** unter
http://wwwzb1.fz-juelich.de/verlagextern1/index.asp

Schlüsseltechnologien / Key Technologies
Band / Volume 241
ISBN 978-3-95806-560-4

Mitglied der Helmholtz-Gemeinschaft

JÜLICH
Forschungszentrum